

**STAND DYNAMICS MODELS OF TROPICAL EUCALYPTUS HYBRID CLONE
PLANTATIONS IN SUMATERA, INDONESIA**

by

Joni Waldy

Bachelor of Science in Statistics, IPB University, 2010

A Thesis Submitted in Partial Fulfillment
of the Requirements for the Degree of

Master of Science in Forestry

in the Graduate Academic Unit of Faculty of Forestry and Environmental Management

Supervisor: John A. Kershaw Jr., PhD, FOREM, University of New Brunswick

Examining Board: Aaron Weiskittel, PhD, University of Maine, U.S.A.
David Wagner, PhD, Education, University of New Brunswick
John A. Kershaw Jr., PhD, FOREM, University of New Brunswick

This thesis accepted by the
Dean of Graduate Studies

THE UNIVERSITY OF NEW BRUNSWICK

March 2021

©Joni Waldy, 2021

ABSTRACT

Eucalyptus is one of the most widely cultivated species and provides raw materials for pulp and paper production in many tropical countries. Growth and yield is essential for forest management decision-making processes such as prediction of future forest yields and exploration of silvicultural options. However, limited publications related to growth and yield of this species exist in Indonesia compared to other regions. In this study, time-based and state-space modeling approaches were evaluated for estimating stand-level attributes of tropical hybrid Eucalyptus clonal plantation in Sumatera over normal rotation periods. Moment-based, percentile-based and hybrid methods for parameter recovery of Weibull distribution parameters for characterizing diameter distributions were also studied. The time-based approach was observed to provide simple and more accurate estimates of stand attributes across relatively short rotation ages. Moment-based parameter recovery methods also was found to give better performance. The combined system of models enables forest managers to evaluate total yield and its distribution across size classes.

DEDICATION

To my teachers from elementary to high school,
who paved the way for my big dreams

ACKNOWLEDGEMENTS

All praises to Allah and His blessing for the completion of my master's degree. I thank Allah for all the opportunities, trials, and strengths that have been showered on me to finish writing the thesis. My humblest gratitude to the Holy Prophet Muhammad (Peace be upon him) whose way of life has been continuous guidance for me.

I would like to thank my supervisor Dr. John A. Kershaw, Jr that was always open whenever I ran into a trouble spot or had a question about my research or writing. Your leadership, technical expertise and knowledge of the various topics which constitute this work were invaluable to the learning process and my future career. I am also deeply indebted to my supervisory committee members: Dr. Aaron Weiskittel (University of Maine, U.S.A) and Dr. Mark Ducey (University of New Hampshire, U.S.A) for their patience and insightful comments, guidance, and inputs that improved the quality of this thesis.

I would like to thank all the Integrated Forest Management Lab members: Ting-Ru Yang, Yung-Han Hsu, Yang Zhan, and Xiao Dai who provided all kinds of help every time when I needed. Even though we had to split up during a pandemic, your inputs and especially your research results are also very meaningful for me and my company. Thanks also to Sandy Loder (Senior Analyst, Remsoft Inc.) who introduced me to my supervisor Dr. John Kershaw Jr, so that I had the opportunity to study directly with him.

I want to special thank PT. Riau Andalan Pulp and Paper, a member of APRIL Group for providing the opportunity through APRIL Overseas Master's Degree Scholarship Program as well as research data to complete my master's study. Also Mr.

Branislav Zoric, Mr. Nawari and Mr. Timothy Charles Fenton as my superiors who had supported me to get this opportunity before I went to Canada. Likewise, Forest Growth and Inventory team members who continued my work to keep supporting the company's business. You have been amazing.

Last but not the least my biggest thanks to my parents Riswandi and Yulianti have given me the freedom to be what I want in my life. For my children Sulthan Ahza Firdaus and Lula Arianna Attahirah, sorry if you lost the figure of a father for two years. For my wife Wildatin Saa'dah, thank you for realizing my dreams since childhood, without which I would have stopped these studies a long time ago. And for my mother-in-law, Paryati Dachrin who has taken good care of my wife and children while I was in Canada.

Table of Contents

ABSTRACT.....	ii
DEDICATION.....	iii
ACKNOWLEDGEMENTS.....	iv
Table of Contents.....	vi
List of Tables.....	ix
List of Figures.....	xii
List of Symbols, Nomenclatures or Abbreviations.....	xv
Chapter 1: General Introduction.....	1
1.1 Pulp and paper industry in Indonesia.....	2
1.2 Indonesia’s eucalyptus plantation.....	3
1.3 Growth and yield modeling.....	5
1.4 Objectives.....	7
1.5 Thesis layout.....	8
1.6 References.....	10
Chapter 2: Comparison of time-based versus state-space stand growth models for tropical hybrid Eucalyptus clonal plantations in Sumatera, Indonesia.....	15
2.1 Introduction.....	16
2.2 Methods.....	20

2.2.1 Study site.....	20
2.2.2 Data collection	21
2.2.3 Time-based model development	22
2.2.4 State-space model development.....	24
2.2.5 Other stand attributes	27
2.2.6 Model evaluation	28
2.3 Results.....	29
2.3.1 Stand volume model	29
2.3.2 Time-based model.....	30
2.3.3 State-space model	32
2.3.4 Model comparison	34
2.4 Discussion.....	35
2.5 Conclusion	40
2.6 References.....	41
Chapter 3: Diameter distribution model development of tropical hybrid Eucalyptus clonal plantations in Sumatera, Indonesia: A comparison of estimation methods	76
3.1 Introduction.....	77
3.2 Methods.....	82
3.2.1 Study site.....	82
3.2.2 Data collection	82

3.2.3 Maximum likelihood estimation (MLE).....	83
3.2.4 Moment-based parameter recovery.....	83
3.2.5 Percentile-based parameter recovery	84
3.2.6 Hybrid method parameter recovery	85
3.2.7 Moment and Percentile Estimation.....	86
3.2.8 Model evaluation	87
3.3 Result	87
3.3.1 Moment and percentile prediction models.....	87
3.3.2 Characteristics of Maximum Likelihood Estimates.....	88
3.3.3 Diameter distribution model evaluation.....	89
3.4 Discussion	90
3.5 Conclusion	93
3.6 References.....	94
Chapter 4: Conclusions.....	117
4.1 Summary of results	118
4.2 Model applications.....	122
4.3 Future work.....	123
4.4 References.....	126
Curriculum Vitae	

List of Tables

<p>Table 2.1 Summarized stand attributes and their increment for the inventory plots (n=2808) used for modeling (A = age; HT = top height; BA = basal area; SD = stand density; RD = relative density; DQ = quadratic mean diameter; and VOL = stand volume).....</p>	48
<p>Table 2.2 Mathematical equation forms evaluated for time-based top height growth model. (A₁ = age (months) at time 1; A₂ = age (months) at time 2; HT₁ = top height (m) at time 1; HT₂ = top height at time 2; h_i = coefficient parameters)</p>	49
<p>Table 2.3 Mathematical equation forms evaluated for time-based stand density models. (A₁ = age (months) at time 1; A₂ = age (months) at time 2; SD₁ = stand density (trees· ha⁻¹) at time 1; SD₂ = stand density (trees·ha⁻¹) at time 2; s_i = coefficient parameters).....</p>	50
<p>Table 2.4 Mathematical equation forms evaluated for time-based basal area growth models. (A₁ = age (months) at time 1; A₂ = age (months) at time 2; BA₁ = basal area (m²ha⁻¹) at time 1; BA₂ = basal area (m²ha⁻¹) at time 2; b_i = coefficient parameters).....</p>	51
<p>Table 2.5 Estimated parameters with their standard errors (in parentheses) and statistical evaluation for volume model</p>	52
<p>Table 2.6 Parameter estimates and their associated standard errors (in parentheses), standard deviations of the random effects and goodness-of-fit statistics model V-4</p>	53
<p>Table 2.7 Derived coefficient (fixed + random effects) of model V-4 by clone and site classes.....</p>	54

Table 2.8 Estimated parameters with their standard errors (in parentheses) of nonlinear least square analysis and goodness-of-fit measures for seven top height models using time-based approach.....	55
Table 2.9 Estimated parameters with their standard errors (in parentheses) of nonlinear least square analysis and goodness-of-fit measures for six stand density models using time-based approach.....	56
Table 2.10 Estimated parameters with their standard errors (in parentheses) of nonlinear least square analysis and goodness-of-fit measures for nine basal area models using time-based approach.....	57
Table 2.11 Parameter estimates and their standard errors (in parentheses), standard deviations of random effects, and goodness-of-fit statistics for time-based mixed-effects models	58
Table 2.12 Derived coefficients (fixed + random effects) of time-based mixed effect models by clone and site class	59
Table 2.13 Parameter estimates and their standard errors (in parentheses), standard deviations of random effects, and goodness-of-fit statistics for state-space mixed-effects models	60
Table 2.14 Derived coefficients (fixed + random effects) of state-space mixed effect models by clone and site classes	61
Table 2.15 Goodness-of-fit statistics and two-one-sided t-test (TOST) equivalence tests for time-based and state-space approach for each stand attributes and their observed increments.....	62

Table 3.1 Parameter estimates and their associated standard errors (in parentheses), random effects standard deviations and goodness-of-fit statistics for arithmetic mean diameter prediction model.....	105
Table 3.2 Parameter estimates and their associated standard errors (in parentheses), random effects standard deviations and goodness-of-fit statistics for 25 th diameter percentile prediction model.....	106
Table 3.3 Parameter estimates and their associated standard errors (in parentheses), random effects standard deviations and goodness-of-fit statistics for 99 th diameter percentile prediction model.....	107
Table 3.4 Coefficient estimates (fixed + random effects) of nonlinear mixed effect model by clone and site classes for arithmetic mean diameter prediction model.	108
Table 3.5 Coefficient estimates (fixed + random effects) of nonlinear mixed effect model by clone and site classes for 25 th diameter percentile prediction model.....	109
Table 3.6 Coefficient estimates (fixed + random effects) of nonlinear mixed effect model by clone and site classes for 99 th diameter percentile prediction model.....	110
Table 3.7 Average of the parameter estimates of the Weibull distribution using fit data and three prediction methods.	111
Table 3.8 Means and standard deviations of the goodness-of-fit statistics produced by three diameter distribution prediction methods.....	112

List of Figures

Figure 2.1 Location of the study area in the Sector Teso East, central region of Sumatera	63
Figure 2.2 Comparison between time-based, state-space and observation for each stand attributes. The dotted line represents the 1:1 line, while the red line is the observed trend using a smoothing line.....	64
Figure 2.3 Comparison between time-based, state-space and observation for each stand attributes increment. The dotted line represents the 1:1 line, while the red line is the observed trend using a smoothing line	65
Figure 2.4 Significance and equivalence test between time-based, state-space and observation for each stand attribute and their increment	66
Figure 2.5 Bakuzis matrix of time-based stand growth model across different level of site class (initial density 1667 trees·ha ⁻¹) for clone A.	67
Figure 2.6 Bakuzis matrix of time-based stand growth models across different level of site class (initial density 1667 trees·ha ⁻¹) for clone B.	68
Figure 2.7 Bakuzis matrix of state-space stand growth model across different level of site class (initial density 1667 trees·ha ⁻¹) for clone A.	69
Figure 2.8 Bakuzis matrix of state-space stand growth model across different level of site class (initial density 1667 trees·ha ⁻¹) for clone B.....	70
Figure 2.9 Bakuzis matrix of time-based stand growth model across different level of initial density (site class 26) for clone A.	71
Figure 2.10 Bakuzis matrix of time-based stand growth model across different level of initial density (site class 26) for clone B.....	72

Figure 2.11 Bakuzis matrix of state-space stand growth model across different level of initial density (site class 26) for clone A.	73
Figure 2.12 Bakuzis matrix of state-space stand growth model across different level of initial density (site class 26) for clone B.....	74
Figure 2.13 Behavior of observed and predicted stand attributes trend over age with initial density 1667 trees·ha ⁻¹ and site class 26 using either a time-based (TB) or state-space (SS) approach.....	75
Figure 3.1 Boxplots of Weibull scale (a) and shape (b) parameter by clone, age and site class estimated from full sample of the trees in the plot using maximum likelihood estimation method.....	113
Figure 3.2 Parameter estimation comparison between MLE's and three parameter recovery estimation methods for scale (a; above) and shape (b; below). The dotted line represents the 1:1 line, while the red line is the observed trend using a smoothing line.	114
Figure 3.3 Model evaluation for the four example plots that represent (a) clone A, 30 months; (b) clone A, 42 months; (c) clone B, 30 months and (d) clone B, 42 months. The histogram represents the observed diameter distribution, and three curves represent diameter distribution models prediction.	115
Figure 3.4 Simulated development of diameter distribution over ages using MOM method. Simulations are based on prediction stand-level variables (SD, BA, HT, RD and DQ) using site class = 26 and initial stand density 1667 trees ha ⁻¹ . AGE indicated stand age in months.....	116

Figure 4.1 Stand dynamic model simulations of *Eucalyptus hybrid* for clone A. (a) Stand volume over time by site class (initial density 1667 trees·ha⁻¹); (b) Diameter distribution by site class for stand age 48, 96 and 144 months (initial density 1667 trees·ha⁻¹); (c) Stand volume over time by initial density (site class 26); (d) Diameter distribution by initial density for stand age 48, 96 and 144 months (site class 26)..... 130

Figure 4.2 Stand dynamic model simulations of *Eucalyptus hybrid* for clone B. (a) Stand volume over time by site class (initial density 1667 trees·ha⁻¹); (b) Diameter distribution by site class for stand age 48, 96 and 144 months (initial density 1667 trees·ha⁻¹); (c) Stand volume over time by initial density (site class 26); (d) Diameter distribution by initial density for stand age 48, 96 and 144 months (site class 26)..... 131

List of Symbols, Nomenclatures or Abbreviations

A	Stand age (months)
APRIL	Asia Pacific Resources International Holdings Limited
BA	Basal area (m^2ha^{-1})
CDF	Cumulative distribution function
CDFR	Cumulative distribution function regression
\bar{D}	Arithmetic mean diameter (cm)
DBH	Individual tree stem diameter at breast height (1.3 meter)
DQ	Quadratic mean diameter (cm)
EI	Error index
HT	Top height (meter)
HYB	Hybrid method
KS	Kolmogorov-Smirnov statistic
MAI	Mean annual increment ($\text{m}^3\text{ha}^{-1}\text{year}^{-1}$)
MLE	Maximum likelihood estimation
MOM	Moment method
OLS	Ordinary least square
PCT	Percentile method
PDF	Probability density function
PPM	Parameter prediction method
PRM	Parameter recovery method
RD	Relative density
rMSE	Root mean square error
SD	Stand density ($\text{trees}\cdot\text{ha}^{-1}$)
SS	State-space approach
TB	Time-based approach
TOST	Two one-sided t-test
VOL	Stand volume (m^3ha^{-1})

Chapter 1: General Introduction

1.1 Pulp and paper industry in Indonesia

The pulp and paper industry is one of the important industries in the national economy of Indonesia (Widyantoro et al. 2006; Mardiana 2012). Pulp and paper commodities have a very strong industrial structure compared to other industries and do not experiencing dependence on imports of raw materials (LPBI Unair 2018). Even raw materials within acacia and eucalyptus forms are available in large quantities for large periods of time (LPBI Unair 2018).

There are six pulp mills operating in Indonesia, all in Sumatera. Five of them produce Kraft pulp, mostly from acacia wood, and a small mill based in North Sumatra produces dissolving pulp from eucalyptus wood (Nambiar et al. 2018). In 2019, Indonesia's pulp production capacity was 11 million tons per year and paper production was 16 million tons per year from 84 companies (Adi 2019). Since 1996, Asia Pulp & Paper Company Ltd. (APP) and Asia Pacific Resources International Holdings Ltd. (APRIL) have emerged as leading players in the pulp and paper sector not only in Indonesia but also in China (Pirard and Cossater 2006). APRIL's pulp and paper mill is located in Pangkalan Kerinci in Riau Province Indonesia, and can produce up to 2.8 million tons of pulp and 1.15 million tons of paper per year (APRIL 2019). This company group manages around one million hectares of land and 448,639 hectares is used for plantations (APRIL 2019).

The social and economic impacts of the pulp and paper sector in Indonesia are important (Nambiar et al. 2018) with main export destination countries including China, Japan, Korea and the United States (Ahmad 2018; Ramdhini 2019). During 2019, this industry contributes 2.4% of Indonesia's export value (US\$ 4.2 billion) annually

(Workman 2020). On the labor side, the pulp and paper industry employs 260,000 direct workers and 1.1 million indirect workers (Setyawati 2017).

The net impacts of the sector on the economy, tax revenue, employment (with high job multiplier effects), and household income are substantial and critical in some regions such as Riau Province in Sumatera (ITS 2011). One company in this region, APRIL employed 71,000 employees in 2018 and contributed Rp 368.51 trillion (US\$ 26.3 billion) to national gross domestic revenues from 1999 to 2018. Of this sum, 93.68 percent - Rp 345.68 trillion (US\$ 24.6 billion) contributed to the GDP of Riau province (LPEM UI 2019). Because the pulp, paper, and timber plantation sectors are seen as the cornerstone of the future of Indonesia's forestry sector, timber plantations and pulp mill investments continue to receive priority consideration by the Indonesian government (Obidzinski and Dermawan 2012).

1.2 Indonesia's eucalyptus plantation

The expansion of the pulp and paper industry in Indonesia started in the late 1970s. Until the 1990s, wood supply for the pulp mills was highly dependent on harvests from native forests (Nambiar et al. 2018). Because of the decline in global wood production from natural forests since the late 1980s (Warman 2014), plantation forests have become increasingly important for the global supply of timber (Jürgensen et al. 2014). Some companies in Indonesia expanded plantation forests with some species (eg. tropical eucalyptus, *Falcataria moluccana*, *Gmelina arborea* and *Acacia mangium*) in Sumatera and Kalimantan based on trial evaluations. *Acacia mangium* plantations began in the mid-1990s enabling a gradual shift of pulpwood supply to plantations and

expanded from the late 1990s by planting *Acacia crassicarpa* on peatlands (Nambiar et al. 2018).

Over 20 years, *Acacia mangium* in mineral soil and *Acacia crassicarpa* in peatland have been the mainstay of the plantation sector in Indonesia (Inail et al. 2019). Currently, *Acacia spp* is still the largest log producer with 32.69 million m³ in 2019 or 56.43% of total log production (BPS 2020). However, since the mid-2000s, *Acacia mangium* has been subject to substantial threats from two fungal diseases. Ganoderma root rot (Francis et al. 2014; Mohammed et al. 2014) and *Ceratocystis spp* (Tarigan et al. 2011), have become epidemic and caused *Acacia mangium* plantations to become unviable in Sumatera (Harwood and Nambiar 2014). Plantation species have rapidly changed from *Acacia mangium* to *Eucalyptus pellita* and related interspecific hybrids because this serious and unanticipated problem threatened wood production on mineral soils without effective control measures (Nambiar et al. 2018).

The main interest in eucalyptus wood for pulp and paper products comes from its low production cost in certain regions, especially because of high volume production and high pulping yield (Magaton et al. 2009). Eucalyptus pulp fibers produced from clonal plantations have emerged as the most desirable fibers in the market, not only the production of tissue, printing and writing papers but also for the manufacture of “new products” (Magaton et al. 2009). In Indonesia, eucalyptus is a type of fast-growing species that can be harvested at the age of seven and the rapid growth of this species is an opportunity to increase carbon uptake more quickly (Muhdi et al. 2019). In Sumatera, the optimum cutting or rotation age is obtained at six years old with an average mean annual increment of 27.54 m³ ha⁻¹ year⁻¹ and total volume of 165.24 m³ ha⁻¹, so the harvesting

time at six years after planting is the desired silvicultural option (Aswandi 2011). In 2018, eucalyptus log production in Indonesia was 9.01 million m³ and 84% of this (6.83 million m³) came from Sumatera (BPS 2020).

1.3 Growth and yield modeling

Forests are long-lived dynamic biological systems that are continuously changing, and it is often necessary to project these changes in order to obtain relevant information for sound decision making (Peng, 2000). The basic management entity in the forest is generally the stand, which can be defined as “*a contiguous group of trees sufficiently uniform in age-class distribution, composition, and structure, and growing on a site of sufficiently uniform quality, to be a distinguishable unit*” (Helms 1998). Quantitative information about trees and stands is required for assessment and management of forests (Burkhart and Tomé, 2012), so reliable growth models are essential for effective long-term planning and decision making (Garcia et al. 2011).

According to Vanclay (1994), growth is defined as the increase in dimensions of one or more individuals in a forest stand over a given period of time (e.g., volume growth in m³ ha⁻¹ year⁻¹) and yield refers to their final dimensions at the end of a certain period (e.g., volume in m³ ha⁻¹). Growth and yield models play an important role in forest mensuration, provide a mechanism for projecting inventory data and provide inventory updates for the time between inventories (Kershaw et al. 2016). Using suitable inventory and other resource data, growth models provide a reliable way to determine the sustainable timber yield, to examine silvicultural and harvesting options, and to examine the impacts of forest management and harvesting on other values of the forest (Vanclay

1994). Regardless the of amount of stand detail provided and the structural complexity, all growth and yield models have a common purpose: to produce estimates of stand characteristics at specified points in time (Burkhart and Tomé 2012).

Burkhart and Tomé (2012) categorized forest modeling approaches into whole-stand models, size class models, and individual tree models. The whole-stand approach commonly estimates volume, basal area, and/or the number of trees per unit area by using age, site index, site quality, and stand density as predictor variables (Burkhart & Tomé 2012). Whole-stand models are not difficult to develop and apply and are often accurate with single species, even-aged stand structures (Weiskittel et al. 2011). Some examples of this approach are yield tables, compatible growth and yield equations, and state-space models (Weiskittel et al. 2011).

The size class model approach is a compromise between whole stand models and single-tree models (Vanclay 1994). Diameter distribution models are a type of size class models that employ a probability density function to represent the number of trees across different diameters at breast height (DBH) classes (Burkhart & Tomé 2012). Diameter structure is an important stand characteristic from which we can evaluate the stability, growth, volume production, structure of assortment, and maturity (Gorgoso and Rojo 2014).

The three-parameter Weibull distribution function is the most widely used distribution function for plantations because of its flexibility, simplicity, and reliability (Bailey and Dell 1973; Whyte 1992). Hyink and Moser (1983) introduced a generalized framework for developing diameter distribution models. In these models, the future parameters of the distribution model are obtained based on the prediction of future stand-

level parameters and then used to predict the number of individual trees across various DBH classes (Kershaw et al. 2016).

A more detailed approach is the single-tree growth models that use the individual tree as the basic unit of forecasting (Vanclay 1994). Individual-tree models can be distance-dependent or distance-independent depending upon whether tree location is used in the modeling and prediction processes (Munro 1974). Distance-dependent individual-tree model requires not only measurements of tree size, but also the measurement of tree location (Daniels and Burkhart 1975; Tennent 1982). Distance independent individual tree models require no spatial information of neighbors (Clutter and Allison 1974; Clutter and Jones 1980). Because spatial locations of trees are costly to measure in the field, distance-independent models are more common than distance-dependent models (Weiskittel et al. 2011).

Combining stand-level models with size-class or individual-tree models is an effective approach for taking full benefit of their strengths and often improving the accuracy of predictions (Weiskittel et al. 2011). The most common examples of this are whole-stand models used to project area-based forest parameters over time and used to estimate or recover distribution parameters to obtain size class distributions (Weiskittel et al. 2011).

1.4 Objectives

The primary objective of this thesis is to develop a system that provides stand-level growth and yield projections for tropical *Eucalyptus hybrid* clones in short-rotation

plantations in Sumatera, Indonesia. The main research objectives to guide the analysis include:

- 1) Development of a stand-level growth and yield models (top height, basal area, and stand density) for two *Eucalyptus hybrid* clones using time-based and state-space approaches and compare performances.
- 2) Evaluate three parameter recovery methods (moment-based, percentile-based and hybrid) to estimate parameters of the Weibull PDF to estimate future DBH distributions in *Eucalyptus hybrid* plantations.

By using two approaches to develop stand growth model and three methods to estimate the DBH distributions, I hope to be able to compare which approaches and methods perform well for short-rotation *Eucalyptus hybrid* plantations where growth trends of this species are different from the species associated with the most well-developed models in North America. In addition to comparing the different approaches, my approach explores incorporating clone and site index as random effects in a nonlinear mixed effects modeling framework. The overall goal is the development of a model package that will be used by the APRIL Group to improve yield forecasts in their forest management systems and enable better sustainable forest management decision making.

1.5 Thesis layout

This thesis is structured around four chapters. Chapter 1: General introduction, provides an overview of the pulp and paper industry in Indonesia and sets the overall objectives of the thesis research. Chapter 2: *Comparison of time-based versus state-space stand growth models for tropical hybrid Eucalyptus clonal plantations in Sumatera,*

Indonesia develops the two whole-stand growth and yield yields (time-based and state-space) and compares their performance in *Eucalyptus hybrid* plantations in Sumatra, Indonesia. This Chapter has been submitted to the Canadian Journal of Forest Research, and is under revision, as part of a special issue (Advances in forest mensuration and biometrics) associated with the 2020 Western Forest Mensurationists Meeting (Virtual). Authorship is: Joni Waldy, John Kershaw, Aaron Weiskittel, and Mark Ducey. Chapter 3: *Diameter distribution model development of tropical hybrid Eucalyptus clonal plantations in Sumatera, Indonesia: A comparison of estimation methods* compares three different methods to recover Weibull distribution parameters using predictions from the whole stand model. This chapter will be submitted for publication in either the New Zealand Journal of Forest Research or the Australian Journal of Forest Research. Authorship will be the same as Chapter 2. Chapter 4: *Conclusions*, summarizes the results of this thesis, demonstrates some model applications and explores future developments to extend and integrate the models developed here into the forest management systems used by the APRIL group.

1.6 References

- Adi, Tri. 2019. Industri pulp dan kertas Indonesia. [accessed 2020 July 28].
<https://analisis.kontan.co.id/news/industri-pulp-dan-kertas-indonesia>
- Ahmad, T., Daryanto, A., Oktaviani, R., & Priyarsono, D. 2018. Global value chain of Indonesian pulp and paper industry. *Jurnal Manajemen & Agribisnis*, 15(2), 118.
<https://doi.org/10.17358/jma.15.2.118>
- APRIL. 2019. Sustainability Report 2019: Beyond Commitments, Asia Pacific Resources International Holdings Ltd, Jakarta, 88 p.
- Aswandi. 2011. Growth and yield model of *Eucalyptus grandis* Hill Ex Maiden di Aek Nauli Simalungun Sumatera Utara. *Widyariset*, 14 (2):313-322.
- Badan Pusat Statistik. 2020. Statistis of Forestry Production 2019. Jakarta: Badan Pusat Statistik
- Bailey, R.L., & Dell, T.R. 1973. Quantifying diameter distributions with the Weibull function. *Forest Sciences*, 19, 97–104.
- Burkhardt, H.E., & Tomé, M. 2012. Modeling forest trees and stands. Dordrecht. New York: Springer.
- Clutter, J.L, and Allison, B.J. 1974. A growth and yield model for *Pinus radiata* in New Zealand, In: Fries, J. (editor) Growth Models for Tree and Stand Simulation, Proceedings of IUFRO Working Party S4.01-4 meetings, Dep. For. Yield Res., Royal Coll. FOL, Stockholm, p.136-160
- Clutter, J.L. and Jones, E.P. 1980. Prediction of growth after thinning in old-field slash pine plantations, USDA Forest Service, Research Paper, SE-217

- Daniels, R.F., and Burkhart, H.E. 1975. Simulation of individual tree growth and stand development in managed loblolly pine plantations, Div. of For. and Wildlife Res., Virginia Polytechnic Institute and State University, FWS-5-75
- Nambiar, E.K.S., Harwood, C.E., & Mendham, D.S. 2018. Paths to sustainable wood supply to the pulp and paper industry in Indonesia after diseases have forced a change of species from acacia to eucalypts, *Australian Forestry*, 81:3, 148-161, DOI:10.1080/00049158.2018.1482798
- Francis, A., Beadle, C., Puspitasari, D., Irianto, R., Agustini, L., Rimbawanto, A., Gafur, A., Hardiyanto, E., Hidyati, N., Tjahjono, B. 2014. Disease progression in plantations of *Acacia mangium* affected by red root rot (*Ganoderma philippii*). *Forest Pathology*. 44:447–459
- García, O., Burkhart, H.E., Amateis, R.L. 2011. A biologically consistent stand growth model for loblolly pine in the piedmont physiographic region, USA. *Forest Ecology and Management* 262 (11): 2035–2041
- Gorgoso-Varela, J. J., and Rojo-Alboreca, A. 2014. Short communication: A comparison of estimation methods for fitting Weibull and Johnson's SB functions to pedunculate oak (*Quercus robur*) and birch (*Betula pubescens*) stands in northwest Spain. *Forest Systems*, 23(3), 500– 505. doi:10.5424/fs/2014233-04939
- Harwood, C.E., Nambiar, E.K.S. 2014. Sustainable plantation forestry in South-East Asia. Canberra: ACIAR. ACIAR Technical Report No. 84.
- Helms, J.A. (ed). 1998. The dictionary of forestry. Society of American Foresters, Bethesda

- Hyink, D.M. and Moser, J.W. 1983. A generalized framework for projecting forest yield and stand structure using diameter distributions. *For. Sci.* 29: 85-95
- Inail, M., Hardiyanto, E. & Mendham, D.S. 2019. Growth Responses of *Eucalyptus pellita* F. Muell Plantations in South Sumatra to Macronutrient Fertilisers Following Several Rotations of *Acacia mangium* Wild. *Forests.* 10. 1054. 10.3390/f10121054.
- ITS. 2011. The economic contribution of Indonesia's forest-based industries. Melbourne: ITS Global
- Jürgensen, C., Kollert, W., Lebedys, A. 2014. Assessment of Industrial Roundwood Production from Planted Forests. Food and Agriculture Organization of the United Nations, Rome
- Kershaw, J.A. Jr, Ducey, M.J., Beers, T.W., Husch, B. 2016. Forest Mensuration, 5th edn. Wiley/Blackwell, Hoboken, NJ
- LPEM FEB UI. 2019. Economic and Fiscal Contribution of APRIL Group (update 2015-2018). Lembaga Penyelidikan Ekonomi dan Masyarakat, Fakultas Ekonomi dan Bisnis. Universitas Indonesia
- Magaton, A.D.S., Colodette, J.L., Gouvea, A.D.F.G., Gomide, J.L., Muguet, M.C.S., Pedrazzi, C. 2009. Eucalyptus wood quality and its impact on kraft pulp production and use. *Tappi J* 8(8):32–39
- Mardiana. 2012. The impact of pulp and paper industry to local financial government in Riau Province (Case on PT. RAPP). *Journal of Economic and Business View* 3(2).

- Muhdi, Sahar, A., Hanafiah, D.S., Zaitunah, A., Nababan, F.W.B. 2019. Analysis of biomass and carbon potential on eucalyptus stand in industrial plantation forest, North Sumatra, Indonesia. IOP Conf. Ser.: Earth Environ. Sci. 374 012054
- Munro, D.D. 1974. Forest growth models-a prognosis. In J. Fries (Ed.), Growth models for tree and stand simulation. Stockholm, Sweden: Royal College of Forestry
- Obidzinski, K., and Dermawan, A. 2012. New round of pulp and paper expansion in Indonesia: What do we know and what do we need to know? Center for International Forestry Research, Bogor: Indonesia
- Peng, C. 2000. Growth and yield models for uneven-aged stands: Past, present and future. Forest Ecology and Management. 132. 259-279. 10.1016/S0378-1127(99)00229-7
- Pirard, R., & Cossalter, C. 2006. The revival of industrial forest plantations in Indonesia's Kalimantan provinces, will they help eliminate fiber shortfalls at Sumatran pulp mills or feed the China market? Center for International Forestry Research, Bogor: Indonesia
- Ramdhini, L. 2019. Ekspor pulp dan kertas ditarget tembus US\$9 miliar tahun ini. [accessed 2020 July 30]. <https://www.alinea.id/bisnis/ekspor-pulp-dan-kertas-ditarget-tembus-us-9-miliar-tahun-ini>.
- Setyawati. 2017. Indonesia-Investments. [accessed 2020 July 28]. <https://www.indonesia-investments.com/news/todays-headlines/pulp-andpaper-industry-indonesia-challenges-and-opportunities/item7738>.
- Tarigan, M., Roux, J., van Week, M., Tjahjono, B., Wingfield, M.J. 2011. A new wilt and die-back disease of *Acacia mangium* associated with *Ceratocystis manginecans* and *Ceratocystis acaciivora* sp. nov. in Indonesia. S. Afr. J. Bot., 77, 292–304.

- Tennent, R.B. 1982. Individual-tree growth model for *Pinus radiata*, New Zealand
Journal of Forestry Science, 12(1): 62-70
- Vanclay, J.K. 1994. Modelling forest growth and yield: applications to mixed tropical
forests.
- Warman, R.D. 2014. Global wood production from natural forests has peaked. Biodivers.
Conserv. 23, 1063–1078, <http://dx.doi.org/10.1007/s10531-014-0633-6>.
- Whyte, A.G.D., and Woollons, R.C.1992. Diameter distribution growth and yield
modelling: recent reviews and perspectives, In: Wood, G.B. and Turner, B.
(editors) Proceedings of IUFRO S4.01 & S4.02 Conference on "Integrating forest
information over space and time", Canberra
- Widyantoro, B., Siregar, H., Sanim, B., Priyarsono, D.S. 2006. Ekonomi industri pulp
dan kertas Indonesia: analisis simulasi kebijakan dan tekanan internasional. Jurnal
Manajemen & Agribisnis 3(2): 103–111.
- Workman, Daniel. 2020. Paper Exports by Country. World's Top Exports. 2 June 2020.
<http://www.worldstopexports.com/paper-exports-by-country/>

Chapter 2: Comparison of time-based versus state-space stand growth models for tropical hybrid Eucalyptus clonal plantations in Sumatera, Indonesia

2.1 Introduction

Industrial forest plantation company commonly involves the establishment of pure, even-aged stands. Due to the large investments required for intensive management for timber production, highly accurate models of tree attributes and stand development are required to estimate tree and stand characteristics (Burkhart and Tomé 2012). There are two general approaches to estimate current or future forest yield of a timber stand: appropriate growth and yield system and conduct a timber cruise using standard forest inventory procedures (Clutter et al. 1983). Forest inventory can be considerably more expensive, especially if precise stand-level results are required (Clutter et al 1983). Therefore, it is not surprising that numerous approaches growth and yield models have been proposed with the variety of stand conditions, diverse objectives, and needs of users (Burkhart et al. 2019).

The company that focuses on the production of a single product by consuming all merchantable wood volume, a stand-level growth, and yield system is already capable of providing enough information to maximize forest profitability (Burkhart and Tomé 2012). Stand models are often simple and robust (Vanclay 1994), often highly accurate in single species, even-aged stands (Weiskittel et al. 2011) and tend to produce accurate estimates of long-term growth (Qin and Cao 2006). Many stand-growth models have been developed around the world for different species and forest stand types (Clutter et al. 1983). Burkhart and Tomé (2012) and Weiskittel et al. (2011) compiled a broad review of forest growth and yield models and several studies about this topic have been completed in the past (Bonet et al. 2012; Burkhart 1971; Clutter 1963; Pienaar 1979; Pienaar and Turnbull 1973; Schumacher 1939; Sullivan and Clutter 1972).

Growth data come in many different sources such as individual stem analysis, temporary plots, and permanent plots (Weiskittel et al. 2011). Differences between successive independent inventories also can be used to estimate net increase at the stand-level (Kershaw et al. 2016). However, these estimates have a high degree of variation since they contain sampling errors from both inventories as well as variation in growth (Kershaw et al. 2016). According to Winner and Stott (1954), permanent sample plots are the most effective approach for estimating growth and yield where the individual trees are permanently identified and measured over time.

Eucalyptus is becoming the most important fiber source for papermaking worldwide (Magaton et al. 2009). This species has desirable wood properties including short fibers and high wood densities, the best for pulp and paper production, charcoal, fuel, and sawn timber (Rockwood et al. 2008). Unfortunately, the estimation of yield and growth model for *Eucalyptus* has not been adequately investigated (Latifah et al. 2011) and only a few publications related to *Eucalyptus* growth models in Indonesia exist, particularly when compared to numerous publications in other regions such as South America and Australia. Some well-developed models include growth and yield of *Eucalyptus sp* in the tropical region of Brazil (Filho et al. 2015), linking individual-tree and stand-level growth models in clonal *Eucalyptus* plantations in Brazil (Scolforo et al. 2019) and a regionalized growth model for *Eucalyptus globulus* plantations in southeastern Australia (Wang and Baker 2007) among them. Until recently, the prediction of growth and yield for the main eucalyptus forests of Indonesia was based on experience from several forestry companies, and they chose not to publish their work. The lack of readily available growth and yield information in Indonesia is the result of both a

relatively short history of the species and because plantations are owned and managed by numerous private companies that are not permitted to share data for model development. Current long-term management plans in some plantation forests in Indonesia use assumptions of the mean annual increment (MAI) to calculate future yield. Typically, these are derived from research by just a few companies and are then widely applied to other companies (Isnaini 2018).

In Indonesia, some studies regarding *Eucalyptus* growth has been reported by some researchers. Aswandi (2011) used 15 permanent sample plots to develop yield prediction for *Eucalyptus grandis* at Aek Nauli, North Sumatera. He reported that the optimum rotation age is obtained at six years old after planted with MAI $27.54 \text{ m}^3\text{ha}^{-1} \text{ year}^{-1}$ or final yield $165.24 \text{ m}^3\text{ha}^{-1}$. Latifah et al. (2014) also developed a prediction model based on 650 plots for five species of *Eucalyptus* plantations in North Sumatera, Indonesia but only focused on yield prediction. They found that each *Eucalyptus* species required a specific model to properly predict growth and yield. Isnaini (2018) also developed a stand growth model for *Eucalyptus pelita* based on 359 permanent sample plots and concluded that a von Bertalanffy-Richards polymorphic model was the best equation for mean top height projections with standard error 2 meter, while the two-parameter Schumacher polymorphic models were the best equation for the basal area and mortality projection with standard error $2.5 \text{ m}^2\text{ha}^{-1}$ and $134 \text{ trees}\cdot\text{ha}^{-1}$, respectively. To our knowledge, these are the only some publicity available stand growth models for *Eucalyptus* in Indonesia. However, the growth and yield model for the *Eucalyptus hybrid* clonal has not been adequately researched.

Typical whole-stand models predict stand volume or biomass as a function of age, site index, and density. Such time-based models might also include height (mean height or top height), stand density (numbers of trees per ha), and basal area predictions as a function of age. Common examples are the traditional normal or empirical yield tables (Johnstone 1977; Kabzems 1971; MacLeod and Blyth 1955; Plonski 1956). Time-based models often are developed for plantations for which there is a single species and a limited number of densities or treatment regimes. Their primary advantages are robustness, ease of application, and simplicity, while some drawbacks can include inconsistency in predictions, high dependency on age, and potential lack of path-invariance (Weiskittel et al. 2011).

State-space models represent another approach for modeling the growth and yield (García 1984, 1994). These models describe the state of the stand at a point in time and predict the rate of change in the state using first-order differential equations (García 2005). Basal area, stand density, and top height are considered the “state” variables for the stand. These state variables must adequately describe stand structure as well as summarize the historical events affecting future stand development (García 2005). Some applications of the state space approach to growth modeling for even-aged stands include: radiata pine (*Pinus radiata*) in New Zealand (García 1984); *Eucalyptus* coppice stands in Spain (García and Ruiz 2003); European beech (*Fagus sylvatica*) in Denmark (Nord-Larsen and Johannsen 2007); interior spruce (*Picea spp.*) in British Columbia, Canada (García 2011); loblolly pine (*Pinus taeda*) in the Piedmont region of the United States (García et al. 2011); and teak (*Tectona grandis*) plantations in India (Tewari et al. 2014). The state space approach can produce accurate predictions, is less dependent on age, has

path invariance, and can provide an effective framework for both managed, single-species plantation, and natural, mixed-species stand growth models (Weiskittel et al. 2011).

Using plantation inventory plots, the goal of this study was to develop stand-level growth models for *Eucalyptus hybrid* species in central of Sumatera island. The specific objectives were to: (1) develop the best time-based approach using the available data; (2) determine the optimal state-space formulation based on the findings from the time-based approach; and (3) compare the modeling approaches based on fit statistics, projection performance, and overall behavior.

2.2 Methods

2.2.1 Study site

The study used inventory plot data from Eucalyptus hybrid plantations in Sector Teso East of PT. Riau Andalan Pulp and Paper, a member of Asia Pacific Resources International Holding Limited (APRIL) Group that operates under a Sustainable Forest Management Policy. Teso East is 19,600 ha in size and is located in the central region of Sumatera Island, Riau Province, Indonesia in the Kampar and Kuantan Singingi regencies between 101° 18' E and 101° 32' E, and 00° 09' N and 00° 03' N (Figure. 2.1). The region is characterized by a wet tropical climate with average rainfall ranging from 2000-3000 mm per year, and the average rainy days is around 160 days per year. The annual average temperature is 27.6 °C with an average minimum of 21.8 °C and an average maximum of 35 °C.

Until now, Estate Teso East has had its fifth rotation. The first rotation was planted with *Acacia mangium* in 1995 and *Eucalyptus sp.* was planted on a large scale starting in the period 2010. Based on the soil characteristics, this study location was dominated by soil horizon B (topsoil) and C (parent material). Most of the minerals from parent material with organic materials, good for both plants and other organisms to live. This plantation area is relatively flat with slope 0-15% and low elevation in the range 30 – 90 meters above sea level.

2.2.2 Data collection

APRIL implements plantation inventories periodically as a basis for assessing yield potentials and for predicting wood availability. Inventory plots were established for entire plantation areas as part of the forest management and planning systems. The plot layout used systematic sampling with random starting points. Initial sampling intensity was 1% of total stand area (one plot represents 4 ha area) with minimum of five plots each stand and an additional 2-5% sampling intensity for a pre-harvest inventory (one year before harvest).

Plots were circular with a radius of 11.28m (0.04 ha). First measurements were made at six months after planting and regularly continued at twelve-month intervals until harvesting. At the first measurement, only mortality and height were recorded. On subsequent measurements, diameter at breast height (DBH; nearest 0.1cm) was measured at 1.3 above ground using a diameter tape. At the initial measurement six months, height was measured directly using a height pole. For subsequent measurements, a hypsometer was used for indirect measurement of tree height.

This study only used the most recently established eucalyptus clone stands that were planted from 2013 to 2016 with an initial spacing of 3 x 2m (1667 trees·ha⁻¹) and had at least three consecutive measurements. There are 2808 measurements in this study, where clones A and B accounted for 2,476 and 332 plots, respectively. Table 2.1 summarizes stand attributes and their associated increments by clone. In comparison to clone A, clone B is recently developed by the APRIL Group concession. The maximum age of existing inventory data for clone B is 42 months. Because of its promising growth (Table 2.1), it was important to include this clone in the modeling framework developed here.

2.2.3 Time-based model development

The selection of appropriate growth functions for tree and stand modeling is an important aspect in the development of growth and yield models (Burkhart and Tomé 2012). To develop a stand growth model, site index or site class is generally considered a required auxiliary variable for predicting stand attributes including stand volume. The time-based growth models developed in this study predicted temporal development of three key stand variables: top height (HT), stand density (SD) and basal area (BA).

Stand height often is the key driving variable in even-aged, stand-level growth models. Height growth is considered relatively independent of initial stand density and is not affected much by thinning activities. There are several expressions of stand height including mean height, dominant height, top height, Lorey's height, and so on. In this study, we used top height defined as the mean total height of the 100 tallest trees per ha (Kershaw et al. 2016) or four tallest trees per plot. Several model forms have been

developed over the years for predicting even-aged height growth (Weiskittel et al. 2011; Burkhart and Tomé 2012). Seven commonly applied sigmoidal equation forms were evaluated (Table 2.2).

Stand density (SD) was the second key stand attribute predicted. Due to high variation in mortality over time, SD often is the most difficult process to model (Weiskittel et al. 2011). Mortality is generally considered to have two components: random (non-competitive) mortality and competition-induced mortality (Oliver and Larson 1996). Random mortality is often driven by processes at the individual tree rather than at the stand (Weiskittel et al. 2011; Bugman et al. 2019; Wykoff et al. 1982). The relatively simple stand-level mortality models do not typically capture random component of stand mortality. Most time-based stand-level mortality models use initial density and time, sometimes site index (Pienaar and Shiver 1981; Bailey et al. 1985), and more rarely mean tree size (Coomes et al. 2003; Muller-Landau et al. 2006). In this study we evaluated six different stand density equations frequently found in the literature (Table 2.4).

The third key stand attribute was total basal area (m^2ha^{-1}) and its growth ($\text{m}^2\text{ha}^{-1}\text{month}^{-1}$). Nine commonly used equation forms were evaluated in this study (Table 2.3). All functions tested here were variations of sigmoidal exponential functions derived from the von Bertalanffy equation (Burkhart & Tomé 2012). All equations tested project BA growth based on BA at time 1 (BA_1) and age at time 1 (A_1) and time 2 (A_2).

2.2.4 State-space model development

A dynamic state-space growth model was developed using the same data as used in the time-based model and followed the formulations presented in García (2011) and García et al. (2013). This model assumed that the behavior of any stand of eucalyptus evolving in time can be approximated by describing its current state with four state variables: top height (HT), stand density (SD), basal area (BA), and a measure of site occupancy, while using transition functions to estimate the changes in the state variables. Top height growth and its relationship to clone and site class were represented by the best model of the time-based approach because it still depends on stand age for growth model development. In this paper, we considered site occupancy as relative density (RD) which is defined as the ratio of actual density to the maximum density attainable in a stand with the same mean tree size. The maximum density was calculated based on Reineke's Stand Density Index (SDI). Reineke (1933) defined the maximum SDI relationship as the logarithm of the number of trees per acre against the logarithm of the quadratic mean diameter of maximally stocked stands in a straight-line relationship:

$$\log(SD_{max}) = a + b \log(DQ) \quad (\text{SS-SDI})$$

Using quantile regression, intercept (a) and slope (b) will be obtained based on 90% quantile. This line is used to define the limit of the maximum stocking. In this study, we determined the maximum SDI relationship for all clones because we do not have enough data in older ages for clone B.

The mortality rate $\left(\frac{dSD}{dA}\right)$ was modeled as a function of SD and HT. The stand density transition function expressed the rate of change in SD relative to the rate of change in HT:

$$\frac{dSD}{dHT} = -\alpha_1 HT^{\alpha_2} SD^{\alpha_3} \quad (\text{SS-SD-1})$$

Grouping like terms of this equation and integrating both sides gives the following invariant equation:

$$\frac{dSD}{SD^{\alpha_3}} = -\alpha_1 HT^{\alpha_2} dHT \Rightarrow SD^{1-\alpha_3} - \frac{\alpha_1(\alpha_3-1)}{\alpha_2+1} HT^{\alpha_2+1} = \text{constant} \quad (\text{SS-SD-2})$$

Equating the invariant equation for times 1 and 2 gives the following transition (prediction) equation for SD:

$$SD_2 = \left[SD_1^{1-\alpha_3} + \alpha_1 \frac{\alpha_3-1}{\alpha_2+1} (HT_2^{\alpha_2+1} - HT_1^{\alpha_2+1}) \right]^{1/(1-\alpha_3)} \quad (\text{SS-SD-3})$$

This equation predicts SD_2 at top height HT_2 given any initial value (SD_1, HT_1) in which no thinning occurred. The parameters α_1 , α_2 , and α_3 were estimated by nonlinear least-squares method over all the consecutive pairs measurements.

Basal area was not predicted directly, but the product of $W = BA \cdot HT$ and was modeled as such instead (García 2011). The rate of change of W was expressed as the difference between two components: the gross increment and the mortality. Because this study used pure, even-aged stands, the gross increment can be written as $\omega_1 RD \cdot HT \cdot SD^{\omega_2}$, where RD is a relative density measure that reduces growth in young or recently thinned stands that do not still fully occupy the site. The mortality component was modeled using:

$$-k \frac{W}{SD} \frac{dSD}{dHT} = -kW \frac{d \log SD}{dHT} \quad (\text{SS-W-1})$$

where k represents the mean size of dying trees relative to the mean size of those surviving and was considered as a constant to be estimated (García 2011). Therefore, the general W growth model is:

$$\frac{dW}{dHT} = \omega_1 RD HT SD^{\omega_2} + kW \frac{d \log SD}{dHT} \quad (\text{SS-W-2})$$

A simple closed-form solution of this differential equation can be achieved in the special case where ω_2 is equal to k :

$$\frac{dW}{dHT} = \omega_1 RD HT SD^k + k \frac{W}{SD} \frac{dSD}{dHT} \quad (\text{SS-W-3})$$

The site occupancy factor represents resource interception (e.g., light, nutrients, moisture). In young stands, occupancy is low and gradually increases approaching 1 when canopies close. We assumed that the rate of RD change initially depended on HT in the same way as the gross increment, and decreased to zero as full closure was approached:

$$\frac{dRD}{dHT} = \tau HT (1 - RD) \quad (\text{SS-RD-1})$$

Integration gives invariant equation:

$$(1 - RD) \exp(\tau HT^2/2) = \text{constant} \quad (\text{SS-RD-2})$$

With this occupancy model, integration of equation SS-W-3 gives the transition equation for basal area:

$$BA_2 = SD_2^k \left(BA_1 HT_1 SD_1^{-k} + \omega_1 \left[\frac{(HT_2^2 - HT_1^2)}{2} - (RD_2 - RD_1)/\tau \right] \right) / HT_2 \quad (\text{SS-BA-1})$$

with

$$RD_2 = 1 - \exp[-\tau(HT_2^2 - HT_1^2)/2](1 - RD_1) \quad (\text{SS-RD-3})$$

2.2.5 Other stand attributes

Quadratic mean diameter (DQ) is an important stand-level attribute because it is an indicator of potential wood products (Essed 1957), wildlife habitat, and other factors. Given that BA and SD are modeled in both the age-based and state-space models, DQ was estimated using the identity:

$$DQ = \sqrt{\frac{BA}{.00007854 \times SD}} \quad (\text{DQ-1})$$

Likewise, volumes per hectare were estimated given model variables and an independent output function. Four different total stand volume equations were fitted and evaluated using top height and basal area. These models have been widely used to estimate total stand volume (see, for instance, Kershaw et al. 2016; van Laar and Akça 2007):

$$VOL = v_0 HT^{v_1} BA^{v_2} \quad (\text{V-1})$$

$$VOL = v_0 (HT BA)^{v_1} \quad (\text{V-2})$$

$$VOL = \frac{BA}{(v_0 + v_1 HT^{-1})} \quad (\text{V-3})$$

$$VOL = (v_0 + v_1 HT)^{-1} (HT BA)^{v_2} \quad (\text{V-4})$$

where VOL is total stand volume (m^3ha^{-1}), HT is top height (m), BA is basal area (m^2ha^{-1}), and v_0, v_1, v_2 are estimated parameters.

2.2.6 Model evaluation

The best set of modeling approach was selected based on goodness-of-fit criteria, residual analyses, and prediction of other stand-level attributes such as quadratic mean diameter (DQ; cm) and volume per ha (VOL; m³ ha⁻¹). The best set of equations were then refit using mixed-effects models with clone and site class as random effects due its general flexibility and robustness in prediction (e.g., Kuehne et al. 2020). APRIL developed a site index equation for eucalyptus using the relationship between height and age of dominant and codominant trees. Site class was calculated using this site index equation at reference age of five years on a stand basis based on the latest inventory age. Therefore, all plots within the same stand have the same site class category.

Mixed-effects models have been used as an alternative to OLS for repeated measurements and grouped data and has wide application within forest growth and yield modeling (Lappi 1991; Lynch et al. 2005, 2012; Budhathoki et al. 2008; Temesgen et al. 2014). All model fitting will be carried out using the R statistical language (R Core Team 2020). The consistency of the models and the fitting method used was evaluated by the root mean square error (rMSE), coefficient determination (R²), and mean bias:

$$rMSE = \sqrt{\frac{\sum_{i=1}^n (Y_i - \hat{Y}_i)^2}{n}} \quad (E-1)$$

$$R^2 = 1 - \frac{\sum_{i=1}^n (Y_i - \hat{Y}_i)^2}{\sum_{i=1}^n (Y_i - \bar{Y})^2} \quad (E-2)$$

$$Bias = \frac{\sum_{i=1}^n (Y_i - \hat{Y}_i)}{n} \quad (E-3)$$

Where Y_i is actual value of Y for observation i; \hat{Y}_i is predicted value of Y for observation I; \bar{Y} is the average of observed values, n is the number of observations.

In addition, equivalence tests using two one-sided t-tests (TOST) and graphical analyses with goodness-of-fit statistics were used to determine whether the predictions matched field measurements and to assess the trend between predicted versus observations for both approaches. A modified Bakuzis matrix (Leary 1997) was used to assess the biological reasonableness of both approaches. This matrix utilized some rules or “law-like” relationships such as Sukachev (stands on good sites self-thin faster than poor sites), Reineke (stands self-thin in a linear way when SD and DQ are log-transformed), and yield density effect (VOL as a function of SD) (Weiskittel et al. 2011). We examined model behavior for extrapolations both beyond the range of densities as well as range of ages contained within the data.

2.3 Results

2.3.1 Stand volume model

Four different total stand volume equations were fitted using independent variables of top height and basal area. All parameters were significant, and all models performed well and nearly equally, although the best goodness-of-fit criteria were obtained in equation V-4 which explained 99.36% of the total stand volume variability, had rMSE of $4.19 \text{ m}^3\text{ha}^{-1}$, and relatively small bias -0.40 (Table 2.5). Using this consideration, we chose model V-4 and develop a mixed-effects model using clone and site class within clone as random effects. Based on the likelihood-ratio test, the best random effects model included v_0 and v_1 as a random effect for both clone and site class within clone, even though the addition of random effects accounted for very little additional variability (Table 2.6).

All parameters of model V-4 were significant ($p < .05$) and the full models with fixed and random effects accounted for over 99% of the variability in volume (Table 2.6). Differences between clones were greater than differences across within clone for both v_0 and v_1 (Table 2.7) and accounted for more variation than site class within clone (Table 2.6). The coefficients shown in Table 2.7 were used to estimate stand-level volume in both the time-based and state-space models developed in this study.

2.3.2 Time-based model

2.3.2.1 Model estimation

The estimated parameters and goodness-of-fit statistics for all top height, stand density and basal area models are shown in Table 2.8, Table 2.9 and Table 2.10, respectively. All parameter estimates for top height were significant ($p < .05$). In terms of rMSE, R^2 , and bias, the best performing model for top height was model TB-HT-7 derived from the von Bertalanffy-Richards equation and accounted for more than 90% variation in top height. It minimized bias and standard error of prediction relative to the other models tested (Table 2.8). Based on likelihood ratio tests, the best mixed-effects model for TB-HT-7 included clone and site class within clone random effects for parameters h_0 and h_1 (Table 2.11). The full model with fixed and random effects accounted for 92% of the variation in HT. The estimated coefficients (fixed + random effects) for equation TB-HT-7 are shown in Table 2.12. Clone A consistently had higher asymptotic heights (larger h_0) than clone B (Table 2.12). Differences across site class within clone were greater than differences between clones (Table 2.12) and accounted for more variation (Table 2.11).

For stand density, model TB-SD-6 from Clutter et al. (1983) was the best fit compared to the other five stand density models. The rMSE was 123 trees·ha⁻¹, R² = 0.64, and bias = 1.52 trees·ha⁻¹ (Table 2.9). For this model, only parameter s_1 had significant random effects associated with clone and site class with clone (Table 2.11). The full model with fixed and random effects only accounted for very little additional variation relative to the fixed effects alone (Table 2.11). The estimated coefficients (fixed + random effects) for equations TB-SD-6 are shown in Table 2.12. Differences between clones were greater than differences across site class within clone (Table 2.12). Clone A had lower survival rates (larger s_1) than clone B (Table 2.12), while site class had very little effect, especially for clone B (Table 2.12).

All estimated parameters of the nine stand basal area models were significant ($p < .05$) and explained 70-80% variability (Table 2.10). Model TB-BA-4, a form of the Schumacher polymorphic equation, was the best fit with maximum R² and minimum rMSE and bias. For this model, only parameter b_0 had significant ($p < .05$) random effects associated with clone and site class within clone (Table 2). The full model with fixed and random effects accounted for 81% in BA variation. Differences across site class within clone was greater than differences between clones (Table 2.12) and accounted for more variation (Table 2.11).

2.3.2.2 Model performance

Figure 2.2 shows predictions versus field observations for basal area, stand density and the two derived attributes (stand volume and quadratic mean diameter) for the time-based model. The time-based model was able to predict stand attributes quite

well. Goodness fit of statistics for the linear regressions between predictions and field observations show the time-based model system was very reliable for predicting VOL and DQ (Table 2.15). Based on the R^2 for these regressions, the time-based model explained 86% in VOL variation and 85% in DQ variation. On-the-other-hand, Figure 2.3 shows similar plots for the associated stand attribute increments. The time-based model only explained 37%, 8%, 29% and 53% of the variation in increments for BA, SD, VOL and DQ, respectively (Table 2.15).

The Bakuzis matrices for clone A (Figure 2.5) and clone B (Figure 2.6) show that the predictions from the time-based model adhered to all of the widely held stand development theories. In particular, Reineke's Self-Thinning Rule and Eichorn's Rule, both based on derived variables, were very closely held for clone A (Figure 2.5). However, for clone B, Eichorn's Rule was not followed (Figure 2.6) with volumes differentiating by site class at the upper HT values. This reflects the differences in mortality rates between clone A and clone B.

2.3.3 State-space model

2.3.3.1 Model estimation

Because top height increment was dependent on stand age, we used TB-HT-7 with mixed-effects (Tables 2.11 & 2.12) as the transition function in the state-space model. The maximum SD relationship (SS-SDI) based on 90% quantile had intercept (a) = 11.5103 (0.5261) and slope (b) = 1.5967 (0.2008). SD_{max} and RD were calculated utilizing this relationship. Table 2.13 presents the nonlinear mixed-effects regression summaries for the other three state-space model equations: relative density (SS-RD-1),

stand density (SS-SD-1) and basal area (SS-W-3). Based on likelihood ratio tests, the only significant ($p < .05$) random effects for RD were associated with the parameter τ in SS-RD-1, parameter α_2 in SS-SD-1 and parameter ω_1 in SS-W-3. The inclusion of additional clone and site class variables to state-space equation system improved the distributions of the residuals, reduced the bias, and increased the predictive power of the models (Table 2.13). The full models with fixed and random effect accounted 72%, 64%, and 73% of variation for SS-RD-1, SS-SD-1, and SS-W-3 models, respectively.

For SS-RD-1, differences in random effects for site class within clone were greater than differences between clones (Table 2.14), although the effects were very small. Site class had a positive trend for parameter τ in clone A, but not for clone B (Table 2.14). For clone B, site class 24 has a higher value than both site class 26 and 28 (Table 2.14). For SS-SD-1, clone was the largest random effect for stand density (Table 2.13). Clone A had relatively higher α_2 values than clone B, except for site class 26 (Table 2.14). For SS-W-3, differences between site classes with clone were greater than differences between clones (Table 2.13) and accounted for more variation, especially for clone A. Table 2.14 shows the estimated coefficients (fixed + random effects) of RD, SD and BA for state-space model.

2.3.3.2 Model performance

The state-space modeling system was relatively good at predicting stand attributes (Figure 2.2), but not for increments (Figure 2.3). The model predictions for BA, VOL and DQ increments are overestimated for larger values and underestimated for smaller values (Figure 2.3). Goodness of fit statistics between predicted and observed stand attribute

values were acceptable for VOL and DQ (Table 2.15). The state-space model explained 82% in VOL variation and 77% in DQ variation, while for stand attribute increments only explain 22%, 9%, 6% and 41% for BA, SD, VOL and DQ increments, respectively (Table 2.15).

The Bakuzis matrices across different levels of site class for the state-space model are shown in Figure 2.7 (clone A) and Figure 2.8 (clone B). As with the time-based model (Figures 2.5 and 2.6) all major stand development theories were closely adhered to. Reineke's Self-Thinning Rule and Eichorn's Rule, both based on derived variables, were very closely held for both clones (Figure 2.7 and 2.8). This behavior is different in clone B, where, as in the time-based model, the lower mortality resulted in volume-HT trends that did not follow Eichorn's Rule exactly (Figure 2.8).

2.3.4 Model comparison

Overall, plots of predicted versus observed variables for each stand attribute (Figure 2.2) and their associated increments (Figure 2.3) were better for the time-based model compared to the state-space model, even though age is the primary independent variable. Most estimates of stand attributes from the two approaches are similar (Figure 2.2) and slightly different for their increment (Figure 2.3). For the increments, state-space estimates have more variability than the time-based estimates, except for SD increment. In terms of goodness-of-fit, the time-based approach has lower rMSE and higher R^2 for BA, DQ, VOL and its increment (Table 2.15). The time-based model gives a slightly better overall performance over time than the state-space with 13% in rMSE improvement for BA, 10% for VOL and 23% for DQ. In addition, the stand attributes

increment from the time-based model are better than those from the state-space model with 11%, 15% and 12% for BA, VOL and DQ improvements, respectively.

Using a 25% relative epsilon (ignorable difference as a percentage of standard deviation) with a two one-sided t-test (TOST) equivalence test, all stand attributes and increments from the two models versus field observations were statistically equivalent (Figure 2.4). Comparisons of predictions between the two modeling systems showed that SD and its increment and DQ increment were not statistically equivalent at a relative epsilon of 25% standard deviation. The minimum detectable non-negligible differences were smaller for the time-based estimates versus field observations than for the state-space estimates, except for DQ (Table 2.15). With the exception of DQ and its increment, all stand attributes and their associated increments from the time-based model were not statistically different from field observations (i.e., the relative confidence interval includes 0; Figure 2.4). In contrast, only BA, DQ and VOL increment were not statistically different for the state-space model (Figure 2.4). Figure 2.9 show the behavior of stand attributes trend over age with initial density 1667 trees·ha⁻¹ and site class 26. Overall, a simple dynamical model using either a time-based or state-space are adequate at predicting stand parameters within the range of conditions modeled here.

2.4 Discussion

The models developed in this study will provide valuable information and understanding about stand dynamics and potential yield of *Eucalyptus hybrid* stands in Indonesia. Even though it is a newly planted species in Indonesia and began to be planted on a large scale in 2010, two modeling approaches were evaluated in this study, which

substantially increases the knowledge base about this species in the tropical region. Eventually, these models will help managers to make better decisions regarding forest management and planning.

We found that the von Bertalanffy-Richards polymorphic equation was the best equation of those tested for predicting top height over time (Table 2.8). In the same region in Indonesia, Isnaini (2018) reported that a von Bertalanffy-Richards polymorphic equation also was the best predictor for mean top height projections for *Acacia mangium*, *Acacia crassicarpa* and *Eucalyptus pellita*. Other researchers found that this model was the most accurate for predicting dominant height growth (Scolforo et al. 2016), top height (Salekin et al. 2020) and mean height (van der Colff and Kimberley 2013) of plantations. In addition, it has been frequently used for site index curves (Burkhardt and Tennent 1977) and for modeling the development of other forest variables (Pienaar and Turnbull 1973). Similar to some studies (e.g., Berrill 2004; Methol 2001; Zhao 1999) we found that the two-parameter Schumacher polymorphic equation was the best equation for predicting basal area in our eucalyptus clones. In this analysis, the Clutter (1983) formulations was the most optimal for stand density. Overall, site class was the primary driving variable for both top height and basal area, while clone was the most important variable for stand density. In particular, clone B was specifically engineered through tree breeding programs that prioritize resistance to pests and diseases resulting in higher survival in the short term compared to clone A (Table 2.12).

The state-space modeling approach developed in this study was similar to stand-level dynamic growth models for loblolly pine (*Pinus taeda* L.) plantations in the USA (García et al. 2011) and teak (*Tectona grandis* L.) plantations in India (Tewari et al.

2014). Both studies included four state variables (top height, stand density, basal area and a measure of stand closure). As in this study, top height growth was projected using stand age, while the other state variables were projected with respect to top height growth. The dynamic models that were presented in these prior studies provided satisfactory estimates within the range of ages and the projection intervals observed. However, neither of these studies compared the state-space approach with a time-based approach as we did in this study. In our study, the equation system for the state-space approach was built using a simultaneous analysis approach. In particular, the von Bertalanffy-Richards formulation was utilized in the transition functions for projecting dominant height growth in our state-space approach. García (2011) and García et al. (2011) also used the transition functions derived from the base differential equation of their respective growth functions, while other researchers preferred to use different techniques such as the Algebraic Difference Approach (ADA; Bailey and Clutter 1974) or its generalization (GADA; Cieszewski 2003).

The stand density transition function in our study was based on the assumption that the rate of change in SD was relative to top height increment and depended on current values of HT and SD. Diéguez-Aranda et al. (2006) accounted for the influence of site quality in their model for Scots pine (*Pinus sylvestris* L.), while García (2009) employed a site-independent relationship for the mortality relative to height growth. Our results indicated that including clone and site class as random effects on α_2 (associated with current HT) improved model performance. Clone explained a greater portion of the variation than did site class. Inclusion of relative density as a fourth state variable resulted in lower model performance and was likely a result of errors compounding from

the prediction based on the other model equations. Finally, the rather short rotation length, limited observed onset of self-thinning, and truncated data beyond rotation age might also explain the generally lower performance of state-space basal area equations. For example, García (2011) reported a simple dynamics model for managed even-aged stand with limited data for interior spruce (*Picea spp.*), while the approach performed very well on a more extensive data set from loblolly pine plantations (García et al. 2011). This may suggest that robustness of the state-space approach is more dependent on the available data than a time-based approach, which deserves further future evaluation.

For both models, stand density was the poorest predicted variables (Table 2.11 & 2.13). Natural tree mortality is a complex process that is neither constant in time nor in space, so it is difficult to predict or explain the factors that control it (van Laar and Acka 2007). Prediction of tree mortality (or stand density) is widely recognized as much more difficult compared to other stand attribute models due to its high variability. Stand density models for both time-based and state-space approaches only explained 64% variability with a relative rMSE over 8%. As noted above, there was significant variation in observed mortality patterns between the two clones, creating further challenges in developing a robust equation. The problem is further exacerbated by the rather limited range of initial densities. In addition, *Eucalyptus* clones in this region have relatively low mortality rates within the observed density range of 1200-1700 trees·ha⁻¹ from planting to harvesting time.

Although growth models are abstractions of reality, they should still provide predictions that are biologically realistic and robust. Evaluating models of stand dynamics on the basis of only one stand attribute or temporal period is limited because it

does not provide insight into how the model arrived at those estimates and may lead to inappropriate applications and erroneous results (Leary 1997). The general stand development rules represented in a modified Bakuzis matrix can be useful in assessing model predictions, although they all often have multiple limitations (Weiskittel et al. 2011). Overall, both the time-based and state-space modeling approaches we examined in this study did not violate the expected trends within the modified Bakuzis matrix. In clone B, there were observed departures from Eichorn's rules at later stages of stand development beyond the normal rotation age in the time-based model. This was understandable since the data that we used for this clone were limited to a maximum of 5.3 years for clone A and 3.5 years for clone B, and it was too early to extend beyond 8-10 years. However, most commercial plantations in this region are not grown beyond this age and the models showed reasonable behavior within the normal rotation lengths (Figure 2.9); however, this was not a problem with the state-space model, which highlights a potential advantage of this particular approach.

Both modeling approaches offer distinct advantages and disadvantages. Our study used hybrid clones that were relatively uniform, had very short rotation ages (6 years), similar silvicultural regimes, and relatively uniform site class conditions. As a result, the time-based model provided slightly better performance than the state-space model based on equivalence tests and goodness-of-fit statistics. The state-space concept allows for continuous updates as more data are obtained for particular conditions. Theoretically, this should lead to more robust model development. The results shown in the Bakuzis matrices showed that both time-based and state-space models provided biological reasonable depictions of stand development patterns. Development of similar models

using other APRIL plantations with a wider range of site conditions, higher mortality rates, and different species (eg. *Acacia mangium* and *Acacia crassicarpa*) may favor state-space models over time-based models, which deserves additional examination and assessment.

2.5 Conclusion

As observed in this analysis, a short rotation species like *Eucalyptus hybrid* clone with uniform growth benefits from mathematical models that involve an explicit expression of time. Time-based models that use age in its mathematical form were observed to provide simple yet accurate estimates of stand attributes across relatively short rotation ages. This stand-level modeling framework requires testing across a wide range of silvicultural treatments, clones, species, and thinning practices before its flexibility as a tool for predicting stand-level growth can be fully understood. Under these expanded conditions, the state-space models may have better performance. Overall, this study directly quantifies the benefits and potential drawbacks to contrasting stand-level growth modeling approaches, which can help guide future efforts.

2.6 References

- Bailey, R.L., Borders, B.E., Ware, K.D., Jones Jr., E.P., 1985. A compatible model for slash pine plantation survival to density, age, site index, and type and intensity of thinning. *Forest Science* 31, 180–189.
- Berrill, J.P. 2004. Preliminary growth and yield models for even-aged *Cupressus lusitanica* and *C. macrocarpa* plantations in New Zealand. *New Zealand Journal of Forestry Science*, 34(3), 272-292.
- Bonet, J.A., De-Miguel, S., Martinez de Aragón, J., Pukkala, T., Palahí, M. 2012. Immediate effect of thinning on the yield of Lactarius group *deliciosus* in *Pinus pinaster* forests in Northeastern Spain. *Forest Ecology and Management* 265: 211-217
- Budhathoki, C.B., Lynch, T.B. and Guldin, J.M. 2008. A mixed-effects model for the dbh–height relationship of shortleaf pine (*Pinus echinata* Mill.). *South. J. Appl. For.* 32, 5–11.
- Bugmann, H., R. Seidl, F. Hartig, F. Bohn, J. Brůna, M. Cailleret, L. François, et al. 2019. Tree mortality submodels drive simulated long-term forest dynamics: assessing 15 models from the stand to global scale. *Ecosphere*. 10(2):e02616.
- Burkhart, H.E. 1971. Slash pine plantation yield estimates based on diameter distributions: an evaluation. *Forest Science* 17: 452-453.
- Burkhart, H.E., & Tennent, R.B. 1977. Site index equations for radiata pine in New Zealand. *New Zealand Journal of Forestry Science*. 7. 408-416.
- Burkhart, H.E., Avery, T.E., & Bullock, B.P. 2019. *Forest measurements*. Waveland Press

- Burkhardt, H.E., & Tomé, M. 2012. Modeling forest trees and stands. Dordrecht. New York: Springer.
- Clutter, J.L. 1963. Compatible growth and yield models for loblolly pine. *Forest Science* 9: 355-371.
- Clutter, J.L., J.C. Fortson, L.V. Pienaar, G.H. Brister, and R.L. Bailey. 1983. Timber management: A quantitative approach. John Wiley & Sons, Inc. 333 p.
- Coomes, D.A., Duncan, R.P., Allen, R.B. & Truscott, J. 2003. Disturbances prevent stem size-density distributions in natural forests from following scaling relationships. *Ecology Letters*, 6, 980–989.
- Essed, F.J. 1957. Measurement of standing timber. PhD Dissertation, Wageningen
- Filho, A., Netto, S., Pelissari, A., Machado, S., Corte, A. 2015. Growth and yield of *Eucalyptus sp.* in tropical region of Brazil. *Australian Journal of Basic and Applied Sciences*. 9. 286-293.
- García, O. 1984. New class of growth models for even-aged stands: *Pinus radiata* in Golden Downs Forest. *N Z J For Sci* 14:65–88
- García, O. 1994. The state-space approach in growth modelling. *Can J For Res* 24:1894–1903
- García, O. 2005. Thinking about time. In Naito, K. (Ed.), *The Role of Forests for Coming Generations – Philosophy and Technology for Forest Resource Management*. Japan Society of Forest Planning Press, Utsunomiya, Japan, pp. 47–54.
- García, O. 2011. A parsimonious dynamic stand model for interior spruce in British Columbia. *For Sci* 57:265–280

- García, O. 2013. Building a dynamic growth model for trembling aspen in western Canada without age data. *Can J For Res* 43(3):256–265
- García, O., Burkhart, H.E., Amateis, R.L. 2011. A biologically consistent stand growth model for loblolly pine in the piedmont physiographic region, USA. *For Ecol Manag* 262(11):2035–2041
- García, O. and Ruiz, F. 2003. A growth model for eucalypt in Galicia. Spain *For Ecol Manage* 173: 49–62
- Isnaini, H.N. 2018. Growth and yield modeling for unthinned *Acacia mangium*, *Acacia crassicarpa* and *Eucalyptus pellita* plantations in Indonesia. University of Canterbury, Christchurch.
- Johnstone, W.D. 1977. Interim equations and tables for the yield of fully stocked spruce-poplar stands in the mixed wood forest section of Alberta. *Can. For. Serv. Inf. Rep.*NOR-X-175.
- Kabzems, A. 1971. The growth and yield of well-stocked white spruce in the mixed wood section of Saskatchewan. *Sask. Dep. Nat. Res. Tech. Bull. No. 5*
- Kershaw, J.A. Jr, Ducey, M.J., Beers, T.W., Husch, B. 2016. *Forest Mensuration*, 5th edn. Wiley/Blackwell, Hoboken, NJ
- Kuehne, C., Russell, M.B., Weiskittel, A.R. and Kershaw Jr, J.A., 2020. Comparing strategies for representing individual-tree secondary growth in mixed-species stands in the Acadian Forest region. *Forest Ecology and Management*, 459, 117823.
- Lappi, J. 1991. Calibration of height and volume equations with random parameters. *For. Sci.* 37, 781–801.

- Latifah, S., Villanueva, T.R., Carandang, M.G., Bantayan, N.C., & Florece, L.M. 2014. Predicting growth and yield models for *Eucalyptus* species in Aek Nauli, North Sumatera, Indonesia. *Journal of Agriculture, Forestry and Fisheries*, 3(4), 209-216
- Leary, R.A., 1997. Testing models of unthinned red pine plantation dynamics using a modified Bakuzis matrix of stand properties. *Ecological Modelling* 98, 35–46.
- Lynch, T.B., Holley, A.G., and Stevenson, D.J. 2005. A random-parameter height–dbh model for cherry bark oak. *South J. Appl. For.* 29, 22–26.
- MacLeod, W.K. and Blyth, A.W. 1955. Yield of even-aged fully stocked spruce-poplar stands in northern Alberta. *Can. Dep. For., For. Res. Br. Tech. Note No. 18*
- Magaton, A.D.S., Colodette, J.L., Gouvea, A.D.F.G., Gomide, J.L., Muguet, M.C.S., Pedrazzi, C. 2009. *Eucalyptus* wood quality and its impact on kraft pulp production and use. *Tappi J* 8(8):32–39
- Methol, R. 2001. Comparisons of approaches to modelling tree taper, stand structure and stand dynamics in forest plantations. University of Canterbury, Christchurch.
- Muller-Landau, H.C. (and 43 others). 2006. Comparing tropical forest tree size distributions with the predictions of metabolic ecology and equilibrium models. *Ecology Letters*, 9, 589–602.
- Nord-Larsen, T., and Johannsen, V.K. 2007. A state-space approach to stand growth modelling of European beech. *Ann For Sci* 64:365–374
- Oliver, C.W., Larson, B.C., 1996. *Forest stand dynamics: Update edition*. John Wiley & Sons, Inc., New York, NY.
- Pienaar, L.V. 1979. An approximation of basal area growth after thinning based on growth in un-thinned plantations. *Forest Science* 25: 223-232.

- Pienaar, L.V., Shiver, B.D. 1981. Survival functions for site-prepared slash pine plantations in the flatwoods of Georgia and northern Florida. *Southern Journal of Applied Forestry* 5, 59–62.
- Pienaar, L.V., Turnbull, K.J. 1973. The Chapman-Richards generalization of Von Bertalanffy's growth model for basal area growth and yield in even-aged stands. *Forest Science* 19: 2-22.
- Plonski, W.L. 1956. Normal yield tables Ontario Dep. Lands and Forests Rep. No. 24
- R Core Team. 2020. R: A Language and Environment for Statistical Computing. R Foundation for Statistical Computing. <https://www.r-project.org/> (accessed on 14 May, 2020).
- Reineke, L.H. 1933. Perfecting a stand-density index for even-aged forests. *J. Agric. Res.* 46, 627–638.
- Rockwood, D.L., Rudie, A.W., Ralph, S.A., Zhu, J.Y., and Winandy, J.E. 2008. Energy product options for Eucalyptus species grown as short rotation woody crops. *Int. J. Sci.* 9: 1361–1378.
- Qin, J., and Cao, Q.V. 2006. Using disaggregation to link individual-tree and whole-stand growth models. *Can. J. For. Res.* 36, 953–960.
- Salekin, S., Mason, E., Morgenroth, J., Meason, D. 2020. A preliminary growth and yield model for *Eucalyptus globoides* Blakely plantations in New Zealand. *New Zealand Journal of Forestry Science.* 50. 10.33494/nzjfs502020x55x.
- Schumacher, X.A. 1939. A new growth curve and its application to timber yield. *Journal of Forestry* 37: 817-820.

- Scolforo, H.F., Castro Neto, F., Scolforo, J.R.S., Burkhart, H., McTague, J.P., Raimundo, M.R., Loos, R.A., Fonseca, S., Sartório, R.C. 2016. Modeling dominant height growth of eucalyptus plantations with parameters conditioned to climatic variations. *For. Ecol. Manage.* 380:182–195.
- Scolforo, H.F., McTague, J., Burkhart, H., Roise, J., Campoe, O., Stape, J. 2019. *Eucalyptus* growth and yield system: Linking individual-tree and stand-level growth models in clonal *Eucalyptus* plantations in Brazil. *Forest Ecology and Management.* 432. 1-16. 10.1016/j.foreco.2018.08.045.
- Sullivan, A.D., Clutter, J.L. 1972. A simultaneous growth and yield model for loblolly pine. *Forest Science* 18: 76-86.
- Temesgen, H., Zhang, C.H., and Zhao, X.H. 2014. Modelling tree height– diameter relationships in multi-species and multi-layered forests: a large observational study from Northeast China. *Forest Ecology and Management.* 316, 78–89
- Tewari, V., Álvarez-González, J., & García, O. 2014. Developing a dynamic growth model for teak plantations in India. *Forest Ecosystems.* 1. 9. 10.1186/2197-5620-1-9.
- van der Colff, M., Kimberley, M.O. 2013. A National height-age model for *Pinus radiata* in New Zealand. *N.Z. Journal of Forestry Science* 43, 4 (2013).
<https://doi.org/10.1186/1179-5395-43-4>
- Van Laar, A., Akça, A. 2007. *Forest Mensuration.* 2nd edition. New York: Springer; 2007:38

- Wang, Y., and Baker, T. 2007. A regionalized growth model for *Eucalyptus globulus* plantations in south-eastern Australia. *Australian Forestry*. 70. 93-107.
10.1080/00049158.2007.10675008.
- Weiskittel, A.R., Hann, D.W., Kershaw, J.A., and Vanclay, J.K. 2011. Forest growth and yield modeling. Hoboken, NJ: Wiley.
- Winner, L., and C. B. Stott. 1954. Forest control by continuous inventory. CFI Notes 2, North Central Forest Experiment Station, USDA Forest Service. 17p.
- Wykoff, W.R., Crookston, N.L., and Stage, A.R. 1982. User's guide to the Stand Prognosis Model. Gen. Tech. Rep. INT-133. U.S. Department of Agriculture, Forest Service, Intermountain Forest and Range Experiment Station, Ogden, Utah, USA.
- Zhao, W. 1999. Growth and yield modelling of *Pinus radiata* in Canterbury, New Zealand. University of Canterbury, Christchurch.

Table 2.1 Summarized stand attributes and their increment for the inventory plots (n=2808) used for modeling (A = age; HT = top height; BA = basal area; SD = stand density; RD = relative density; DQ = quadratic mean diameter; and VOL = stand volume)

Stand attributes	Clone A (n = 2476)				Clone B (n = 332)			
	Mean	Min	Max	Stdev	Mean	Min	Max	Stdev
A (month)	34.3	12	63.6	14.4	29.1	18	42	9.6
HT (m)	17.3	5.8	30	5.7	18	10.6	27.7	4.4
BA (m ² ha ⁻¹)	12.4	1.8	26.9	5.2	14.2	3.9	22.9	3.8
SD (trees ha ⁻¹)	1,536	175	2,101	209	1,569	450	1,851	203
RD	0.59	0.11	1.16	0.21	0.68	0.21	1.02	0.16
DQ (cm)	9.7	3.4	18.5	2.5	10.6	7.8	14.5	1.4
VOL (m ³ ha ⁻¹)	73	0.05	234.4	53.37	85.71	14.69	189.8	42.63
dHT/dA (m month ⁻¹)	0.4	0.01	1.22	0.12	0.45	0.12	0.75	0.11
dBA/dA (m ² ha ⁻¹ month ⁻¹)	0.32	-0.42	1.18	0.13	0.35	0.14	0.66	0.1
dSD/dA (trees ha ⁻¹ month ⁻¹)	-5	-106	0	7	-1	-21	0	3
MAI (m ³ ha ⁻¹ month ⁻¹)	1.85	0.00	4.37	0.89	2.79	0.82	4.52	0.72
PAI (m ³ ha ⁻¹ month ⁻¹)	3.19	-0.90	11.16	1.04	4.22	2.09	7.30	0.87

Table 2.2 Mathematical equation forms evaluated for time-based top height growth model. (A_1 = age (months) at time 1; A_2 = age (months) at time 2; HT_1 = top height (m) at time 1; HT_2 = top height at time 2; h_i = coefficient parameters)

Model	Equation form	Reference
TB-HT-1	$HT_2 = HT_1 \left(\frac{1 - \exp(h_0 \cdot A_2)}{1 - \exp(h_0 \cdot A_1)} \right)^{h_1}$	Chapman-Richard function
TB-HT-2	$HT_2 = \exp \left(\ln(HT_1) + h_0 \cdot \left(\frac{1}{A_2} - \frac{1}{A_1} \right) \right)$	Clutter et. al, 1983
TB-HT-3	$HT_2 = \exp \left(\ln(HT_1) + h_0 \cdot SI \cdot \left(\frac{1}{A_2} - \frac{1}{A_1} \right) \right)$	Clutter et. al, 1983
TB-HT-4	$HT_2 = \exp \left(\ln(HT_1) \cdot \left(\frac{A_1}{A_2} \right)^{h_1} + h_0 \cdot \left(1 - \left(\frac{A_1}{A_2} \right)^{h_1} \right) \right)$	Schumacher Function (1939)
TB-HT-5	$HT_2 = HT_1^{\left(\frac{A_1}{A_2} \right)} \exp \left(h_0 \cdot \left(1 - \frac{A_1}{A_2} \right)^{h_1} \right)$	Schumacher Function (1939)
TB-HT-6	$HT_2 = \exp \left(\ln(HT_1) - (h_0 + h_1 \cdot HT_1) \left(\frac{1}{A_2} - \frac{1}{A_1} \right) \right)$	Schumacher Function (1939)
TB-HT-7	$HT_2 = h_0 \left[1 - \left(1 - \frac{HT_1^{h_2}}{h_0^{h_2}} \right) \exp(-h_1(A_2 - A_1)) \right]^{\frac{1}{h_2}}$	Bertalanffy-Richard model (Garcia, 1983)

Table 2.3 Mathematical equation forms evaluated for time-based stand density models.

(A_1 = age (months) at time 1; A_2 = age (months) at time 2; SD_1 = stand density (trees·ha⁻¹) at time 1; SD_2 = stand density (trees·ha⁻¹) at time 2; s_i = coefficient parameters)

Model	Equation form	Reference
TB-SD-1	$SD_2 = SD_1 \cdot \exp(SI \cdot (A_2^{s_0} - A_1^{s_0}))$	Pienaar and Shiver, 1981
TB-SD-2	$SD_2 = SD_1 \cdot \exp(A_2^{s_0} - A_1^{s_0})$	Pienaar and Shiver, 1981
TB-SD-3	$SD_2 = SD_1 \cdot \left(\frac{A_1}{A_2}\right)^{s_0} \cdot \exp((s_1 + s_2 \cdot SI) \cdot (A_2 - A_1))$	Bailey et al., 1985
TB-SD-4	$SD_2 = SD_1 \cdot \left(\frac{A_1}{A_2}\right)^{s_0} \cdot \exp(s_1(A_2 - A_1))$	Bailey et al., 1985
TB-SD-5	$SD_2 = SD_1 \cdot \left(\frac{A_1}{A_2}\right)^{s_0} \cdot \exp(s_1(A_2 - A_1)^{s_2})$	Bailey et al., 1985
TB-SD-6	$SD_2 = \exp(\ln(SD_1) + s_0 * (A_2^{s_1} - A_1^{s_1}))$	Clutter et al., 1983

Table 2.4 Mathematical equation forms evaluated for time-based basal area growth models. (A_1 = age (months) at time 1; A_2 = age (months) at time 2; BA_1 = basal area (m^2ha^{-1}) at time 1; BA_2 = basal area (m^2ha^{-1}) at time 2; b_i = coefficient parameters)

Model	Equation form	Reference
TB-BA-1	$BA_2 = \exp \left[\left(\frac{A_1}{A_2} \right) \ln BA_1 + b_0 \left(1 - \frac{A_1}{A_2} \right) + b_1 \cdot SI \left(1 - \frac{A_1}{A_2} \right) \right]$	Sullivan & Clutter, 1972
TB-BA-2	$BA_2 = \exp \left(\left(\frac{A_1}{A_2} \right) \cdot \ln(BA_1) + b_0 \cdot \left(1 - \left(\frac{A_1}{A_2} \right) \right) \right)$	Bennet, 1970
TB-BA-3	$BA_2 = BA_1 \left(\frac{1 - \exp(b_0 \cdot A_2)}{1 - \exp(b_0 \cdot A_1)} \right)^{b_1}$	Chapman-Richard form
TB-BA-4	$BA_2 = \exp \left(\ln(BA_1) \cdot \left(\frac{A_1}{A_2} \right)^{b_1} + b_0 \cdot \left(1 - \left(\frac{A_1}{A_2} \right)^{b_1} \right) \right)$	Schumacher Function (1939)
TB-BA-5	$BA_2 = BA_1^{\left(\frac{A_1}{A_2} \right)} \exp \left(b_0 \cdot \left(1 - \frac{A_1}{A_2} \right)^{b_1} \right)$	Schumacher Function (1939)
TB-BA-6	$BA_2 = \exp \left(\ln(BA_1) - (b_0 + b_1 \cdot BA_1) \left(\frac{1}{A_2} - \frac{1}{A_1} \right) \right)$	Schumacher Function (1939)
TB-BA-7	$BA_2 = BA_1 \cdot \exp \left(\frac{b_0}{A_2 + b_1} - \frac{b_0}{A_1 + b_1} \right)$	Johnson- Schumacher (Grosenbaugh 1965)
TB-BA-8	$BA_2 = BA_1 \left(\frac{1 - \exp(b_0 \cdot A_2^{b_1})}{1 - \exp(b_0 \cdot A_1^{b_1})} \right)$	Weibull function (Yang et al. 1978)
TB-BA-9	$BA_2 = BA_1 \left(\frac{1 - b_0 \cdot \exp(b_1 \cdot A_2)}{1 - b_0 \cdot \exp(b_1 \cdot A_1)} \right)$	Monomolecular Function (Zeide 1993)

Table 2.5 Estimated parameters with their standard errors (in parentheses) and statistical evaluation for volume model

Model	Estimated parameters			Goodness-of-fit		
	v_0	v_1	v_2	rMSE	R ²	Bias
V-1	0.1804 (0.0030)	0.9938 (0.0079)	1.2032 (0.0058)	4.2973	0.9933	-0.4557
V-2	0.1566 (0.0024)	1.1177 (0.0025)		4.4966	0.9926	-0.4060
V-3	-0.0301 (0.0011)	3.8523 (0.0251)		5.3422	0.9896	-1.1436
V-4	8.3202 (0.1528)	0.1329 (0.0107)	1.2138 (0.0022)	4.1916	0.9936	-0.3953

Table 2.6 Parameter estimates and their associated standard errors (in parentheses), standard deviations of the random effects and goodness-of-fit statistics model V-4

Factor	Parameter	Estimate
Fixed effects	v_0	7.8598 (0.6330)
	v_1	0.1238 (0.0272)
	v_2	1.2050 (0.0054)
Random effects		
(Clone)	$s(v_0)$	0.8115
	$s(v_1)$	0.0322
(Site Class Clone)	$s(v_0)$	0.5571
	$s(v_1)$	0.0275
Goodness-of-fit		
Fixed	rMSE	4.2855
	R^2	0.9933
	Bias	-1.2267
Fixed + random	rMSE	4.0250
	R^2	0.9941
	Bias	-0.3753

Table 2.7 Derived coefficient (fixed + random effects) of model V-4 by clone and site classes

Parameter	Estimate coefficient by clone and site class						
	A:22	A:24	A:26	A:28	B:24	B:26	B:28
v_0	9.6990	8.0446	8.2677	8.6693	7.3133	6.7142	7.1158
v_1	0.0409	0.1224	0.1114	0.0916	0.1429	0.1725	0.1526
v_2	1.2052	1.2052	1.2052	1.2052	1.2052	1.2052	1.2052

Table 2.8 Estimated parameters with their standard errors (in parentheses) of nonlinear least square analysis and goodness-of-fit measures for seven top height models using time-based approach

Model	Estimated parameters			Goodness-of-fit		
	h_1	h_2	h_3	rMSE	R^2	Bias
TB-HT-1	-0.0131 (0.0009)	0.8932 (0.0130)		2.05	0.7738	0.1624
TB-HT-2	-18.107 (0.0688)			2.71	0.6017	0.6796
TB-HT-3	-0.7138 (0.0028)			2.83	0.5677	0.8191
TB-HT-4	4.2215 (0.0377)	0.5070 (0.0134)		1.66	0.8507	0.0551
TB-HT-5	3.4905 (0.0063)	0.9797 (0.0027)		1.85	0.8151	-0.1015
TB-HT-6	14.2198 (0.2745)	0.3921 (0.0266)		2.64	0.6223	0.4724
TB-HT-7	31.8304 (0.5876)	0.0361 (0.0024)	0.2659 (0.0909)	1.35	0.9017	-0.0147

Table 2.9 Estimated parameters with their standard errors (in parentheses) of nonlinear least square analysis and goodness-of-fit measures for six stand density models using time-based approach

Model	Estimated parameters			Goodness-of-fit		
	s ₁	s ₂	s ₃	rMSE	R ²	Bias
TB-SD-1	-0.0036 (0.0001)			134.53	0.5706	-1.8694
TB-SD-2	-0.1304 (0.0053)			135.67	0.5634	-5.1168
TB-SD-3	-0.1304 (0.0088)	-0.0036 (0.0011)	-0.00016 (0.00004)	124.52	0.6321	2.3943
TB-SD-4	-0.1309 (0.0088)	-0.0078 (0.0003)		124.73	0.6308	2.7267
TB-SD-5	-0.1241 (0.0089)	-0.0058 (0.0006)	1.0779 (0.0221)	124.52	0.6321	-0.3566
TB-SD-6	-0.0000008 (0.0000004)	3.0360 (0.1230)		123.13	0.6403	1.5218

Table 2.10 Estimated parameters with their standard errors (in parentheses) of nonlinear least square analysis and goodness-of-fit measures for nine basal area models using time-based approach

Model	Estimated parameters		Goodness-of-fit		
	h_1	h_2	rMSE	R^2	Bias
TB-BA-1	2.4999 (0.0711)	0.0325 (0.0028)	1.94	0.7895	-0.0619
TB-BA-2	3.3115 (0.0042)		1.97	0.7823	-0.0833
TB-BA-3	-0.0440 (0.0011)	1.6938 (0.0317)	2.32	0.7003	0.1858
TB-BA-4	3.6941 (0.0272)	0.6796 (0.0151)	1.89	0.8010	-0.0364
TB-BA-5	3.2969 (0.0092)	0.9925 (0.0042)	1.97	0.7825	-0.1046
TB-BA-6	23.9126 (0.2087)	-0.3011 (0.0292)	2.27	0.7121	0.3835
TB-BA-7	-27.3250 (0.6020)	2.6294 (0.2791)	2.27	0.7120	0.2066
TB-BA-8	-0.0087 (0.0003)	1.3760 (0.0142)	2.34	0.6951	0.1869
TB-BA-9	1.1833 (0.0084)	-0.0325 (0.0007)	2.26	0.7132	0.1739

Table 2.11 Parameter estimates and their standard errors (in parentheses), standard deviations of random effects, and goodness-of-fit statistics for time-based mixed-effects models

Factor	Model TB-HT-7		Model TB-SD-6		Model TB-BA-4	
	Parameter	Estimate	Parameter	Estimate	Parameter	Estimate
Fixed effects	h ₀	30.0040 (1.5446)	s ₀	-0.000003 (0.000001)	b ₀	3.6635 (0.0368)
	h ₁	0.0474 (0.0047)	s ₁	2.4858 (0.1993)	b ₁	0.6972 (0.0158)
	h ₂	0.0698 (0.0862)				
Random effects						
(Clone)	s(h ₀)	<0.0001			s(b ₀)	0.0003
	s(h ₁)	0.0046	s(s ₁)	0.2049		
(Site Class Clone)	s(h ₀)	3.8311			s(b ₀)	0.0648
	s(h ₁)	0.0059	s(s ₁)	0.0681		
Goodness-of-fit						
Fixed	rMSE	1.47	rMSE	123.14	rMSE	1.89
	R ²	0.8830	R ²	0.6402	R ²	0.8009
	Bias	1.4715	Bias	2.7098	Bias	-0.0382
Fixed + random	rMSE	1.22	rMSE	122.68	rMSE	1.87
	R ²	0.9192	R ²	0.6429	R ²	0.8057
	Bias	-0.0180	Bias	1.2171	Bias	-0.0233

Table 2.12 Derived coefficients (fixed + random effects) of time-based mixed effect models by clone and site class

Model	Parameter	Clone : Site Class						
		A:22	A:24	A:26	A:28	B:24	B:26	B:28
TB-HT-7	h ₀	26.6838	28.1532	31.9327	36.1523	24.5601	29.1716	33.3742
	h ₁	0.0450	0.0484	0.0385	0.0355	0.0600	0.0530	0.0472
	h ₂	0.0698	0.0698	0.0698	0.0698	0.0698	0.0698	0.0698
TB-SD-6	s ₀	-0.000003	-0.000003	-0.000003	-0.000003	-0.000003	-0.000003	-0.000003
	s ₁	2.5838	2.6887	2.7013	2.7430	2.2964	2.2874	2.2882
TB-BA-4	b ₀	3.5633	3.6622	3.6562	3.7692	3.7051	3.6204	3.6680
	b ₁	0.6972	0.6972	0.6972	0.6972	0.6972	0.6972	0.6972

Table 2.13 Parameter estimates and their standard errors (in parentheses), standard deviations of random effects, and goodness-of-fit statistics for state-space mixed-effects models

Factor	Model SS-RD-1		Model SS-SD-1		Model SS-W-3	
	Parameter	Estimate	Parameter	Estimate	Parameter	Estimate
Fixed effects	τ	0.0051	α_1	0.0001	k	0.2116
		(0.0002)		(0.0002)		(0.0284)
				2.9946		ω_1
		α_2	(0.1996)		(0.0450)	
		α_3	0.4073			
			(0.1756)			
Random effects						
(Clone)	$s(\tau)$	<0.0001	$s(\alpha_2)$	0.1241	$s(\omega_1)$	<0.0001
(Site Class Clone)	$s(\tau)$	0.0006	$s(\alpha_2)$	0.0439	$s(\omega_1)$	0.0111
Goodness-of-fit						
Fixed	rMSE	0.0911	rMSE	124.49	rMSE	2.2262
	R ²	0.7086	R ²	0.6323	R ²	0.7231
	Bias	-0.0086	Bias	0.6136	Bias	0.0171
Fixed + random	rMSE	0.0892	rMSE	123.65	rMSE	2.2039
	R ²	0.7207	R ²	0.6372	R ²	0.7287
	Bias	0.0042	Bias	1.1099	Bias	0.0226

Table 2.14 Derived coefficients (fixed + random effects) of state-space mixed effect models by clone and site classes

Model	Parameter	Estimate coefficient by clone and site class						
		A:22	A:24	A:26	A:28	B:24	B:26	B:28
SS-RD-1	τ	0.0045	0.0046	0.0047	0.0057	0.0061	0.0052	0.0052
SS-SD-1	α_1	0.0001	0.0001	0.0001	0.0001	0.0001	0.0001	0.0001
	α_2	3.0375	3.0876	3.0434	2.9879	2.7999	2.7978	2.7856
	α_3	0.4072	0.4072	0.4072	0.4072	0.4072	0.4072	0.4072
SS-W-3	k	0.2137	0.2137	0.2137	0.2137	0.2137	0.2137	0.2137
	ω_1	0.2156	0.2306	0.2299	0.2408	0.2626	0.2460	0.2521

Table 2.15 Goodness-of-fit statistics and two-one-sided t-test (TOST) equivalence tests for time-based and state-space approach for each stand attributes and their observed increments

Stand attributes	Goodness-of-fit					Equivalence test ^b		
	TB		SS		rMSE improvement ^a (%)	TB vs Obs	SS vs Obs.	TB vs SS
	rMSE	R ²	rMSE	R ²				
BA (m ² ha ⁻¹)	1.86	0.81	2.1	0.75	13%	0.039	0.037	0.064
SD (trees·ha ⁻¹)	123	0.64	124	0.64	1%	0.036	0.200	0.974
VOL (m ³ ha ⁻¹)	17.75	0.86	19.56	0.82	10%	0.030	0.074	0.146
DQ (cm)	0.72	0.85	0.89	0.77	23%	0.120	0.048	0.220
Δ BA (m ² ha ⁻¹ month ⁻¹)	0.1	0.37	0.11	0.22	11%	0.049	0.080	0.087
Δ SD (trees·ha ⁻¹ month ⁻¹)	7.43	0.08	7.4	0.09	0%	0.034	0.170	1.026
Δ VOL (m ³ ha ⁻¹ month ⁻¹)	0.9	0.29	1.03	0.06	15%	0.039	0.036	0.074
Δ DQ (cm month ⁻¹)	0.04	0.53	0.05	0.41	12%	0.101	0.116	0.280

^a % improvement = 100 * (SS – TB) / TB

^b The minimum detectable non-negligible differences

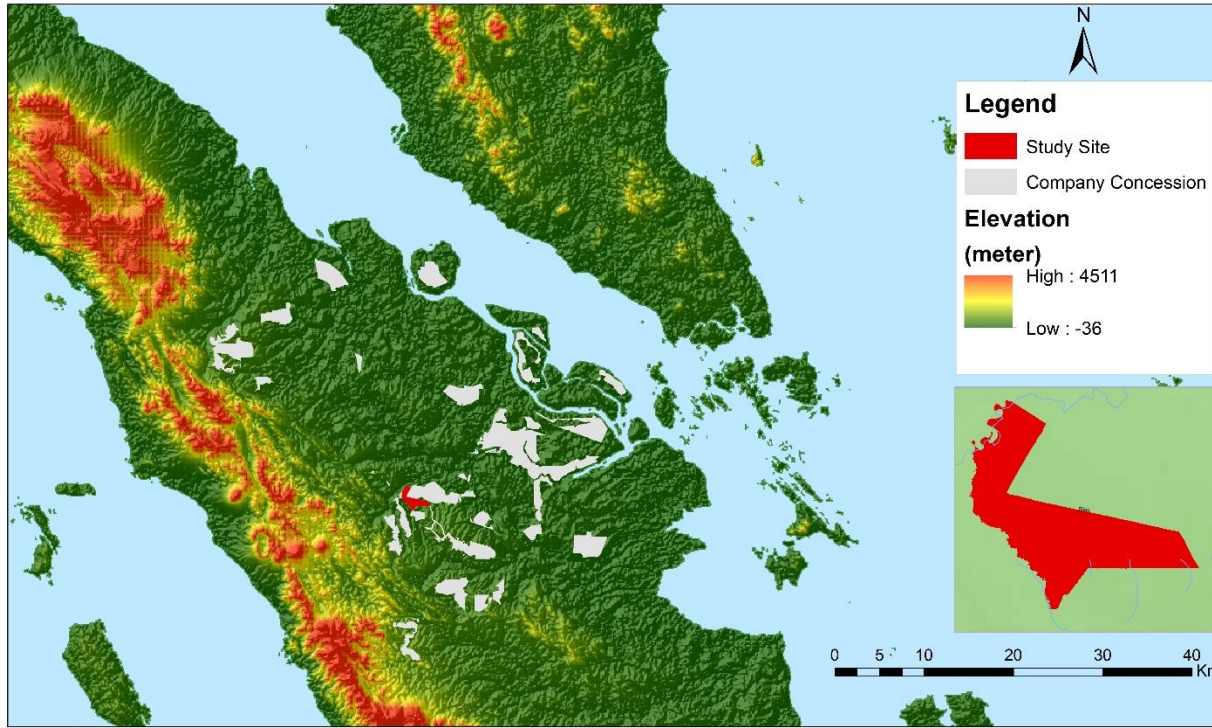


Figure 2.1 Location of the study area in the Sector Teso East, central region of Sumatra

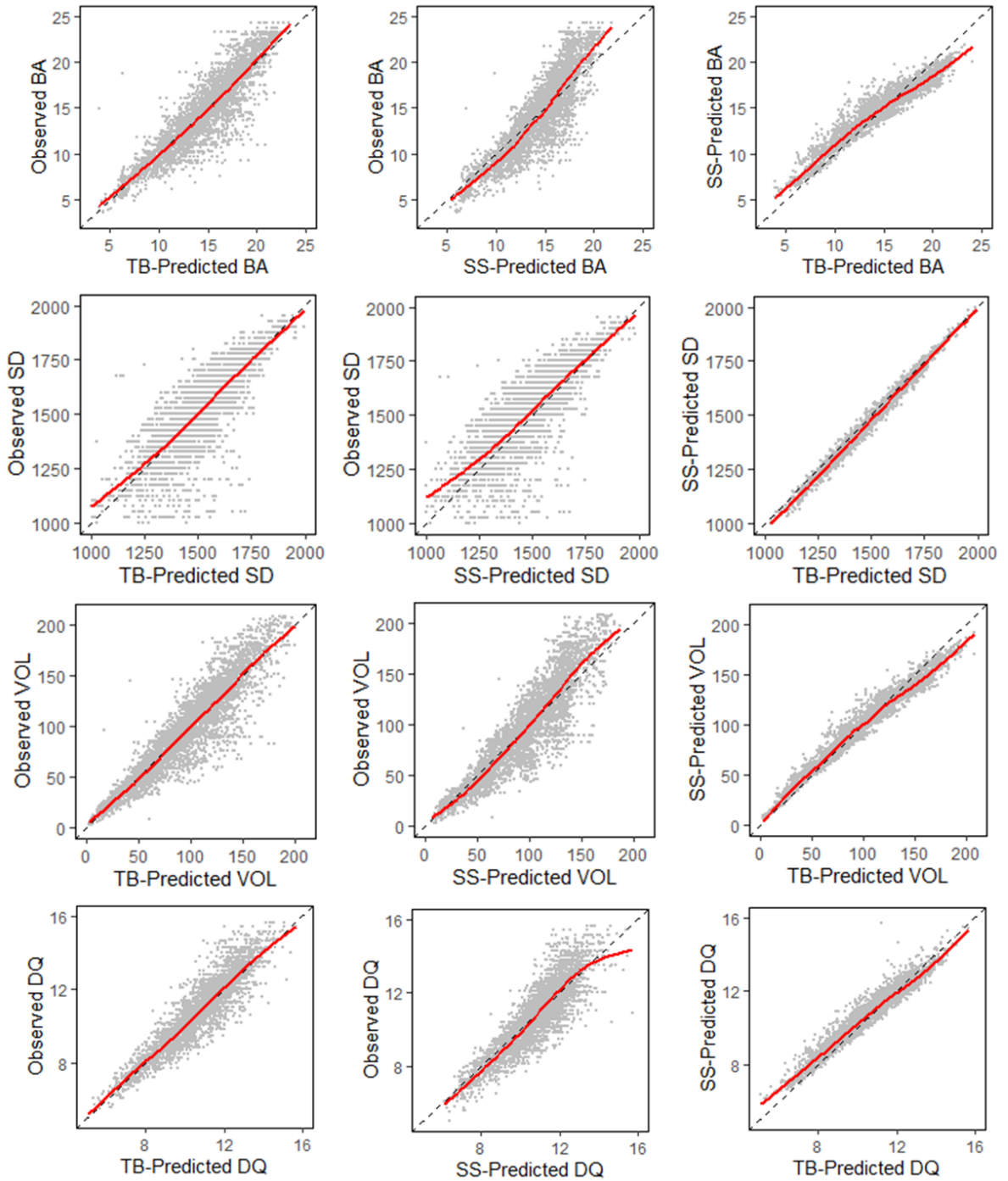


Figure 2.2 Comparison between time-based, state-space and observation for each stand attributes. The dotted line represents the 1:1 line, while the red line is the observed trend

using a smoothing line

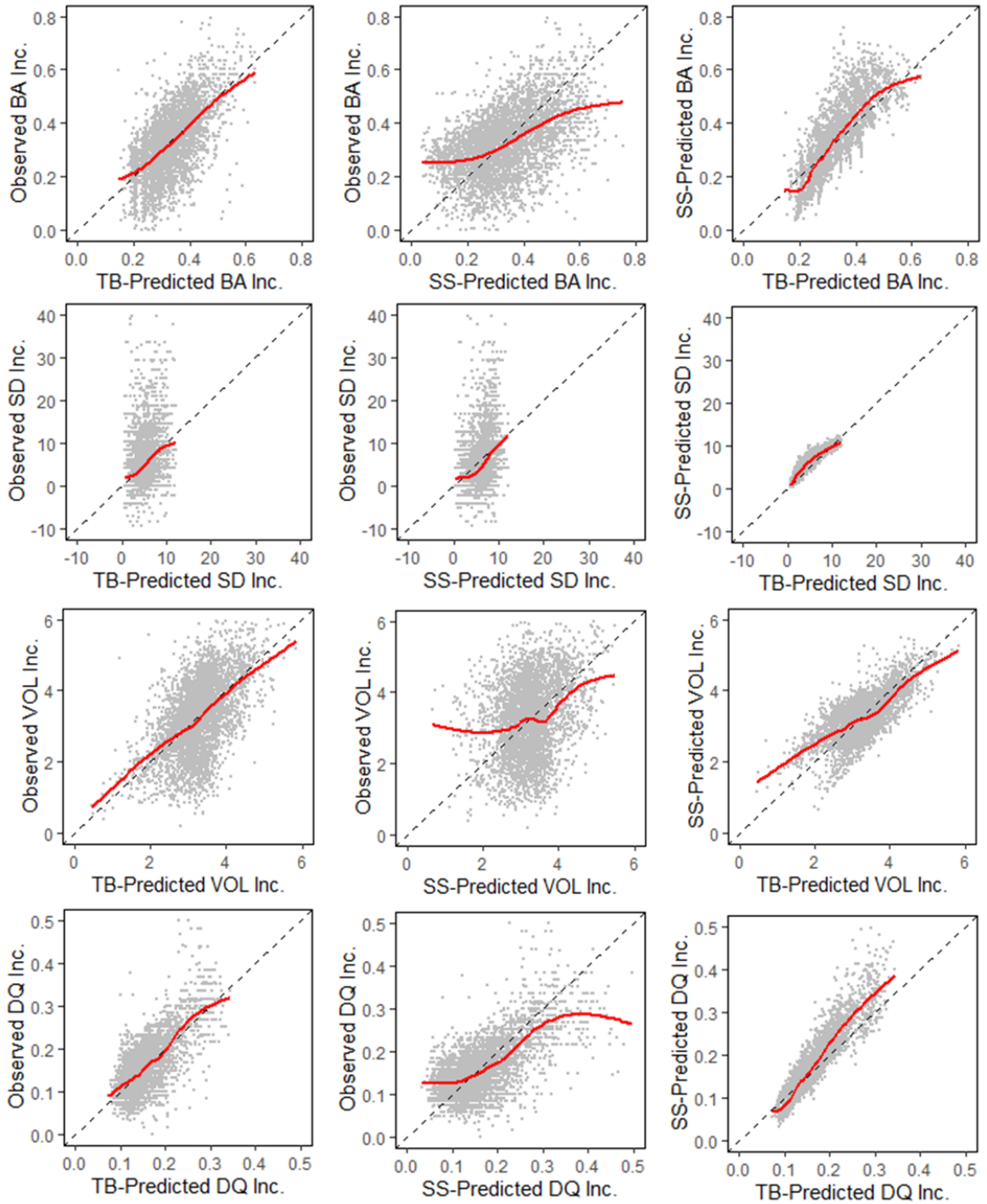


Figure 2.3 Comparison between time-based, state-space and observation for each stand attributes increment. The dotted line represents the 1:1 line, while the red line is the observed trend using a smoothing line

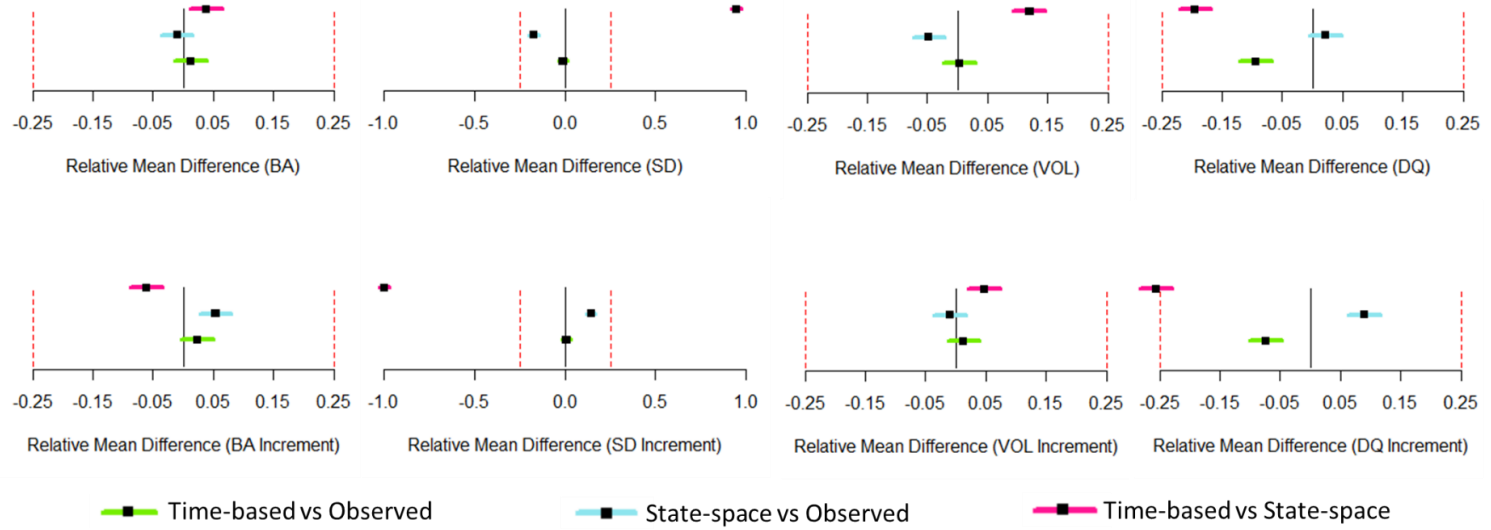


Figure 2.4 Significance and equivalence test between time-based, state-space and observation for each stand attribute and their increment

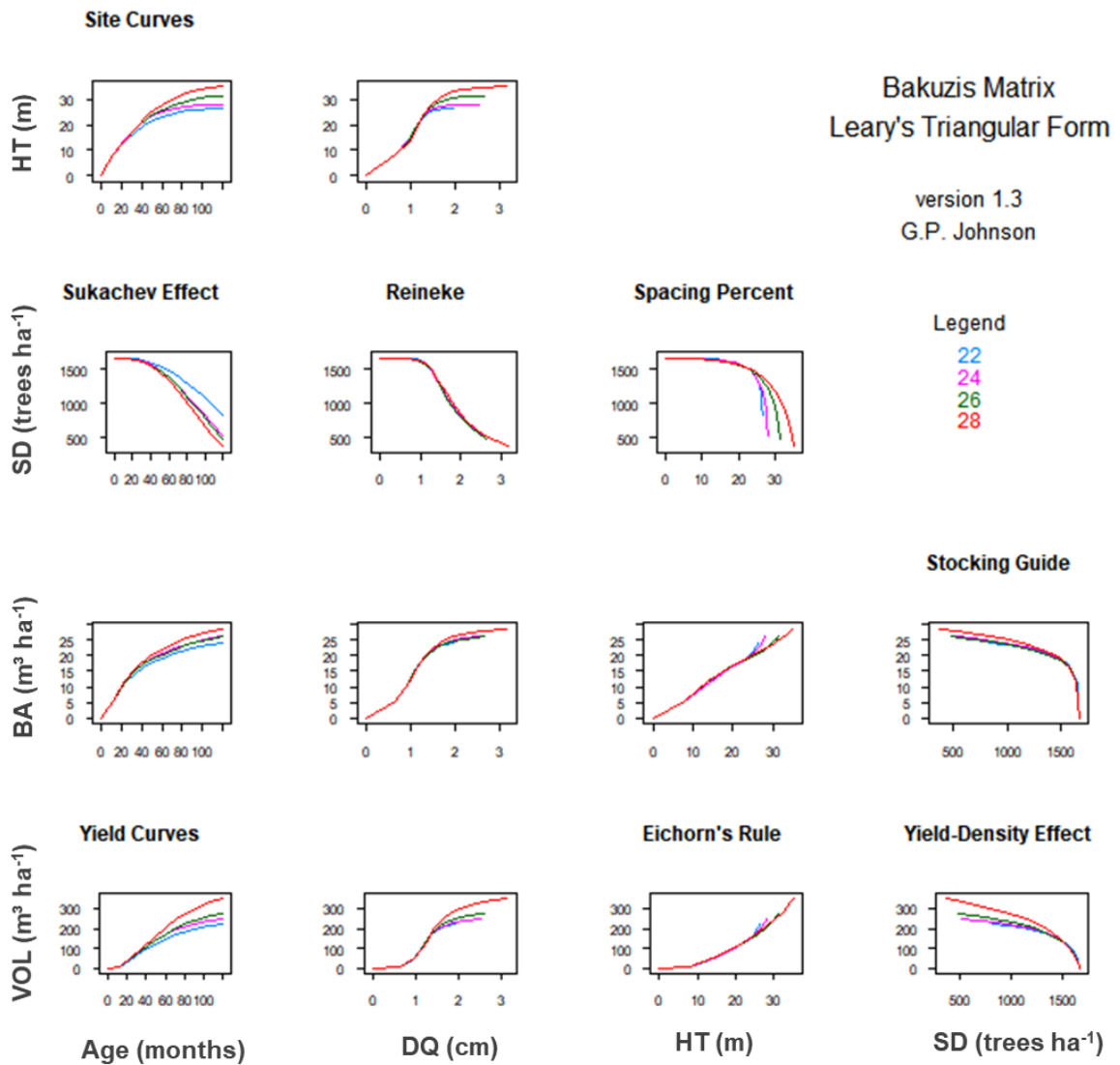


Figure 2.5 Bakuzis matrix of time-based stand growth model across different level of site class (initial density 1667 trees·ha⁻¹) for clone A.

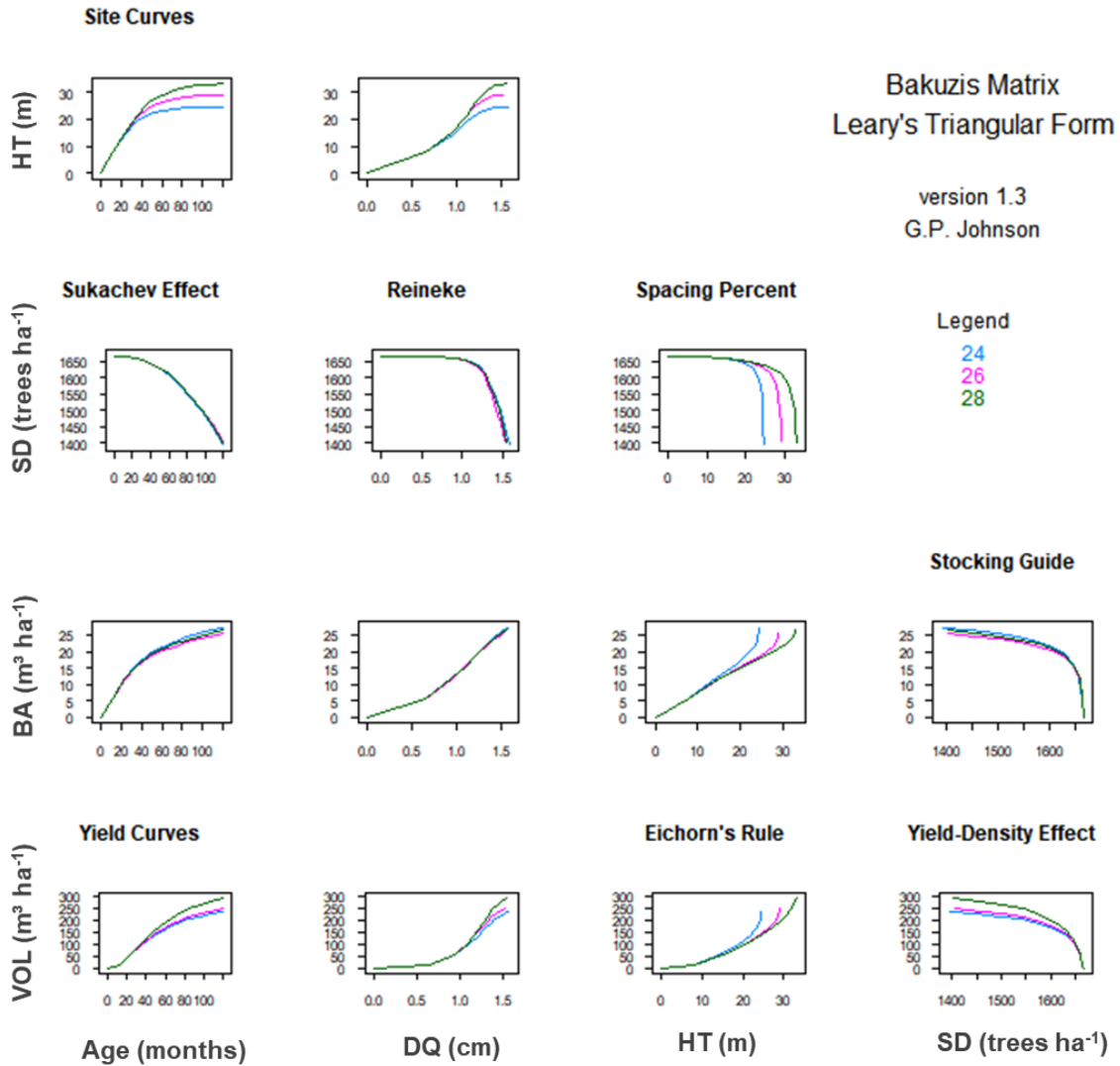


Figure 2.6 Bakuzis matrix of time-based stand growth models across different level of site class (initial density 1667 trees·ha⁻¹) for clone B.

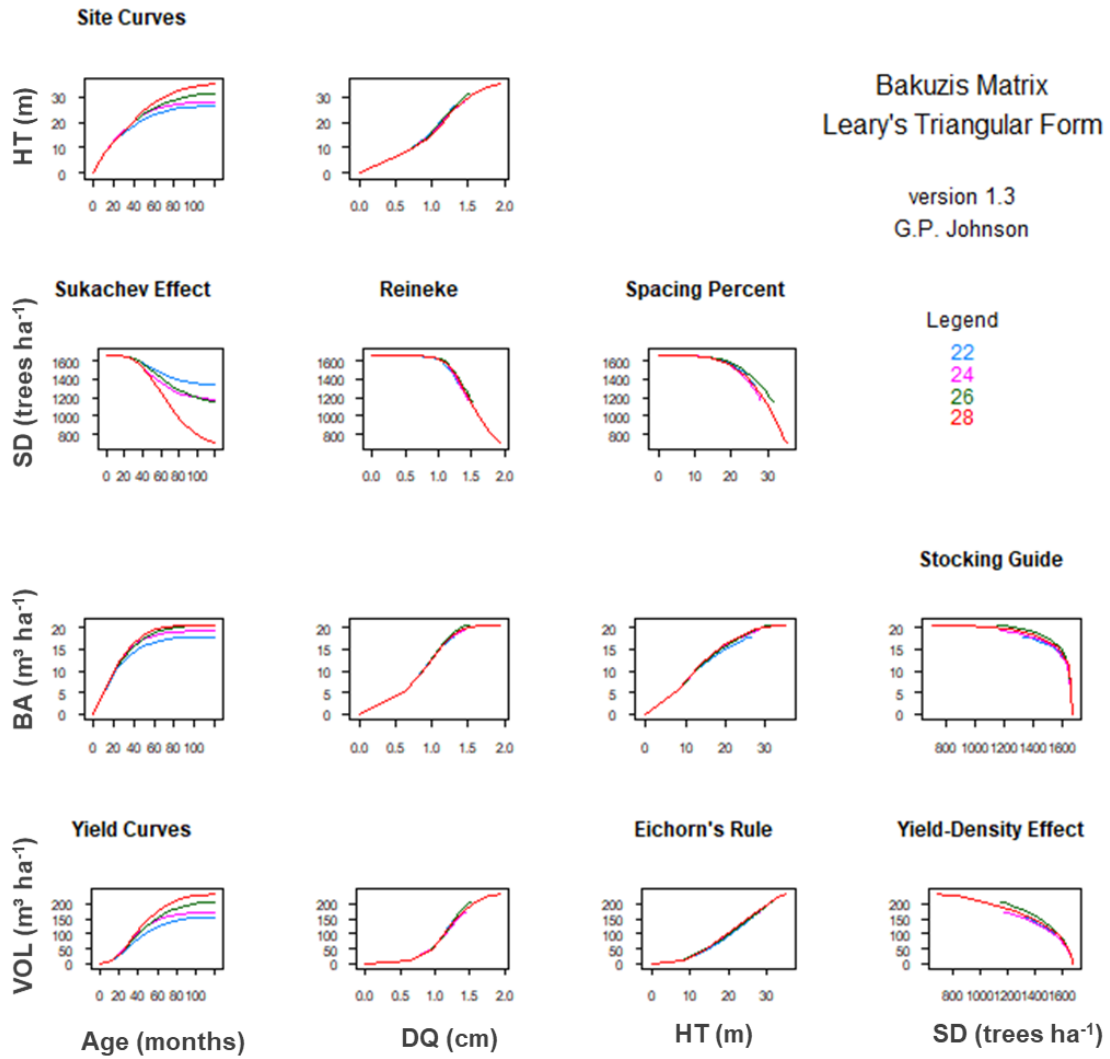


Figure 2.7 Bakuzis matrix of state-space stand growth model across different level of site class (initial density 1667 trees·ha⁻¹) for clone A.

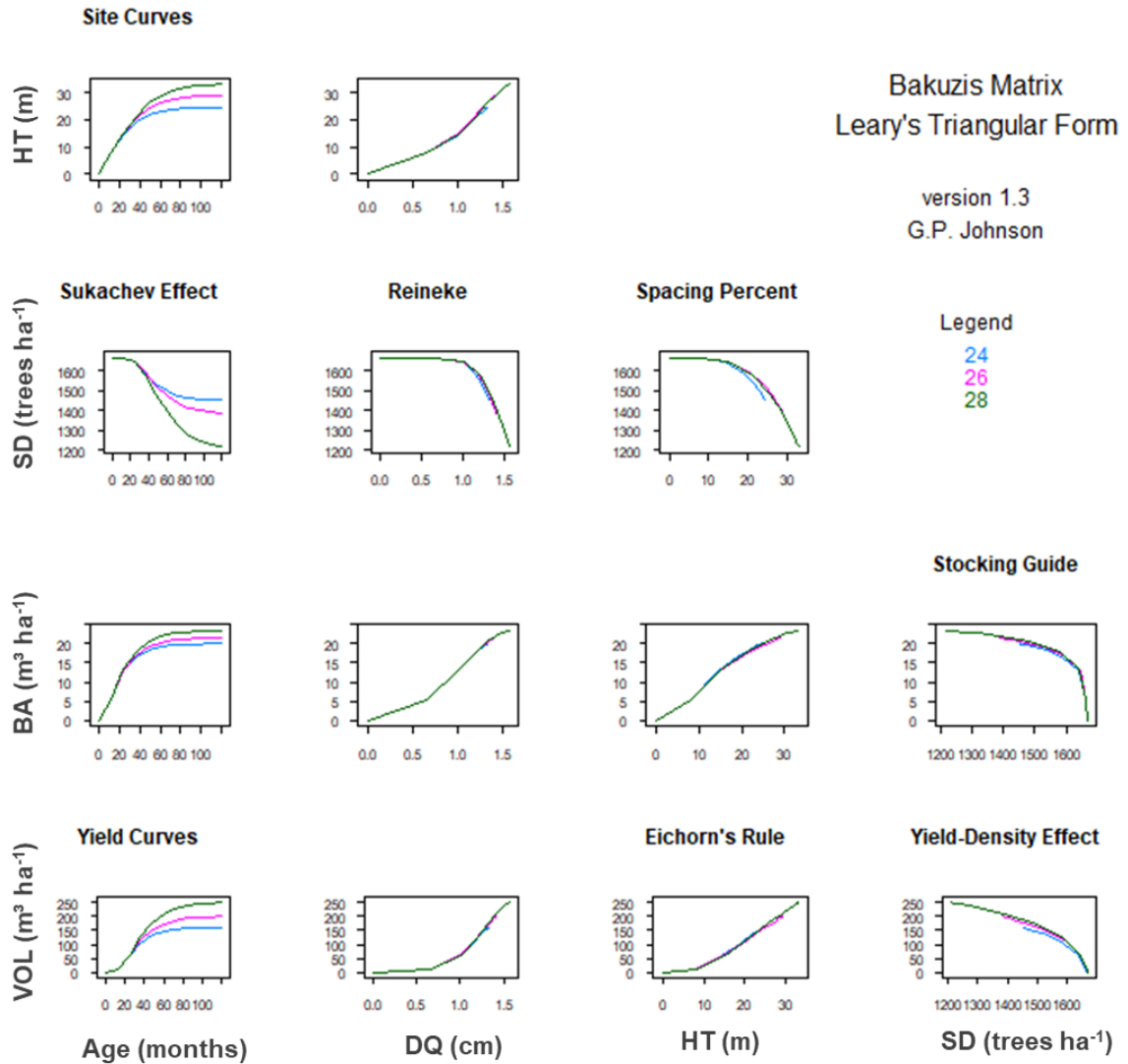


Figure 2.8 Bakuzis matrix of state-space stand growth model across different level of site class (initial density $1667 \text{ trees} \cdot \text{ha}^{-1}$) for clone B.

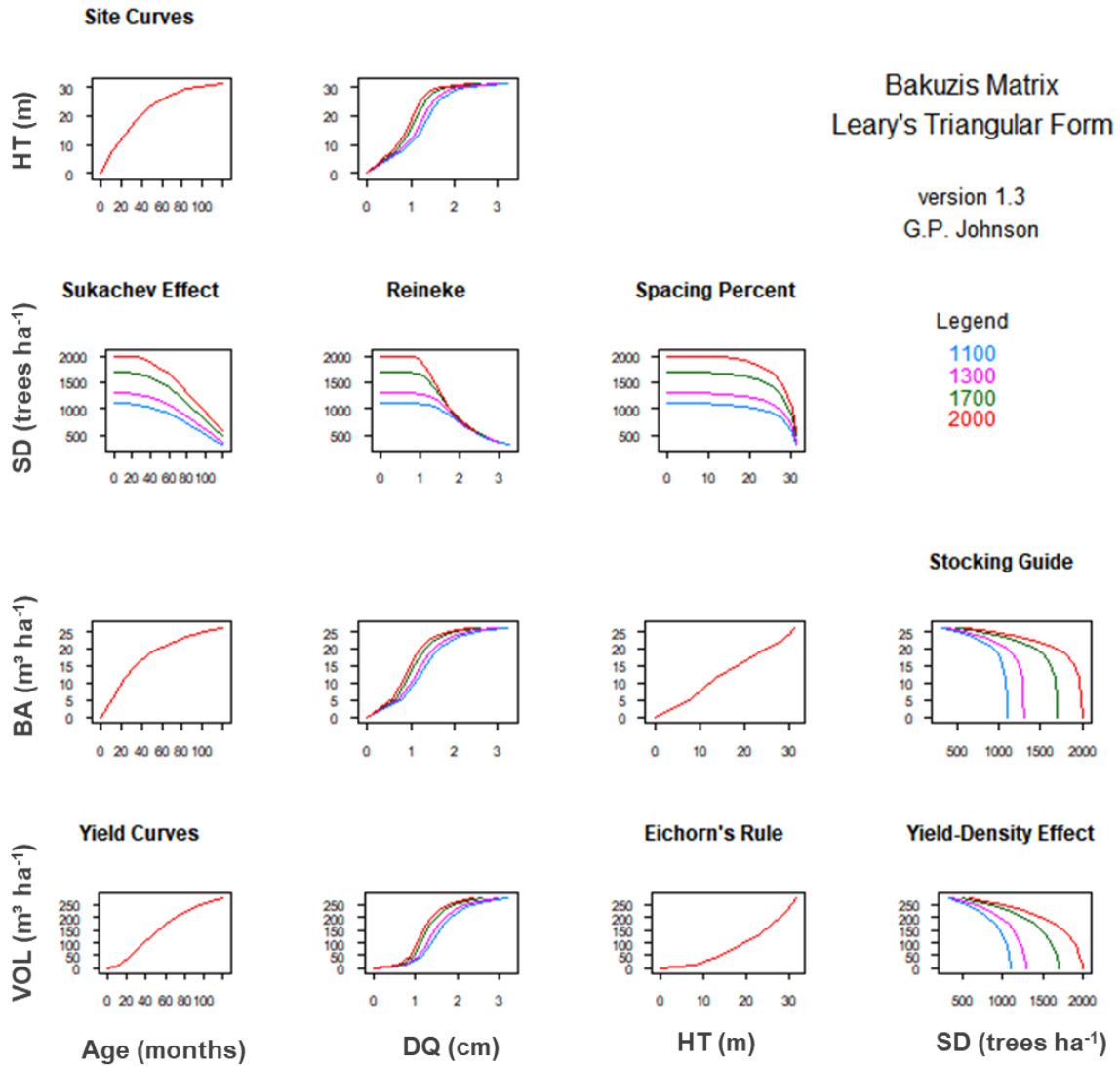


Figure 2.9 Bakuzis matrix of time-based stand growth model across different level of initial density (site class 26) for clone A.

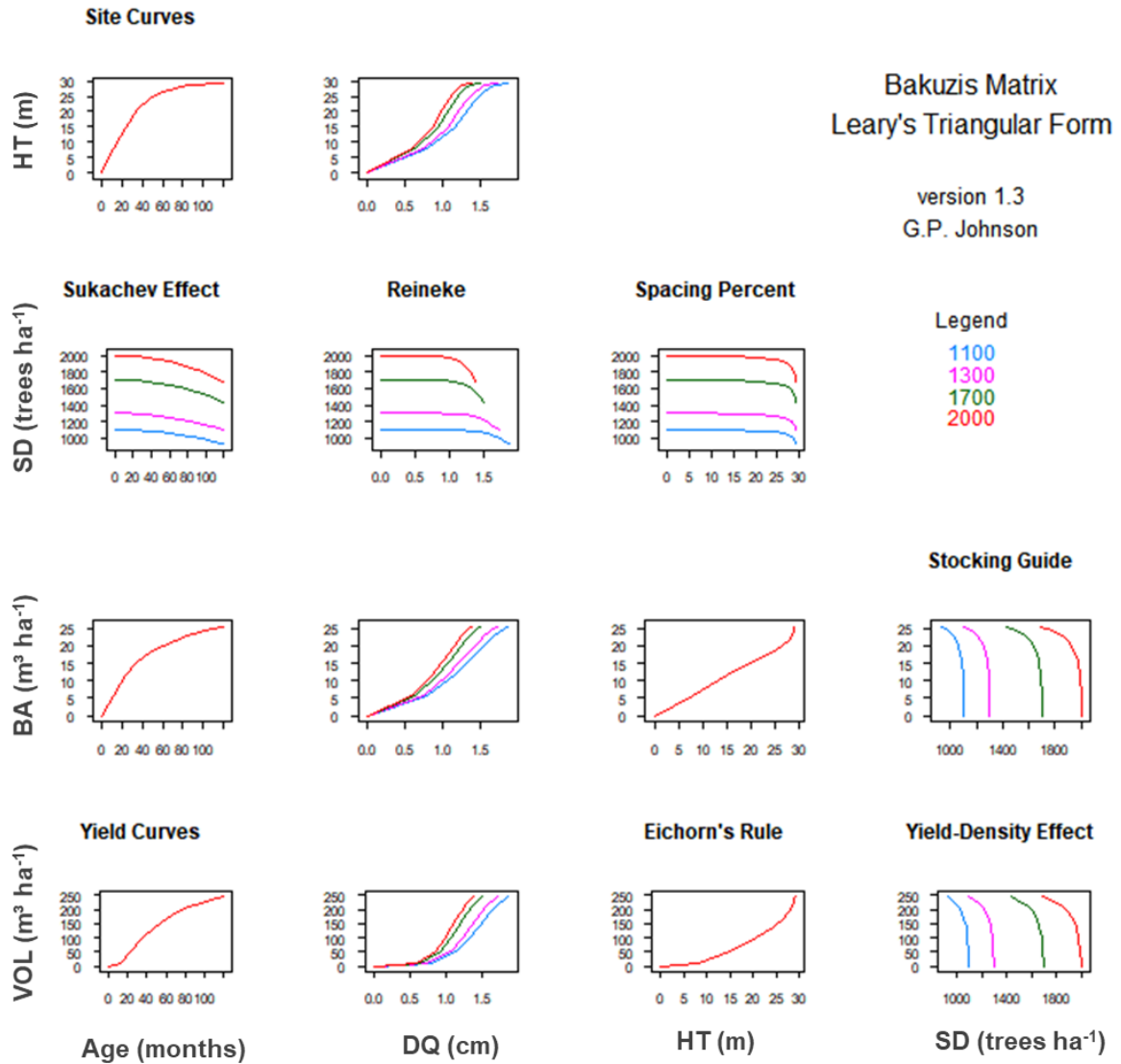


Figure 2.10 Bakuzis matrix of time-based stand growth model across different level of initial density (site class 26) for clone B.

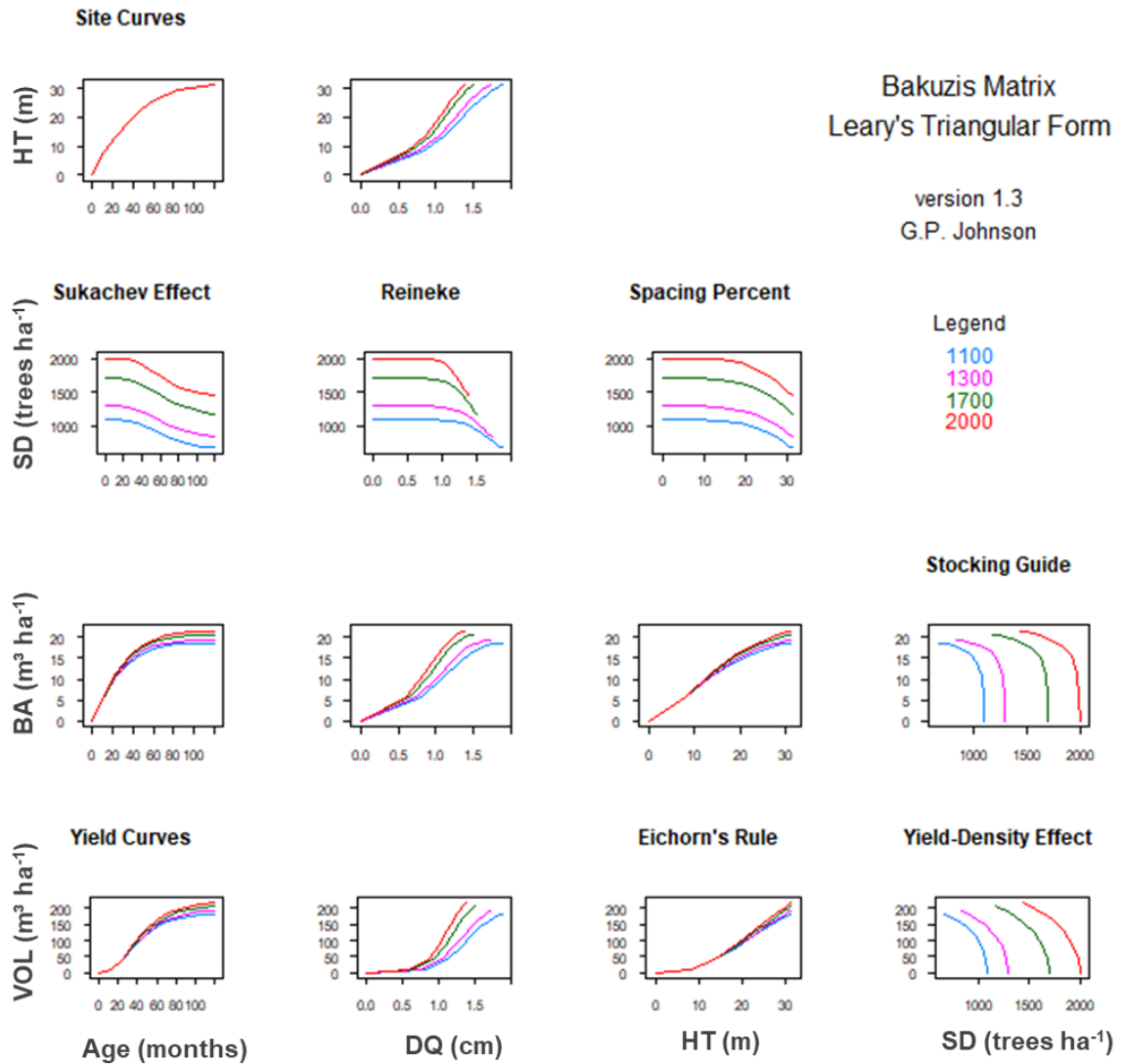


Figure 2.11 Bakuzis matrix of state-space stand growth model across different level of initial density (site class 26) for clone A.

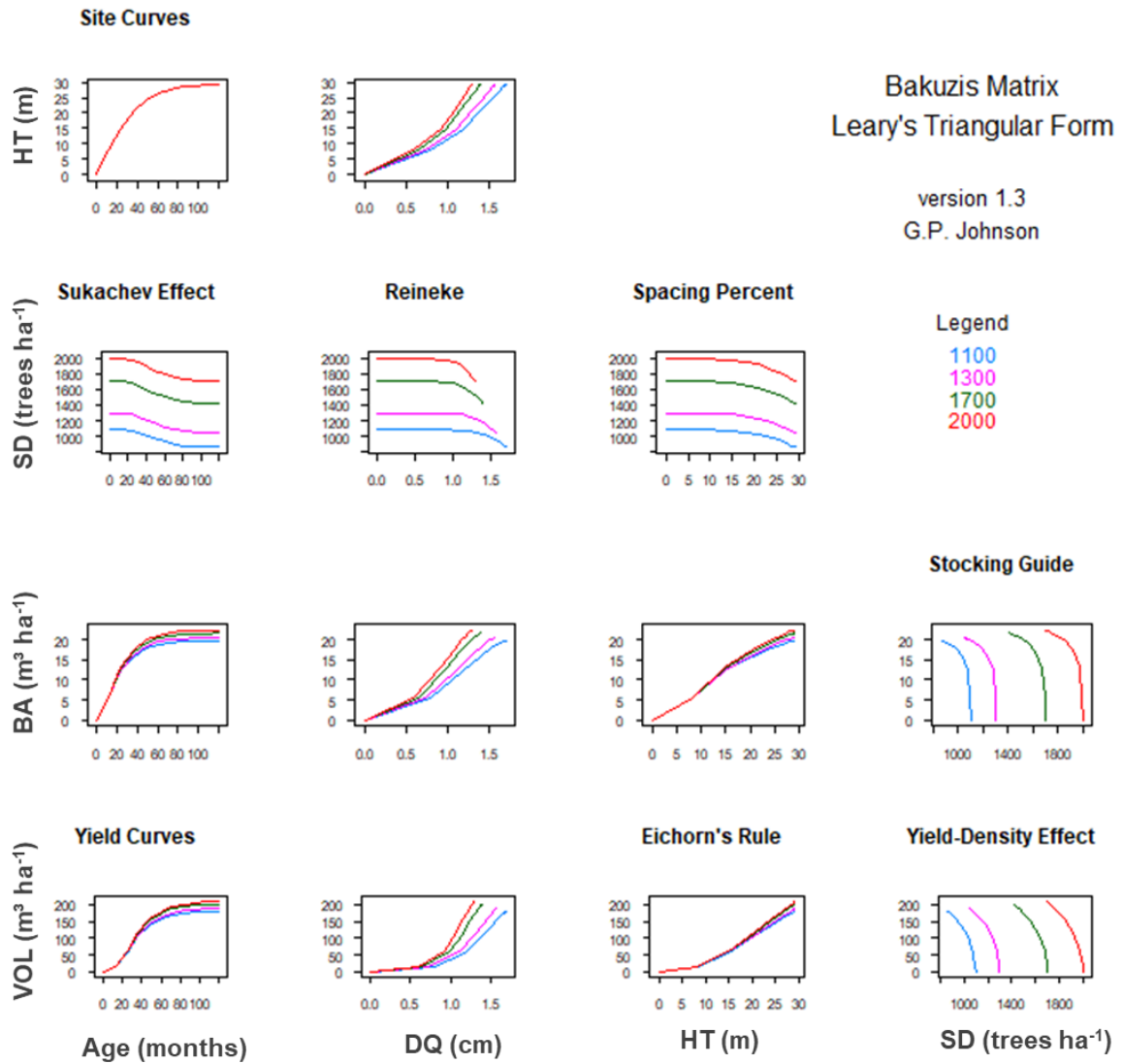


Figure 2.12 Bakuzis matrix of state-space stand growth model across different level of initial density (site class 26) for clone B.

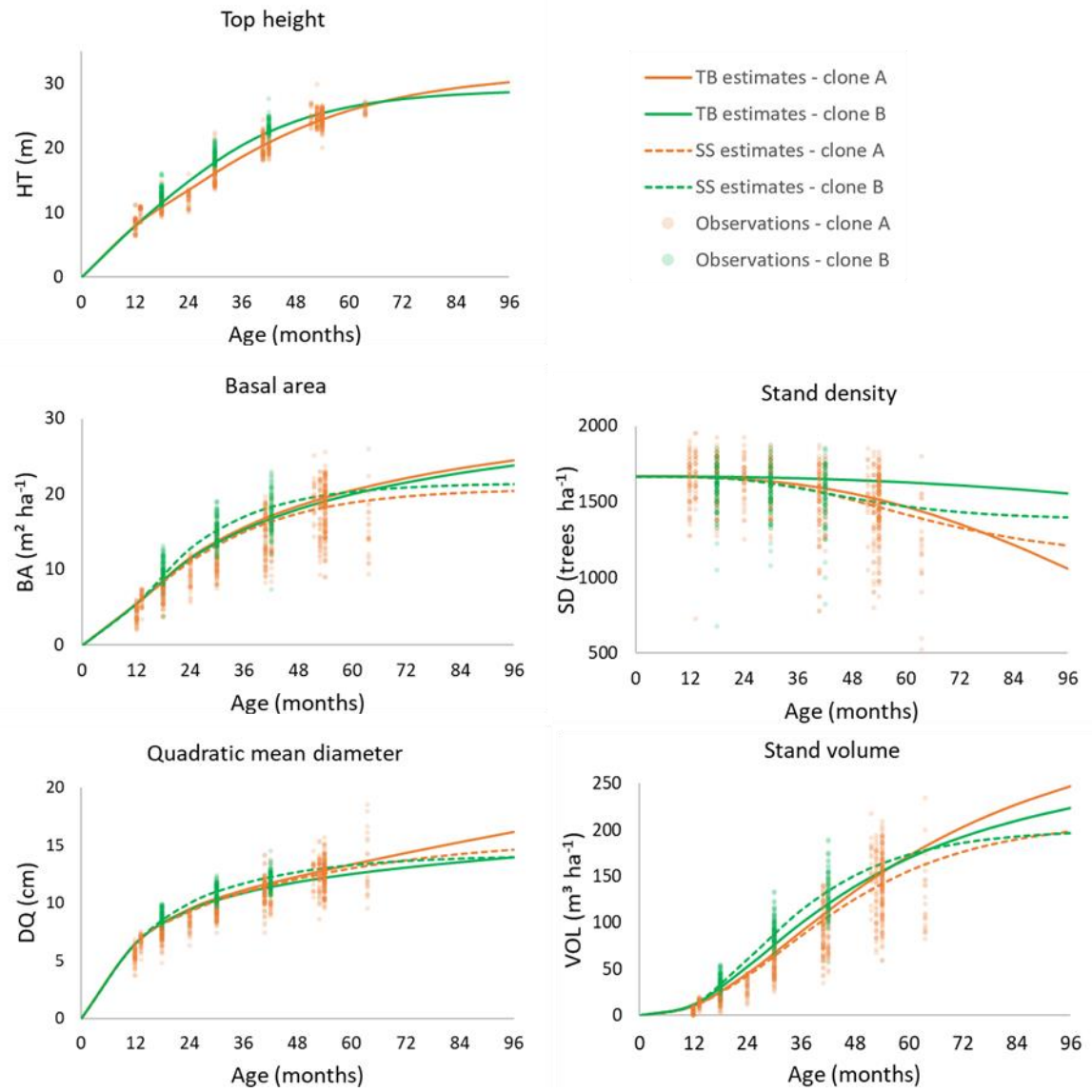


Figure 2.13 Behavior of observed and predicted stand attributes trend over age with initial density 1667 trees·ha⁻¹ and site class 26 using either a time-based (TB) or state-space (SS) approach

**Chapter 3: Diameter distribution model development of tropical hybrid
Eucalyptus clonal plantations in Sumatera, Indonesia: A comparison of
estimation methods**

3.1 Introduction

Whole-stand models are advantageous when management focus is on a single product (Burkhart and Tomé 2012) and provide accurate estimates of long-term growth at low resolutions (Qin and Cao 2006). However, effective forest management and planning often requires information about the distribution of volume by size and product classes (Burkhart and Tomé 2012). Size-class and individual-tree models are required for predicting distributions of multiple products (Vanclay 1994), since they provide detailed yield estimates by size (Miguel et al. 2010). Size-class models predict diameter distributions and provide estimates of forest attributes (such as the number of trees, basal area, and volume per unit area) by diameter class (Poudel and Cao 2013).

Diameter distributions are indicators of growing-stock structure (Loetsch et al. 1973). The concept of diameter distributions is not new to forestry literature (DeLiocourt 1898). Several probability density functions are used to describe the structure of forest stands, including the beta (Bennett and Clutter 1968; Lenhart and Clutter 1971; Loetsch et al. 1973; Burkhart and Strub 1974; Bennett et al. 1978; Gorgoso et al. 2012; Ogana et al. 2015), Johnson's SB (Hafley and Schreuder 1977; Knoebel and Burkhart 1991; Zhou and McTague 1996; Gorgoso and Rojo-Alboreca 2014), gamma (Nelson 1964; Zhang and Zhou 2010; Eslami et al. 2011; Ogana et al. 2015) and Weibull distributions (Bailey and Dell 1973). The Weibull distribution is the most widely used diameter distribution models (Burkhart & Tomé 2012) and one of the best-performing among other distributions (Eisfeld et al. 2005).

The Weibull distribution is a flexible distribution function capable of fitting a variety of distribution shapes (Poudel and Cao 2013). It has a lower bound and

calculations of proportions of trees across diameter classes is straightforward and does not require numeric integration (Cao 2012). In addition, the parameters of the Weibull distribution are generally well correlated with several stand-level attributes (Bailey and Dell 1973), such as dominant height, quadratic mean diameter, and mean diameter (Sghaier et al. 2016). Because of its flexibility, the Weibull distribution is applicable to many different species and forest structures from pure, single cohort, even-aged stands to multispecies, multicohort, uneven-aged stands (Matney and Sullivan 1982; Knowe et al. 1994; Knowe and Stein 1995; Siipilehto 1999; Cao 2004; Newton et al. 2005).

The three-parameter Weibull distribution function is commonly used to quantify tree diameter distributions because of its flexibility in fitting a variety of shapes and degrees of skewness, the relative simplicity of estimating its parameters, and the distribution has a closed-form solution for the cumulative density function (Bailey and Dell 1973; Bowling et al. 1989; Little 1983; Matney and Sullivan 1982; Rennolls et al. 1985; Schreuder and Swank 1974; Zarnoch et al. 1991). The probability density function (PDF) for the three-parameter Weibull distribution is:

$$f(x) = \frac{c}{b} \left(\frac{x-a}{b}\right)^{c-1} \exp\left[-\left(\frac{x-a}{b}\right)^c\right] \quad (a \leq x < \infty) \quad (3.1)$$

$$= 0, \text{ otherwise}$$

Integration yields a closed-form cumulative distribution function (CDF):

$$F(X \leq x) = 1 - \exp\left[-\left(\frac{x-a}{b}\right)^c\right] \quad (a \leq x < \infty) \quad (3.2)$$

The parameter a is referred to as the location parameter, b is the scale parameter, c is the shape parameter and x is diameter at breast height (Clutter et al. 1983). The b and c

parameters must be positive, while mathematically a can be positive, zero, or negative (provided $x - a \geq 0$). For diameter distribution applications a is nonnegative.

For shape (c) parameters less than 1, the Weibull distribution assumes the classic inverse J-shape found in uneven-aged stands, while when c equals 1, the negative exponential distribution results. Mound shape curves typical of even-aged stands are produced for c greater than 1 (Burkhardt and Tomé 2012). When c is equal 3.6 the Weibull distribution is symmetrical, approximating a normal distribution shape. Right skewed curves are defined for c less than 3.6 and left-skewed curves for c greater than 3.6. As c approaches infinity the distribution approaches a spike over a single point (Burkhardt and Tomé 2012). The location parameter often is assumed known in many cases, so it is logical to set this parameter to the smallest value or the lower limit of diameter measurement (Kershaw et al. 2016).

Parameter estimates based on maximum likelihood methods for the Weibull distribution requires individual tree data (Bolker 2008). Maximum likelihood estimation has several desirable statistical properties, such as consistency and asymptotic normality (Royle and Dozario 2008), and provides better estimates compared to other methods (Zhou and McTague 1996). However, it requires more computational resources (Cao and McCarty 2006) and individual tree measurements. In most forestry applications, diameter distributions are generally predicted from characteristics measured in a stand of interest. Hyink and Moser (1983) presented a generalized framework for estimating diameter distributions using parameter prediction methods (PPM) and parameter recovery methods (PRM). In the PPM approach, the future parameters of the distribution model are directly predicted from the current parameters and other information about the stand such as

density, basal area, volume, etc. (Kershaw et al. 2016). The PPM uses the location (a), scale (b), and shape (c) parameters as the dependent variables, which have been previously estimated using maximum likelihood methods (Cao 2004). In the PRM approach, future values of stand parameters are directly predicted, and the parameters of the diameter distribution are derived from the stand parameters (Kershaw et al. 2016).

The parameter prediction approach with the Weibull distribution has been applied to many different species and forest types: pine (*Pinus taeda* L. and *Pinus echinate* Mill.) plantations (Smalley and Bailey 1974 a,b); slash pine (*Pinus elliottii*) plantations (Dell et al. 1979); longleaf pine (*Pinus palustris* Mill.) plantations (Leduc et al. 2001); loblolly pine (*Pinus taeda*) plantations (Clutter et al. 1984; Feduccia et al. 1979; Smalley and Bailey 1974a); natural slash pine (*Pinus elliotti*) stands (Schreuder et al. 1979); mixed stands of western hemlock and Douglas-fir (*Pseudotsuga menziesii* and *Tsuga heterophylla*) (Little 1983); Sitka spruce (*Picea sitchensis*) plantations (Rennolls et al. 1985); and Norway spruce (*Picea abies*) plantations (Kilikki and Päivinen 1986; Kilikki et al. 1989; Siipilehto 1999). While parameter predictions can be easily derived from regression equations fit to precisely estimated diameter distributions, these models often produce poor parameter predictions, low R^2 values for the a and c parameters, and are not responsive to silvicultural treatments (Hyink and Moser 1983). Because PPM does not work very well in many cases, this approach is not considered in this study.

According to Siipilehto and Mehtätalo (2013), there are two main options for PRM approaches: moment-based and percentile-based estimation. The PRM moment-based approach solves for the Weibull parameters using the moments of the diameter distribution that are estimated from regression equations using a variety of stand

characteristics (Bowling et al. 1989; Hyink and Moser 1983; Knoebel et al. 1986; Lindsay et al. 1996; Matney and Sullivan 1982; Newton et al. 2004; Strub and Burkhart 1975). The percentile-based method predicts the Weibull parameters using percentiles of the diameter distribution that are also estimated from stand characteristics (Bailey et al. 1989; Brooks et al. 1992; Lohrey and Bailey 1976; Knowe 1992; Magnussen 1986; McTague and Bailey 1987). In addition, some other methods have been proposed such as a hybrid approach (McTague and Bailey 1987), cumulative distribution function regressions (CDFR; Cao 2004), and modified CDFRs (Poudel and Cao 2013).

A successful diameter-distribution model requires good predictions of its parameters. The PRM approach was proposed to compatibly with stand-average growth and yield models developed from the underlying diameter distribution data (Hyink and Moser 1983). The overall objective of this analysis was to evaluate different parameter recovery methods for predicting parameters of the Weibull PDF for characterizing diameter distributions of Eucalyptus hybrid clone plantation in Sumatera, Indonesia. The specific objectives were to: (1) compare moment-based, percentile-based and hybrid methods; (2) determine the best approach for robustly deriving diameter distributions across a full range of conditions; and (3) based on observed performance, predict moments and/or percentiles from stand and site characteristics using nonlinear regression analyses.

3.2 Methods

3.2.1 Study site

This study was conducted in Sector Teso East of PT. Riau Andalan Pulp and Paper, a member of Asia Pacific Resources International Holding Limited (APRIL) Group and used inventory plot data from *Eucalyptus hybrid* plantations. Teso East is 19,600 ha in size and is located in the central region of Sumatera Island, Riau Province, Indonesia in the Kampar and Kuantan Singingi regencies between 101° 18' E and 101° 32' E, and 00° 09' N and 00° 03' N. The region is characterized by a wet tropical climate with average rainfall ranging from 2000-3000 mm per year, and the average rainy days is around 160 days per year. The annual average temperature is 27.6 °C with an average minimum of 21.8 °C and an average maximum of 35 °C.

Until now, Estate Teso East has had its fifth rotation. The first rotation was planted with *Acacia mangium* in 1995 and then *Eucalyptus sp.* was planted on a large scale starting in 2010. Based on the soil characteristics, this study location was dominated by soil horizon B (topsoil) and C (parent material). Most of the minerals derived from parent material with organic materials, good for both plants and other organisms to live. This plantation area is relatively flat with slopes ranging from 0 – 15% and low elevation ranging from 30 – 90 meters above sea level.

3.2.2 Data collection

In APRIL plantations, DBHs are measured beginning at 18 months. All live trees with DBH of 1.0 cm and greater on each plot (0.04 ha in size) are measured using a diameter tape at 1.3 meters above the ground as measured from the uphill side of the

stem. Each tree is assigned a status (live or dead), and assessed for wind damage, pest, and diseases. Plots are remeasured on an annual basis after initial plot establishment.

3.2.3 Maximum likelihood estimation (MLE)

Weibull parameters were estimated using the individual tree DBH measurements from each plot at each measurement period using maximum likelihood estimation (MLE) methods (Johnson et al. 1995; Casella and Berger 2001). The location parameter (a) was set to 1 cm in this study, and the MLE estimates of the scale (b) and shape (c) parameters were used as reference distributions to compare with the recovered parameter estimates.

The likelihood function of the Weibull PDF (eq. 3.1):

$$L(x_1, \dots, x_n; b, c) = \prod_{i=1}^n \frac{c}{b} \left(\frac{x}{b}\right)^{c-1} \exp\left(-\left(\frac{D}{b}\right)^c\right) \quad (3.3)$$

MLEs were obtained by minimizing the negative of the logarithm of the likelihood function.

3.2.4 Moment-based parameter recovery

In moment-based parameter recovery, regression equations, as a function of mean top height, stand density, age, or relative density, are used to predict the arithmetic mean diameter (\bar{D} , the first moment) and the quadratic mean diameter (DQ, the square root of the second moment). As with the MLE estimates, we set $a = 1$, our minimum measured DBH. Weibull parameters are then recovered from the arithmetic mean diameter (\bar{D}) and quadratic mean diameter (DQ) using (Burkhardt and Tomé 2012):

$$b = \frac{(\hat{\bar{D}} - a)}{\Gamma_1} \quad (3.4)$$

$$\widehat{DQ}^2 - a^2 2a\widehat{D} - b^2 \Gamma_2 = 0 \quad (3.5)$$

where \widehat{DQ} is predicted DQ, \widehat{D} is predicted \bar{D} , $\Gamma_i = \Gamma\left(1 + \frac{i}{c}\right)$ and a , b , and c are recovered Weibull parameters. Equations 3.4 and 3.5 were numerically solved to recover the parameters.

3.2.5 Percentile-based parameter recovery

Percentile estimation of the Weibull parameters are relatively. Like the moments, the percentiles are functions of the distribution parameters and are often highly correlated with stand characteristics (Borders et al. 1987; Knowe 1992; Knowe et al. 1992). If three sample percentiles are known, each can be equated to its corresponding Weibull cumulative distribution function value and the three equations can be solved iteratively for estimates of a , b , and c (Burkhart and Tomé 2012). If the location parameter is assumed known, then only two percentiles are required to estimate b and c . Given the Weibull cumulative distribution function (Equation 2), and letting \widehat{D}_p represent the estimated p^{th} percentile value of diameter in the sample, then

$$p = 1 - \exp\left\{-\left[\frac{(\widehat{D}_p - a)}{b}\right]^c\right\} \quad (3.6)$$

Solving Equation 3.6 for \widehat{D}_p yields:

$$\widehat{D}_p = a + b[-\ln(1 - p)]^{\frac{1}{c}} \quad (3.7)$$

The scale parameter, b , is given by:

$$b = \frac{\widehat{D}_p - a}{[-\ln(1 - p)]^{\frac{1}{c}}} \quad (3.8)$$

Given two percentiles p_1 and p_2 where $p_1 < p_2$, c is estimated using:

$$c = \frac{\ln\left(\frac{\ln(1-p_2)}{\ln(1-p_1)}\right)}{\ln(\widehat{D}_{p_2} - a) - \ln(\widehat{D}_{p_1} - a)} \quad (3.9)$$

Theoretically, any two percentiles can be used; however, Bailey et al. (1989) found best performance resulted when percentiles represented a broader proportion of the distribution. In this study, I used the 25th and 99th diameter percentiles to recover parameters b and c of Weibull distribution.

3.2.6 Hybrid method parameter recovery

The hybrid approach uses a combination moments and percentiles (Bailey et al. 1989; Brooks et al. 1992; Knowe et al. 2005; Lee and Coble 2006; Coble and Lee 2008; Jiang and Brooks 2009). As in both the moment-based approach and the percentile-based approach, the location parameter was assumed known (i.e., $a = 1$), and the b and c parameters were recovered from a moment estimate and two percentile estimates using (Bailey et al. 1989):

$$b = -a \frac{\Gamma_1}{\Gamma_2} + \left[\left(\frac{a}{\Gamma_2} \right)^2 (\Gamma_1^2 - \Gamma_2) + \frac{\widehat{DQ}^2}{\Gamma_2} \right]^{0.5} \quad (3.10)$$

$$c = \frac{\ln\left(\frac{\ln(1-p_2)}{\ln(1-p_1)}\right)}{\ln(\widehat{D}_{p_2} - a) - \ln(\widehat{D}_{p_1} - a)} \quad (3.11)$$

Here we used estimates of DQ, 25th and 99th diameter percentiles to estimate b and c .

3.2.7 Moment and Percentile Estimation

The quadratic mean diameter, arithmetic mean diameter, and the percentiles were calculated for each plot and measurement period using the individual tree DBH data. To relate with the stand characteristic, regression equation forms used to predict the diameter moments or percentiles (e.g., Matney and Farrar 1992; Baldwin and Feduccia 1987; Cao 2004). In this study, the logistic form is used to predict arithmetic mean diameter (\bar{D}) and a modified general form of the regression equation from Cao (2004) to predict diameter percentiles with additional DQ variables to be compatible with stand-level models.

DQ was estimated using the relationship of basal area and stand density. In Chapter 2, the stand density model from Clutter et al. (1983) and basal area model derived from the Schumacher polymorphic equation were the best fit based on evaluation of several models tested, and project future attributes to any point in time. These time-based models gave DQ estimation with rMSE = 0.72 cm and explained 85% of the variability (Table 2.15).

Arithmetic mean diameter (\bar{D}) was estimated from the derived DQ using:

$$\bar{D} = DQ \left(\frac{\exp(b_0 + b_1 RD + b_2 \ln HT + b_3/A)}{1 + \exp(b_0 + b_1 RD + b_2 \ln HT + b_3/A)} \right) + \epsilon \quad (3.12)$$

and percentiles were estimated using:

$$D_i = \exp[b_0 + DQ (b_1 RD + b_2 \ln HT + b_3/A)] + \epsilon_i \quad (3.13)$$

where \bar{D} is arithmetic mean diameter (cm); D_i is the i^{th} diameter percentile (cm); DQ is the quadratic mean diameter (cm); RD is a relative density which is defined as the ratio of actual density to the maximum density attainable in a stand with the same mean tree size; HT is the top height (m); A is stand age (months); b_i are regression parameters and ϵ is

random error. Equation (12) assures the required relationship $DQ > \bar{D}$ because the logistic component, $\frac{\exp(b_0 + \dots + b_4/A)}{1 + \exp(b_0 + \dots + b_4/A)} < 1$, and $\exp(x) > 0$. Fitted Eqs. 3.12 and 3.13 were used to predict each plot \times measurement period moments.

Nonlinear regression was used to evaluate the goodness of fit for moment and percentiles estimation, initially. Then I included clone and site class as random effects into the regression equations and nonlinear mixed effects methods to estimate fixed and random effects in each model. A likelihood ratio test used to assess if the random effect significantly improved model fit (Weiskittel et al. 2011).

3.2.8 Model evaluation

The Kolmogorov-Smirnov (KS) statistic (Massey 1951) and an error-index (EI; Reynolds et al. 1988) were computed for each method to evaluate the three prediction methods. Using a significance level 5%, the KS test was used to compare the estimated cumulative frequency and the observed frequency. The method producing the lowest average KS statistics and error-index values was the best method. All estimation and analyses were carried out using the R statistical language (R Core Team 2020).

3.3 Result

3.3.1 Moment and percentile prediction models

Using nonlinear least square analysis, all coefficients for Equation 3.12 and 3.13 to predict arithmetic mean diameter and diameter percentiles were significant ($p < 0.05$). Consequently, all parameters associated with stand characteristics (DQ, RD, HT, and A) were included for mixed-effect analysis that involved clone and site class within clone as

random effects (Tables 3.1 – 3.3). Based on the likelihood ratio test, the best random-effects models included all coefficients as random effects of clone and site class within the clone (Tables 3.1 – 3.3). Parameter estimates and their associated standard errors (in parentheses), random effects standard deviations, and goodness-of-fit statistics for the arithmetic mean diameter, 25th and 99th diameter percentiles were shown in Tables 3.1 – 3.3. The full model with fixed and random effect accounted for 99%, 77% and 93% of the variation for \bar{D} (Table 3.1), D_{25} (Table 3.2) and D_{99} (Table 3.3) prediction models, respectively (Table 1). The D_{25} percentile model has the lowest performance compare to \bar{D} and D_{99} models. Differences between clones were greater than differences across sites within clones for almost all modeling parameters, except b_1 and b_2 that associated with D_{99} model prediction (Table 3.1 – 3.3). Coefficient estimates of random effect model by clone and site classes for all prediction models were shown in Tables 3.4 – 3.6.

3.3.2 Characteristics of Maximum Likelihood Estimates

The estimated Weibull scale parameters, b , based on the MLE method ranged 3.95 to 15.11 and the shape parameters, c , ranged from 1.68 - 11.50 (Table 3.7). Based on the K-S test, estimated diameter distributions were not significantly ($p > .05$) different from the observed diameter distributions for 68% (CI = 95%) and 80% (CI = 99%) of the observed Eucalyptus hybrid clone diameter distributions (Table 3.8). The scale parameter increased, and the shape parameter decreased, with increasing age and site class for both clones (Figure 3.1). For a similar stand age, clone A had lower scale and shape parameters than clone B. In addition, clone B had smaller variation in scale parameter but higher variation in shape parameter than clone A (Figure 3.1).

3.3.3 Diameter distribution model evaluation

Table 3.7 summarizes the parameter estimates for fit data using maximum likelihood (MLE) and the three parameter recovery methods (MOM, PCT, and HYB). The results of the three prediction methods indicated that all the three recovery methods provided relatively similar mean parameter estimates for the Weibull distribution function, with the average scale parameter in the range of 9.53 - 10.37, and the average shape parameter in the range of 2.80 – 3.46. The MOM and HYB methods were more similar to the MLE based on the average scale parameter, the PCT and HYB methods were relatively closer to the MLE based on the average shape parameter (Table 3.7; Figure 3.2). Shape parameters for HYB method were similar with the PCT that derived from the same variables and formulation (Table 3.7; Figure 3.2). Like most other applications, the shape parameter is more difficult to model than the scale parameter (Figure 3.2).

Based on the statistical model evaluation of three prediction methods, the MOM has the best fit based on the KS statistic at 0.1757, followed by the HYB and PCT with KS statistic at 0.1988 and 0.2125, respectively (Table 3.8). The KS statistic also indicated the coverage of estimated distributions fit the observed diameter distributions were 49% (MOM), 26% (PCT), and 37% (HYB) fall within 95% confidence intervals; and 66% (MOM), 44% (PCT), and 54% (HYB) that fall within 99% confidence intervals (Table 3.8). The MOM also had the lowest mean error-index at 26.5218, followed by HYB (27.7307) and PCT (31.4708) (Table 3.8). In terms of the differences in precision for predicting the Weibull parameter, the MOM has the lowest variability with the standard deviation of error index at 6.7118 and the PCT had the highest variability at 9.7699.

Although all approaches allow for a direct mathematical link between the predicted overall stand characteristics and a diameter distribution that is consistent with those characteristics, the moment-based method (MOM) indicated the best fit to the observed data when compared to other methods (PCT and HYB).

For evaluation, some graphical examination of the performance of the three recovery methods were conducted. Figure 3.3 illustrates the three methods for typical plots of the diameter distributions observed in the Eucalyptus hybrid clone plantations. The plots represent a range of clones, stand ages, and the variance of distribution typically observed in the region. Figure 3.3 (a) shows a unimodal distribution for clone A at 30 months and illustrates that three methods perform equally well for modeling the distribution of the plot. Figure 3.3 (b) shows a multimodal distribution. In this case, none of the three methods fitted the plot well and all missed the valley (8-9 cm) and the peak (13-14 cm). However, the MOM and PCT were better fits for the peak (6-7 cm) than the HYB. In Figure 3.3 (c) for clone B at 30 months with a distribution that is close to normal, the MOM is the best fit than the others. The PCT and HYB show a similar pattern for this plot. While in Figure 3.3 (d) with an irregular distribution, the MOM tends to deal with tails of both sides and MOM exhibited slightly greater flexibility in describing the larger variance than the two other methods.

3.4 Discussion

To be compatible with a recently developed stand-level growth and yield model (Chapter 2; Waldy et al., In Review), the predicted quadratic mean diameter played an important role in recovering parameters of the Weibull distribution that characterized the

future diameter distributions. In this study, the prediction models were quite good at predicting arithmetic mean diameter and 99th percentiles but relatively poor at predicting the 25th percentile. This means that stand attributes, especially DQ and A, have a stronger correlation with the arithmetic mean diameter and higher percentiles than lower percentiles, which has been found in similar analyses. For example, Cao (2012) found similar trends in predicting future diameter distributions of loblolly pine (*Pinus taeda* L.). He found that stand attributes explained more variability in estimating higher percentiles (50th percentile and above) than lower percentiles.

The method of moments is one of the most accurate methods for estimating the Weibull distribution parameters (Al-Fawzan 2000; Nanang 1998; Ueno and Osawa 1987; Shifley and Lentz 1985). Moments are the preferred method in growth and yield models because they ensure numeric compatibility and generally require fewer equations (Weiskittel et al. 2011). Our study indicated the MOM had a higher percentage of coverage for estimated distributions that fit the observed diameter distributions than PCT and HYB. This higher percentage for MOM in this study was likely because of sufficient sample sizes to model moment based recovery with an average number of trees of 60 trees per plot (plot size 0.04 ha). Bankston (2019) reported that larger plot sizes resulted in more accurate predicted diameter distributions. However, he suggested a plot size of 0.08 ha might be sufficient for model building for data from unthinned stands. A substantial decrease in error was no longer evident when plot size increased from 0.08 to 0.10 hectares. Shiver (1988) suggested a sample size of not less than 50 trees is required to obtain satisfactorily accurate estimates of the Weibull parameters, while simulation studies from Saborowski (1994) indicated that a sample with $n = 80$ could generally be

expected to produce satisfactory results. To get a better diameter distribution that represented plot-level measurements, modifying the plot size is not a logical decision for a well-established forest inventory system for the APRIL group. Instead of using Weibull distributions, other probability density functions (e.g., beta, Johnson's SB, gamma or lognormal) are potentially worth examining to describe the structure of a *Eucalyptus hybrid* clone in this region. Goodwin (2020) suggested several variants of the Weibull distribution. While some of those models produced better estimates of diameter distributions, Goodwin's recommendation for plantation was to use the 3-P Weibull distribution as done in this study.

Using simulated development of the MOM model predictions, the peakedness of the distribution is reduced for both clones with increasing stand age. The diameter distribution of clone A tends to become more positively skewed and the variation increases with increasing stand age (Figure 3.4), partly because of mortality in the lower tree strata, and thinnings from below, which remove the dominated trees or crown thinning (thinning from above), which remove dominating and co-dominating trees (van Laar and Akca 2007). The number of trees decreases in lower diameter classes and increases in upper classes, shifting curves to the right and increasing the flattening degree with increasing age. In clone B, the shape curves for all ages were almost similar and no significant increases in variation. These findings are relatively logical because the mortality for this clone is very low, so the diameter growth tends to uniform.

3.5 Conclusion

The aim of the present study was to compare different recovery methods for predicting parameters of the Weibull distribution for characterizing diameter distributions of Eucalyptus hybrid clone plantation in Indonesia. This diameter distribution prediction approach will help the company to differentiate its final product based on species, clone, and wood characteristics include diameter classes. In this study, the moment method was found to give the lowest mean error-index and KS statistic, followed by the hybrid and percentile methods. Although all three methods had difficulty in describing the multimodal diameter distributions, the moment method tends to be more robust with tails on both sides of the distribution and exhibited slightly greater flexibility in describing the larger variance than the two other methods. Overall, the Weibull approach appeared relatively robust in determining diameter distributions of Eucalyptus hybrid clone plantation in Indonesia, yet some refinements may be necessary to characterize more complex distributions.

3.6 References

- Al-Fawzan, M.A. 2000. Methods for estimating the parameters of the Weibull distribution. InterStat, statistics on the Internet. Online in Internet: URL:<http://www.ip.statjournals.net:2002/InterStat/ARTICLES/2000/abstracts/OO0001.html-ssi> [Cited 2020-09-10]
- Bailey, R.L., and Dell, T.R. 1973. Quantifying diameter distributions with the Weibull function. *Forest Sciences*, 19, 97–104.
- Bailey, R.L., Burgan, T.M., Jokela, E.J. 1989. Fertilized mid-rotation-aged slash pine plantations-stand structure and yield prediction models. *South J Appl For.* 13:76-80
- Baldwin, V. Clark, Jr., Feduccia, D.P. 1987. Loblolly pine growth and yield prediction for managed West Gulf plantations. Res. Pap. SO-236. New Orleans, LA: U.S. Department of Agriculture, Forest Service, Southern Forest Experiment Station. 27 p.
- Bankston, S. 2019. Sample-plot size and diameter moments/percentiles prediction model effects on stand diameter distribution recovery accuracy. Thesis. Department of Forestry, Mississippi State University
- Bennett, F.A., and J.L. Clutter. 1968. Multiple-product yield estimates for un-thinned slash pine plantations-Pulpwood, saw timber, gum. USDA For. Serv., Res. Paper SE-35. 21 p.

- Bennett, F.A., Lloyd, F.T, Swindel, B.F., and Whitehorne, E.W. 1978. Yields of veneer and associated products from un-thinned, old-field plantations of slash pine in the north Florida and South Georgia flatwoods. USDA For. Serv., Res. Paper SE-176. 80 p.
- Bolker, B.M. 2008. Ecological models and data in R. 1st ed. Princeton Univ. Press, Princeton, NJ. 396 p.
- Borders, B.E., Patterson, W.D. 1990. Projecting stand tables: a comparison of the Weibull diameter distribution method, a percentile-based projection method, and a basal area growth projection method. *Forest Sci.* 36, 413–424.
- Borders, B.E., Souter, R.A., Bailey, R.L., and Ware, K.D. 1987. Percentile-based distributions characterize forest stand tables. *For. Sci.* 33: 570–576.
- Bowling, E.H., Burkhart, H.E., Burk, T.E., and Beck, D.E. 1989. A stand-level multispecies growth model for Appalachian hardwoods. *Can. J. For. Res.* 19: 405-412.
- Brooks, J.R, Borders, B.E, Bailey, R.L. 1992. Predicting diameter distributions for site-prepared loblolly and slash pine plantations *South. J. Appl. For.* 16 130–133
- Burkhart, H.E., and Strub, M.R. 1974. A model for simulation of planted loblolly pine stands. P. 128–135 in *Growth models for tree and stand simulation*, Fries, J. (ed.). Royal College of Forestry, Stockholm.
- Burkhart, H.E., and Tomé, M. 2012. *Modeling forest trees and stands*. Dordrecht; New York: Springer.
- Cao, Q.V. 2004. Predicting parameters of a Weibull function for modelling diameter distribution. *Forest Sci.* 50, 682–685.

- Cao, Q.V. 2012. Use of the Weibull function to predict future diameter distributions from current plot data. In: Butnor, John R., ed. 2012. Proceedings of the 16th biennial southern silvicultural research conference. e-Gen. Tech. Rep. SRS-156. Asheville, NC: U.S. Department of Agriculture Forest Service, Southern Research Station. 53-58.
- Cao Q.V., Burkhart, H.E., Lemin, R.C. Jr. 1982. Diameter distributions and yields of thinned loblolly pine plantations. Virginia Polytechnic Institute and State University, Blacksburg, Pub FWS-1-82
- Cao, Q.V., and McCarty, S.M. 2006. New methods for estimating parameters of Weibull functions to characterize future diameter distributions in forest stands. Proc South Silv Res Conf USDA For Serv Gen Tech Rep SRS-92:338-340
- Casella, G., Berger, R.L. 2001. Statistical inference, 2nd ed. Duxbury, Thomson Learning, 660 pp.
- Clutter, J.L., J.C. Fortson, L.V. Pienaar, G.H. Brister, and R.L. Bailey. 1983. Timber management: A quantitative approach. John Wiley & Sons, Inc. 333 p.
- Clutter, J.L., Harms, R.W., Brister, G.H., and Rheney, J.W. 1984. Stand structure and yields of site-prepared loblolly pine plantations in the lower coastal plain of the Carolinas, Georgia, and north Florida. USDA For. Serv. Gen. Tech. Rep. SE-27.
- Coble, D.W., and Y.J. Lee. 2008. A new diameter distribution model for unmanaged slash pine plantations in east Texas. South. J. Appl. For. 32(2):89-94.
- de Liocourt, F. 1898. De l'amenagement des sapinieres. Bulletin Trimestriel, Societe Forestiere de Franche-Comte et Belfort, Julliet. pp. 396-409.

- Dell, T.R., Fedducia, D.P., Campbell, T.E., Mann, W.F. Jr, Polmer, B.H. 1979. Yields of un-thinned slash pine plantations on cutover sites in the west Gulf region. USDA Forest Service, Southern Forest Experiment Station, New Orleans, Research Paper SO-147
- Eisfeld, R.L., Sanquetta, C.R., Arce, J.E., Maestri, R., and Weber, K.S. 2005. Growth and yield modelling of *Pinus taeda* L. using probability function. *Floresta* 35(2): 317-328. doi:10.5380/rf.v35i2.4619
- Eslami, A.R., Karimi, B., Payam, H., and Derakhshan, O.K. 2011. Investigation of the structure and distribution diameter classes models in beech forests of northern Iran. *African Journal of Agricultural Research*, 6(10), 2157–2165.
- Feduccia, D.P., Dell, T.R., Mann, W.F. Jr, Campbell, T.E., Polmer, B.H. 1979. Yields of un-thinned loblolly pine plantations on cutover sites in the west Gulf region. USDA Forest Service, Southern Forest Experiment Station, New Orleans, Research Paper SO-148
- Goodwin, A.N. 2020. A blind spot in the use of the Weibull function for modeling diameter distributions. *Forest Science*. <https://doi.org/10.1093/forsci/fxaa042>
- Gorgoso, J. J., Rojo, A., Camara-Obregon, A., and Dieguez-Aranda, U. 2012. A comparison of estimation methods for fitting Weibull, Johnson's SB and beta functions to *Pinus pinaster*, *Pinus radiata* and *Pinus sylvestris* stands in northwest Spain. *Forest Systems*, 21(3), 446–459. doi:10.5424/fs/2012213-02736

- Gorgoso-Varela, J. J., and Rojo-Alboreca, A. 2014. Short communication: A comparison of estimation methods for fitting Weibull and Johnson's SB functions to pedunculate oak (*Quercus robur*) and birch (*Betula pubescens*) stands in northwest Spain. *Forest Systems*, 23(3), 500– 505. doi:10.5424/fs/2014233-04939
- Hafley, W.L., and Schreuder, H.T. 1977. A useful bivariate distribution for describing stand structure of tree heights and diameters. *Biometrics*, 33, 471–478. doi:10.2307/2529361
- Hyink, D.M. and Moser, J.W. 1983. A generalized framework for projecting forest yield and stand structure using diameter distributions. *For. Sci.* 29: 85-95
- Jiang, L., and Brooks, J. R. 2009. Predicting diameter distributions for young longleaf pine plantations in Southwest Georgia, *Southern Journal of Applied Forestry*, Volume 33, Issue 1, February 2009, Pages 25–28, <https://doi.org/10.1093/sjaf/33.1.25>
- Johnson, N.L., Kotz, S., Balakrishnan, N. 1995. *Continuous univariate distributions*, 2nd ed. Wiley. 756 pp.
- Kershaw, J.A. Jr., Ducey, M.J., Beers, T.W., Husch, B. 2016. *Forest Mensuration*, 5th edn. Wiley/Blackwell, Hoboken, NJ
- Kilkki, P., and Paivinen, R. 1986. Weibull function in the estimation of the basal area dbh-distribution. *Silva Fenn.* 20: 149–156
- Kilkki, P., Maltamo, M., Mykkanen, R., Paivinen, R. 1989. Use of the Weibull function in estimating the basal area dbh-distribution. *Silva Fennica*, 23: 311–318

- Knoebel, B.R., and Burkhart, H.E. 1991. A bivariate distribution approach to modeling forest diameter distributions at two points in time. *Biometrics*, 47, 241–253.
doi:10.2307/2532509
- Knoebel, B.R., Burkhart, H.E., Beck, D.E. 1986. A growth and yield model for thinned stands of yellow-poplar, *Forest Science*, Volume 32, Issue suppl_2, June 1986,
<https://doi.org/10.1093/forestscience/32.s2.a0001>
- Knowe, S.A. 1992. Basal area and diameter distribution models for loblolly pine plantations with hardwood competition in the piedmont and upper coastal plain. *South. J. Appl. For.* 16: 93–98.
- Knowe, S.A., Foster, G.S., Roussau, R.J., Nance, W.L. 1994. Eastern cottonwood clonal mixing study: predicted diameter distributions. *Can. J. Forest Res.* 24, 405–414.
- Knowe, S.A., Harrington, T.B., and Shula, R.G. 1992. Incorporating the effects of interspecific competition and vegetation management treatments in diameter distribution models for Douglas-fir saplings. *Can. J. For. Res.* 22: 1255–1262.
- Knowe, S.A., Radosevich, S.R. and Shula, R.G. 2005. Basal area and diameter distribution prediction equations for young Douglas-Fir plantations with hardwood competition: coast ranges. *West. J. Appl. For.* 20 (2), 73–93.
- Knowe, S.A., Stein, W.I., 1995. Predicting the effects of site preparation and protection on development of young Douglas-fir plantations. *Can. J. Forest Res.* 25, 1538–1547
- Leduc, D.J., Matney, T.G., Belli, K.L., and Baldwin, V.C., Jr. 2001. Predicting diameter distributions of longleaf pine plantations: a comparison between artificial neural networks and other accepted methodologies. *USDA For. Serv. Res Pap.* SRS-25.

- Lee, Y.J., and Coble, D.W. 2006. A new diameter distribution model for unmanaged loblolly pine plantations in east Texas. *South. J. Appl. For.* 30(1):13–20.
- Lenhart, J.D., and J.L. Clutter. 1971. Cubic-foot yield tables for old-field loblolly pine plantations in the Georgia Piedmont. *GA For. Res. Council Rep.* 22—Ser. 3. 12 p.
- Lindsay, S.R., Wood, G.R., and Wollons, R.C. 1996. Stand table modelling through the Weibull distribution and usage of skewness information. *For Ecol Manag.* 81(1–3):19–23.
- Little, S.N. 1983 Weibull diameter distributions for mixed stands of western conifers. *Can. J. For. Res.* 13, 85–88.
- Loetsch, F., Zöhrer, F., & Haller, K.E. 1973. *Forest inventory 2*. Munich, Germany: BLV.
- Lohrey, R.E., Bailey, R.L. 1976. Yield tables and stand structure for un-thinned longleaf pine plantations in Louisiana and Texas. *Res. Pap. SO-133*. New Orleans, LA: U.S. Department of Agriculture, Forest Service, Southern Forest Experiment Station. 53 p
- Magnussen, S. 1986. Diameter distributions in *Picea abies* described by the Weibull model. *Scandinavian Journal of Forest Research* 1: 493-502.
- Massey, F.G.J.R. 1951. The Kolmogorov-Smirnov test for goodness of fit. *J. Am. Stat. Assoc.* 46:68–78.
- Matney, T.G., and Farrar, R.M. 1992. A thinned/un-thinned loblolly pine growth and yield simulator for planted cutover site-prepared land in the Mid-Gulf South. *South. J. Appl. For.* 16(2):70-75.

- Matney, T.G., Sullivan, A.D. 1982. Compatible stand and stock tables for thinned and unthinned loblolly pine stands. *Forest Sci.* 28, 161–171.
- McTague, J.P., Bailey, R.L. 1987. Compatible basal area and diameter distribution models for thinned loblolly pine plantations in Santa Catarina, Brazil. *Forest Science* 33, 43–51.
- Miguel, E.P., Machado, S.A., Figueiredo Filho, A., and Arce, J.E. 2010. Using the Weibull function for prognosis of yield by diameter class in *Eucalyptus europphylla* stands. *Cerne* 16(1): 94-104. doi:10.1590/S0104-77602010000100011
- Nanang, D.M. 1998. Suitability of the Normal, Log-normal and Weibull distributions for fitting diameter distributions of neem plantations in Northern Ghana. *For Ecol Manage* 103(1):1–7
- Nelson, T.C. 1964. Diameter distribution and growth of loblolly pine. *Forest Sciences*, 10, 105–115.
- Newton, P.F., Lei, Y., Zhang, S.Y. 2004. A parameter recovery model for estimating black spruce diameter distribution within the context of a stand density management diagram. *The Forestry Chronicle*, 3: 349–358
- Newton, P.F., Lei, Y., Zhang, S.Y. 2005. Stand-level diameter distribution yield model for black spruce plantations. *Forest Ecol. Manage.* 209, 181–192.
- Ogana, F. N., and Gorgoso-Varela, J. J. 2015. Comparison of estimation methods for fitting Weibull distribution to the natural stand of Oluwa Forest Reserve, Ondo State, Nigeria. *Journal of Research in Forestry, Wildlife & Environment*, 7(2), 82–90.

- Ogana, F.N., Osho, J.S.A., and Gorgoso-Varela, J. J. 2015. Comparison of beta, gamma and Weibull distributions for characterizing tree diameter in Oluwa Forest Reserve, Ondo State, Nigeria. *Journal of Natural Sciences Research*, 5(4), 28–36.
- Poudel, K.P., and Cao, Q.V. 2013. Evaluation of methods to predict Weibull parameters for characterizing diameter distributions. *For. Sci.* 59(2): 243-252.
doi:10.5849/forsci.12-001
- Qin, J., and Cao, Q.V. 2006. Using disaggregation to link individual-tree and whole-stand growth models. *Can. J. For. Res.* 36: 953–960.
- R Core Team. 2020. *R: A Language and Environment for Statistical Computing*. R Foundation for Statistical Computing. <https://www.R-project.org/> (accessed on 14 May 2020).
- Rennolls, K., Geary, D.N. & Rollinson, T.J.D. 1985. Characterizing diameter distributions by the use of Weibull distribution. *Forestry* 58: 57-66.
- Reynolds, M.R., Burk, T.E., and Huang, W.C. 1988. Goodness of-fit tests and model selection procedures for diameter distribution models. *For. Sci.* 34:373–399
- Royle, J.A., and Dorazio, R.M. 2008. *Hierarchical modeling and inference in ecology: The analysis of data from populations, metapopulations and communities*. Academic Press, San Diego, CA. 444 p
- Saborowski, J. 1995. Minimum sample size for estimating the Weibull parameters of diameter distributions. *Proc. IUFRO Symp., Stellenbosch*, pp 1–7
- Schreuder, H.T., Hafley, W.L., Bennet, F.A. 1979. Yield prediction for un-thinned natural slash pine stands. *Forest Sci.* 25, 25–30.

- Schreuder, H.T., and Swank, W.T. 1974. Coniferous stands characterized with the Weibull distribution. *Can J For Res* 4: 518–523
- Sghaier, T., Cañellas, I., Calama, R., and Sánchez-González, M. 2016. Modelling diameter distribution of *Tetraclinis articulata* in Tunisia using normal and Weibull distributions with parameters depending on stand variables. *iForest* 9: 702-709. doi: 10.3832/ifor1688-008
- Shifley, S.R., Lentz, E. 1985. Quick estimation of the three-parameter Weibull to describe tree size distributions. *Forest Ecology and Management* 12:195–203
- Shiver, R.D. 1988. Sample size and estimation methods for the Weibull distribution in un-thinned and thinned pine plantation diameter distributions. *For. Sci.* 24(3): 809–814
- Siipilehto, J. 1999. Improving the accuracy of predicted basal-area diameter distribution in advanced stands by determining stem number. *Silva Fennica* 33, 281–301.
- Siipilehto J., and Mehtätalo L. 2013. Parameter recovery vs. parameter prediction for the Weibull distribution validated for Scots pine stands in Finland. *Silva Fennica*. 47(4): 1-22. doi:10.14214/sf.1057
- Smalley, G.W., Bailey, R.L. 1974a. Yield tables and stand structure for loblolly pine plantations in Tennessee, Alabama, and Georgia highlands. USDA Forest Service, Southern Forest Experiment Station, New Orleans, Research Paper SO-96
- Smalley, G.W., Bailey, R.L. 1974b. Yield tables and stand structure for shortleaf pine plantations in Tennessee, Alabama, and Georgia highlands. USDA Forest Service, Southern Forest Experiment Station, New Orleans, Research Paper SO-97

- Strub, M.R. and Burkhart, H.E. 1975. A class-interval-free method for obtaining expected yields from diameter distributions. *For Sci* 27:67–69
- Ueno, Y., Osawa, Y. 1987. The applicability of the Weibull and the expanded Weibull distributions. *J Jpn For Soc* 69(1):24–28
- van Laar, A., Akça, A. 2007. *Forest Mensuration*. 2nd edition. New York: Springer; 2007:38
- Vanclay, J.K. 1994. *Modelling forest growth and yield: applications to mixed tropical forests*.
- Weiskittel, A.R., Hann, D.W., Kershaw, J.A., and Vanclay, J.K. 2011. *Forest growth and yield modeling*. Hoboken, NJ: Wiley.
- Zarnoch, S.J., D.P. Feduccia, V.C. Baldwin, Jr., and T.R. Dell. 1991. Growth and yield predictions for thinned and un-thinned slash pine plantations on cutover sites in the West Gulf region. *USDA For. Serv. Res. Pap. SO-264*. 32p.
- Zhang, L., and Zhou, X. 2010. Diameter distribution of trees in natural stands managed on polycyclic cutting system. *Forestry Studies in China*, 12(1), 21–25.
- Zhous, B., and McTague, J.P. 1996. Comparison and evaluation of five methods of estimation of the Johnson system parameters. *Canadian Journal of Forest Research. Journal Canadien de la Recherche Forestiere*, 26, 928–935.
doi:10.1139/x26-102

Table 3.1 Parameter estimates and their associated standard errors (in parentheses), random effects standard deviations and goodness-of-fit statistics for arithmetic mean diameter prediction model.

Factor	Parameter	Estimate	
Fixed effects	b_0	3.7564 (1.1495)	
	b_1	1.5021 (0.4841)	
	b_2	-0.7535 (0.2975)	
	b_3	15.3432 (6.7380)	
Random effects	(Clone)	$s(b_0)$	2.8489
		$s(b_1)$	0.7263
		$s(b_2)$	0.6312
		$s(b_3)$	13.2230
	(Site Class Clone)	$s(b_0)$	2.8490
		$s(b_1)$	1.1114
		$s(b_2)$	0.7182
		$s(b_3)$	16.0999
Goodness-of-fit	Fixed	rMSE	0.2874
		R^2	0.9821
		Bias	0.0829
	Fixed + random	rMSE	0.2156
		R^2	0.9899
		Bias	0.0038

Table 3.2 Parameter estimates and their associated standard errors (in parentheses), random effects standard deviations and goodness-of-fit statistics for 25th diameter percentile prediction model

Factor	Parameter	Estimate	
Fixed effects	b_0	1.2951 (0.1785)	
	b_1	0.0269 (0.0088)	
	b_2	0.0127 (0.0036)	
	b_3	0.6449 (0.1969)	
Random effects	(Clone)	$s(b_0)$	0.2334
		$s(b_1)$	0.0096
		$s(b_2)$	0.0040
		$s(b_3)$	0.2348
	(Site Class Clone)	$s(b_0)$	0.1454
		$s(b_1)$	0.0129
		$s(b_2)$	0.0050
		$s(b_3)$	0.2332
Goodness-of-fit	Fixed	rMSE	1.1311
		R ²	0.5451
		Bias	-0.5099
	Fixed + random	rMSE	0.7953
		R ²	0.7738
		Bias	-0.0046

Table 3.3 Parameter estimates and their associated standard errors (in parentheses), random effects standard deviations and goodness-of-fit statistics for 99th diameter percentile prediction model

Factor	Parameter	Estimate	
Fixed effects	b_0	1.9872 (0.1591)	
	b_1	-0.0155 (0.0029)	
	b_2	0.0288 (0.0012)	
	b_3	-0.3663 (0.3397)	
Random effects	(Clone)	$s(b_0)$	0.2135
		$s(b_1)$	<0.0001
		$s(b_2)$	<0.0001
		$s(b_3)$	0.4693
	(Site Class Clone)	$s(b_0)$	0.1070
		$s(b_1)$	0.0064
		$s(b_2)$	0.0027
		$s(b_3)$	0.1466
Goodness-of-fit	Fixed	rMSE	1.1510
		R ²	0.8631
		Bias	0.7320
Fixed + random		rMSE	1.0592
		R ²	0.9327
		Bias	-0.0117

Table 3.4 Coefficient estimates (fixed + random effects) of nonlinear mixed effect model by clone and site classes for arithmetic mean diameter prediction model.

Parameter	Estimate coefficient by clone and site class						
	A:22	A:24	A:26	A:28	B:24	B:26	B:28
b_0	5.0580	6.8023	6.4207	5.9698	1.4566	-0.6481	1.2354
b_1	0.1972	0.6093	0.3989	1.7608	2.7261	3.2856	2.0468
b_2	-0.8457	-1.5070	-1.3428	-1.6237	-0.2855	0.2443	-0.0292
b_3	2.6035	0.2958	-0.3092	7.9372	31.4552	41.3175	27.9144

Table 3.5 Coefficient estimates (fixed + random effects) of nonlinear mixed effect model by clone and site classes for 25th diameter percentile prediction model.

Parameter	Estimate coefficient by clone and site class						
	A:22	A:24	A:26	A:28	B:24	B:26	B:28
b_0	0.9454	1.1477	1.2233	0.9345	1.4989	1.4012	1.6833
b_1	0.0070	0.0174	0.0041	0.0415	0.0351	0.0320	0.0421
b_2	0.0237	0.0155	0.0178	0.0096	0.0101	0.0125	0.0039
b_3	0.9622	0.8341	0.5222	1.1938	0.4514	0.5397	0.2436

Table 3.6 Coefficient estimates (fixed + random effects) of nonlinear mixed effect model by clone and site classes for 99th diameter percentile prediction model

Parameter	Estimate coefficient by clone and site class						
	A:22	A:24	A:26	A:28	B:24	B:26	B:28
b_0	2.1217	2.1818	2.3095	2.3301	1.7646	1.7967	1.6186
b_1	-0.0063	-0.0224	-0.0156	-0.0165	-0.0126	-0.0115	-0.0235
b_2	0.0289	0.0302	0.0269	0.0257	0.0285	0.0278	0.0333
b_3	-0.7517	-0.7901	-1.0401	-0.9254	0.1114	0.0389	0.3257

Table 3.7 Average of the parameter estimates of the Weibull distribution using fit data and three prediction methods.

Method	Scale parameter				Shape parameter			
	Mean	Stdev	Min	Max	Mean	Stdev	Min	Max
MLE	10.23	1.85	3.95	15.11	3.39	1.20	1.68	11.50
MOM	10.24	1.71	4.29	15.08	2.80	0.78	1.89	14.02
PCT	9.53	1.59	5.10	14.58	3.46	0.97	2.35	7.98
HYB	10.37	1.79	4.24	15.85	3.46	0.97	2.35	7.98

Table 3.8 Means and standard deviations of the goodness-of-fit statistics produced by three diameter distribution prediction methods.

Method	KS			EI	
	Mean	Stdev	% Coverage ^a	Mean	Stdev
MLE	0.1499	0.0699	68%, 80%	23.6921	6.4569
MOM	0.1757	0.0724	49%, 66%	26.5218	6.7118
PCT	0.2125	0.0759	26%, 44%	31.4708	9.7966
HYB	0.1988	0.0825	37%, 54%	27.7307	8.1979

^a Percentage of distributions that fall within 95% or 99% confidence intervals of the KS

D_{\max}

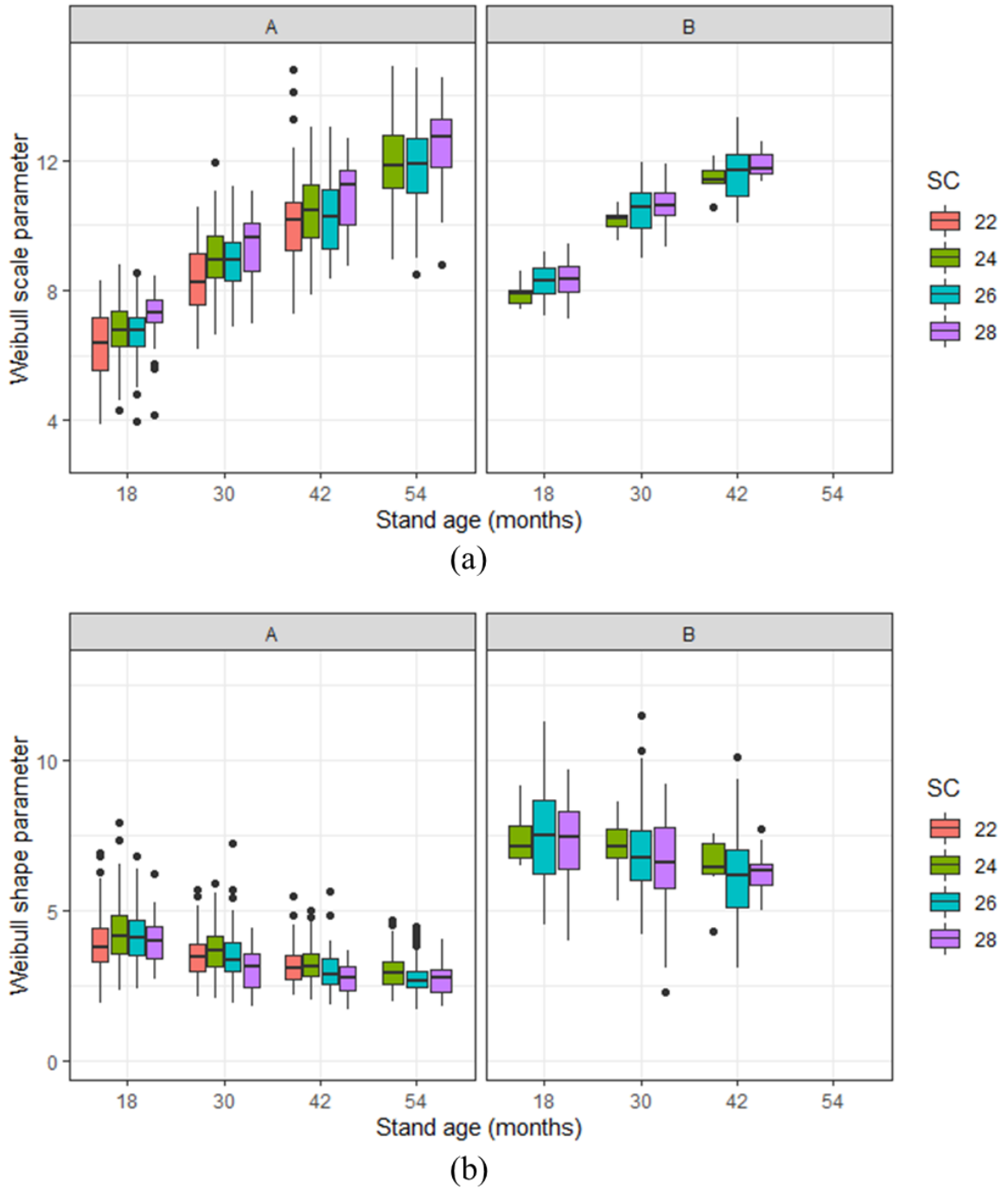


Figure 3.1 Boxplots of Weibull scale (a) and shape (b) parameter by clone, age and site class estimated from full sample of the trees in the plot using maximum likelihood estimation method.

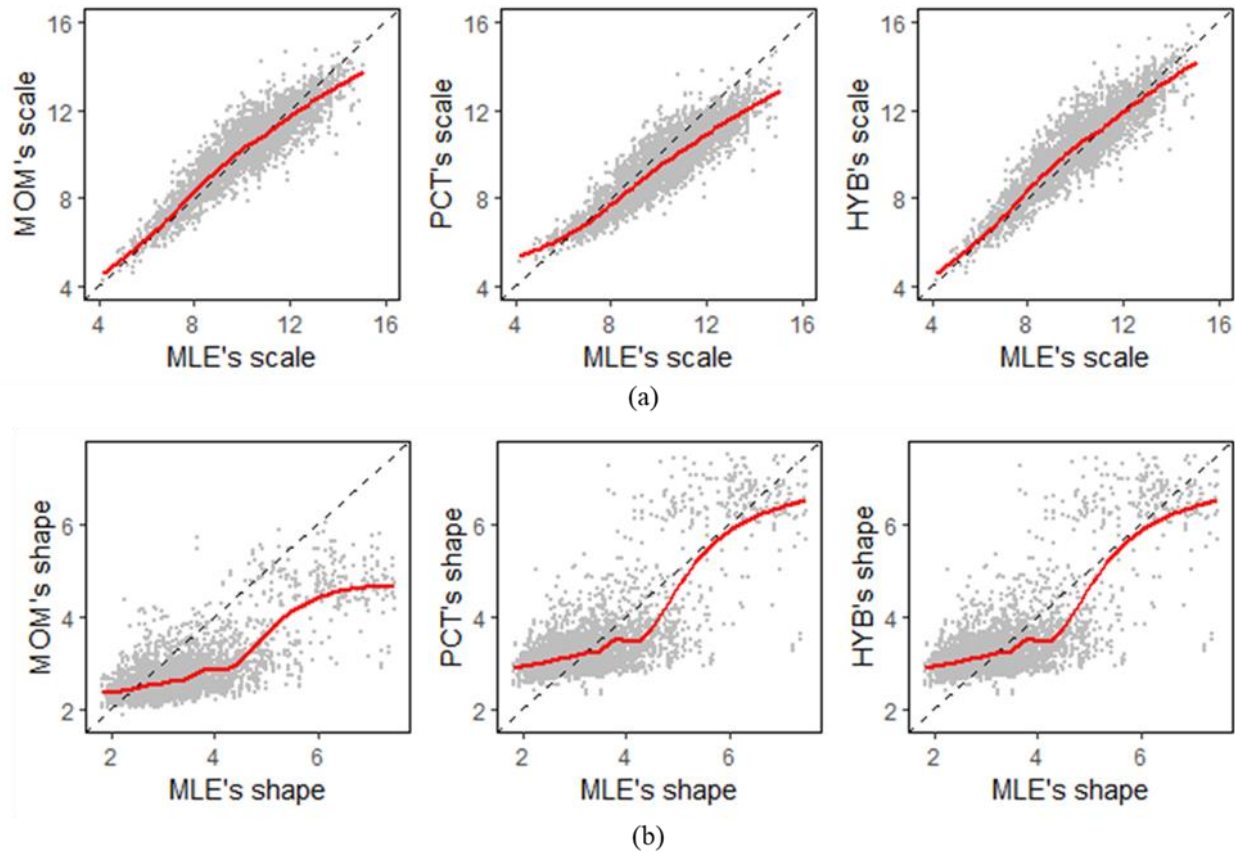


Figure 3.2 Parameter estimation comparison between MLE's and three parameter recovery estimation methods for scale (a; above) and shape (b; below). The dotted line represents the 1:1 line, while the red line is the observed trend using a smoothing line.

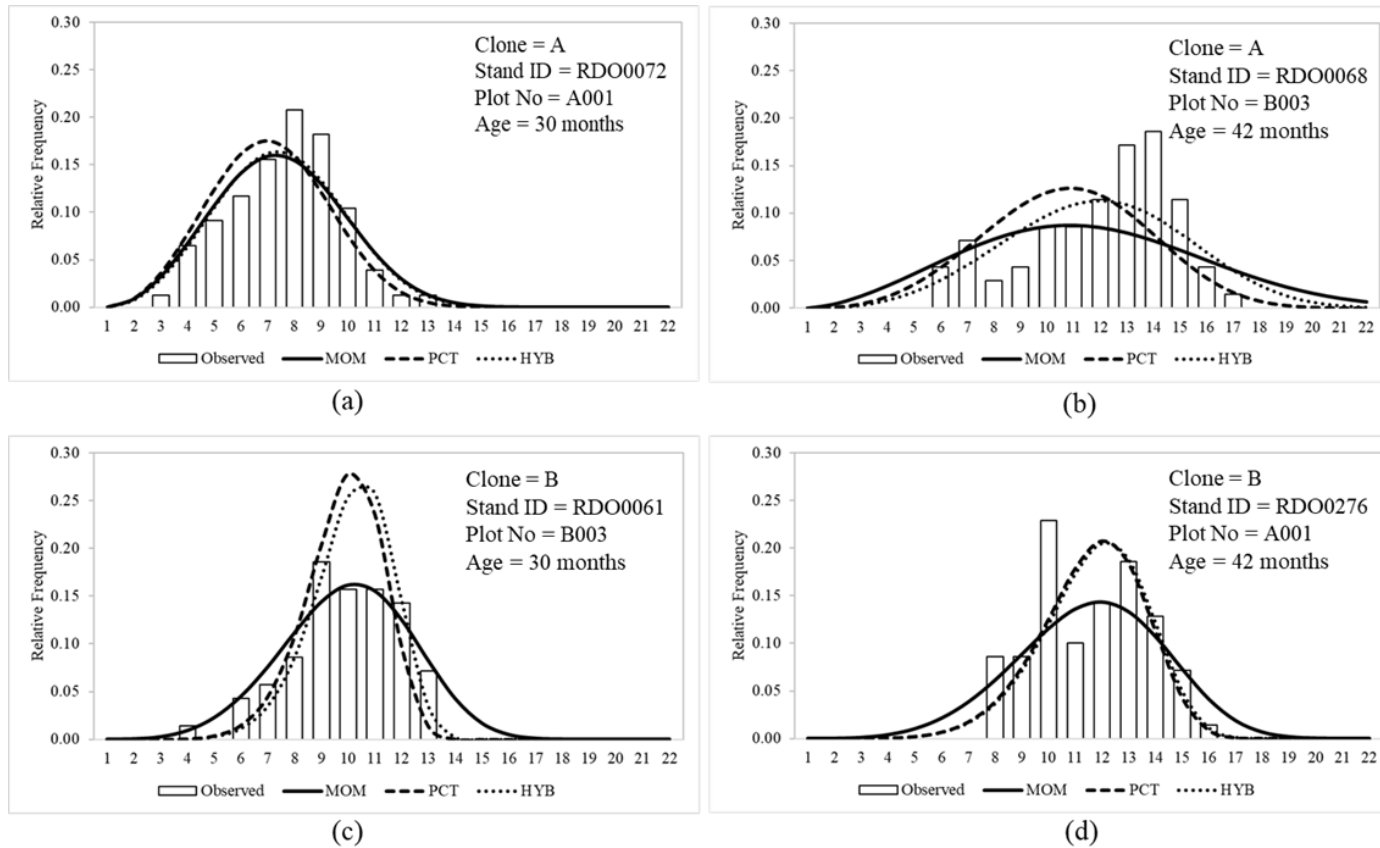


Figure 3.3 Model evaluation for the four example plots that represent (a) clone A, 30 months; (b) clone A, 42 months; (c) clone B, 30 months and (d) clone B, 42 months. The histogram represents the observed diameter distribution, and three curves represent diameter distribution models prediction.

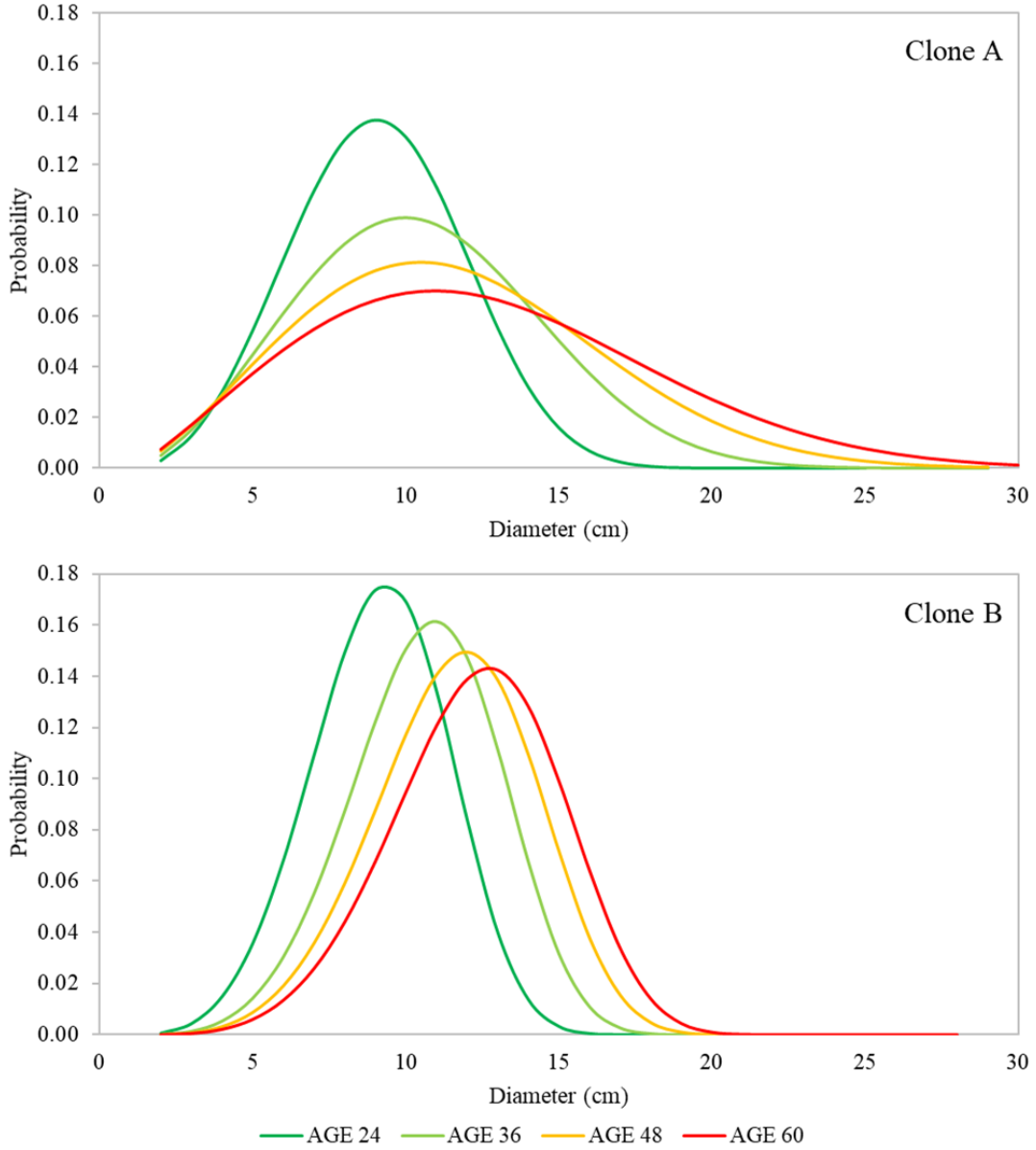


Figure 3.4 Simulated development of diameter distribution over ages using MOM method. Simulations are based on prediction stand-level variables (SD, BA, HT, RD and DQ) using site class = 26 and initial stand density 1667 trees ha⁻¹. AGE indicated stand age in months.

Chapter 4: Conclusions

4.1 Summary of results

Commercial plantations, established to provide a sustainable supply of raw materials for the pulp and paper industry, are a significant land use in Sumatra and Kalimantan Island (Inail et al. 2019). With existing land, plantation growing companies must find ways to increase forest productivity in a sustainable manner. Applying good silvicultural treatments or finding clones that grow fast and are less susceptible to disease are examples of how companies can increase yields. Using suitable inventory and other resource data, growth models provide a reliable way to determine sustainable timber yields, to examine silvicultural and harvesting options, and to examine impacts of forest management and harvesting on other forest values (Vanclay 1994). This thesis explored approaches for both stand-level and diameter distribution modeling, and developed these dynamic models using forest inventory data for *Eucalyptus* clonal plantations in Sumatra Island, Indonesia. In Chapter 2, I compared time-based and state-space approaches to determine which approach was best suited for describing stand-level dynamics in this system; and in Chapter 3, I explored three different methods to recover parameters of the Weibull distribution for predicting future diameter distributions in these systems. The models developed in this study will provide valuable information and understanding about stand dynamics and potential yield of *Eucalyptus hybrid* stands in Indonesia.

Our first study (Chapter 2; Waldy et al., In Review) indicated that both time-based and state-space approaches were adequate for predicting stand parameters within the range of conditions modeled here (Figure 2.9) and Bakuzis matrices showed that both models provided biologically reasonable depictions of stand development patterns (Figures 2.5 – 2.8). However, considering all statistical evaluations (goodness-of-fit

statistics and two one-sided t-test equivalence tests), the time-based models that use age in their mathematical form produced a simple and reliable estimation system for *Eucalyptus hybrid* clones that minimized overall prediction errors. We found that the von Bertalanffy-Richards and two-parameter Schumacher polymorphic equations were the best equations among those tested for predicting top height (Table 2.8) and basal area (Table 2.10) over time, while the Clutter (1983) formulation was most optimal for predicting stand density (Figure 2.9). Several studies have shown that the state-space approach give better predictions and provides more effective framework for predicting plantation growth development. However, Garcia (1988) cautioned that these methods are not recommended for general development and use by “casual” growth modelers; an expertise to understand the techniques and modify them as necessary is essential in developing state-space models.

In our study, all plantations had the same initial planting density, thus reducing the complexity of the mortality dynamics which often limit time-based modeling approaches (Weiskittel et al. 2011; García 1988; Hyink and Moser 1984). In addition, the rotation lengths of the *Eucalyptus hybrid* plantations used in this study were shorter than the time required to reach the onset of competition-induced mortality (stand self-thinning), so the observed mortality was only random mortality (random in the sense that neither model explicitly considers causes). Like traditional yield tables, time-based models are often limited to a narrow range of silvicultural treatment regimes (Weiskittel et al. 2011) while state-space models are more flexible, general prediction systems (García 1988). When compared using different initial densities, both models produced biologically reasonable estimates (Figures 2.9 – 2.12) but there were no data available to

compare their statistical accuracies under different initial densities. The very short rotation ages with a single initial planting density favored time-based models over state-space models. As experience with plantation performance improves and the need to expand silvicultural options to meet a more diverse product mix develops, more complex or variable plantations management regimes may develop. In these cases, state-space models may become better suited for predicting plantation dynamics and the time-based versus state-space approaches reassessed.

The use of clone and site index as random effects in the models should enable APRIL to rapidly calibrate these models as new clones are developed or as they expand the range of site qualities over which Eucalyptus clones are planted. Temesgen et al. (2008) propose several methods for estimating random effects for new data.

Parameter recovery methods were proposed as a compatible approach for size-distribution modeling derived from stand-average growth and yield models (Hyink and Moser 1983). Moment-based (Matney and Sullivan 1982; Knoebel et al. 1986; Lindsay et al. 1996; Newton et al. 2004) and percentile-based parameter recovery methods (Lohrey and Bailey 1976; McTague and Bailey 1987; Bailey et al. 1989; Brooks et al. 1992; Knowe 1992) are widely used in forest growth and yield modeling. More recently, a hybrid approach using both moments and percentiles was proposed as an alternative approach (Brooks et al. 1992; Bullock and Burkhart 2005; Knowe et al. 2005; Lee and Coble 2006; Coble and Lee 2008; and Jiang and Brooks 2009). In our second study (Chapter 3), moment-based, percentile-based and hybrid parameter recovery approaches were compared using the Weibull distribution fitted to observed diameter distributions for Eucalyptus clones in Sumatra, Indonesia. The growth model developed in Chapter 2

provides independent predictions of top height, basal area and density. Both moments and percentiles were predicted from future stand attributes, which were predicted from current stand attributes using the regression from which an estimate of the quadratic mean diameter (the square root of the second moment) can be calculated. Using field data, I then fitted a nonlinear mixed effects model to estimate mean diameter (the first moment) based on estimated quadratic mean diameter and other stand-level estimates for the growth model (Table 3.1). Similarly, nonlinear mixed effects equations were developed for percentile estimation based on field data (Tables 3.2 and 3.3). The hybrid approach uses a combination of moments (QMD in this study) and percentile estimates to recover distribution parameters. Based on the KS test and an error index, we found that moment-based methods performed better than hybrid methods which performed better than percentile methods (Table 3.8). Given that hybrid methods use a combination of moments and percentiles, these results were not really surprising, although Cao (2004) found hybrid approaches outperformed moment-based approaches in loblolly pine plantations. Again, the single initial planting density and the short rotation length may have favored moment-based methods over the other two approaches. All three methods had difficulty in describing multimodal diameter distributions; however, the moment-based method was better able to fit distributions with more skewed tails on either side of the distribution and exhibited slightly greater flexibility in describing distributions with larger variances. As the growth models, as new management regimes evolve, these results will need to be re-evaluated.

4.2 Model applications

A forest growth model is a simplification of the forest and its dynamics that allows forecasting of forest development under different management alternatives (Burkart and Tome 2012). The models developed in this study are applied at the stand level (Chapter 2) and then used to produce estimates by diameter classes based on the Weibull distribution function (Chapter 3). The input data required by these models are site index, clone, age (A_1), top height (HT_1), basal area (BA_1) and stand density (SD_1) at the beginning of the projection period; and age at the end of the projection period (A_2). Model output can be used with the equations developed in chapter 3 to estimate distributions of trees across diameters.

Figures 4.1 and 4.2 display simulations of stand dynamic models of Eucalyptus hybrid for clone A and B, respectively. Panels (a) and (b) in both figures illustrate stand volume and diameter distributions over time by site class using an initial density of 1667 trees·ha⁻¹. Site class had a very significant effect on stand volume for both clones. Stand volumes for clone A at rotation ages (72 months) were 174 m³ha⁻¹ for Site Class 22, 188 m³ha⁻¹ for Site Class 24, 205 m³ha⁻¹ for Site Class 26, and 221 m³ha⁻¹ for Site Class 28 (Figure 4.1 a). Stand volumes for clone B were 186 m³ha⁻¹ for Site Class 24, 203 m³ha⁻¹ for Site Class 26 and 222 m³ha⁻¹ for Site Class 28 (Figure 4.2 a). While the random effect associated with site class was significant in the modeling phase (Table 3.1), its effect on diameter distributions was relatively small and not clearly visible even though the scale parameter for poor sites was smaller than predicted for good sites (Figure 4.1.b and 4.2.b). Again, the short rotation lengths and lack of significant competition induced

mortality might not allow for the effects of site index on diameter distributions to be observed.

Using site class 26 for simulations, panels (c) and (d) in Figures 4.1 and 4.2 show effects of different initial planting densities on stand volumes and diameter distributions. At 72 months, stand volumes for clone A were $191 \text{ m}^3\text{ha}^{-1}$ for a planting density of $1111 \text{ trees}\cdot\text{ha}^{-1}$, $203 \text{ m}^3\text{ha}^{-1}$ for a planting density of $1333 \text{ trees}\cdot\text{ha}^{-1}$, and $220 \text{ m}^3\text{ha}^{-1}$ for a planting density of $1667 \text{ trees}\cdot\text{ha}^{-1}$. For clone B stand volumes were $182 \text{ m}^3\text{ha}^{-1}$ for a planting density of $1111 \text{ trees}\cdot\text{ha}^{-1}$, $193 \text{ m}^3\text{ha}^{-1}$ for a planting density of $1333 \text{ trees}\cdot\text{ha}^{-1}$ and $212 \text{ m}^3\text{ha}^{-1}$ for a planting density of $1667 \text{ trees}\cdot\text{ha}^{-1}$. The effect of initial density on diameter distributions is much clearer than site index effects. Higher planting density shifts the distribution curves to the left (smaller trees) for a given age (Figures 4.1.d and 4.2.d). Smaller trees at higher densities are expected as competition begins earlier, thus reducing individual tree growth through crown recession and reduced photosynthetic capacity (Oliver and Larson 1996).

4.3 Future work

This thesis represents an attempt to develop dynamic growth and yield models for tropical short-rotation *Eucalyptus hybrid* plantations in Indonesia, and, to our knowledge, it is the first attempt at using state-space in these systems. However, because our field data only had a single initial establishment density and a very short rotation length, the state-space model, which is theoretically more responsive to changes in management regimes (García 1988), did not perform as well as the time-based models developed here. Establishing plantation trials that examine different planting densities and monitoring

these trials over longer periods of time are essential for assessing current management regimes. Given the current emphasis on pulp production with paper as the primary product, the management regimes are adequate for meeting mill demands. Development of new pulp-based products may require different wood properties or increased quantity and quality of wood volumes flowing to the mill. Developing such silvicultural trials ahead of market demands will enable the company to tune their management regimes more quickly. Retaining a portion of the existing inventory plots or permanent sample plots beyond the normal rotation ages is another approach the APRIL group could use to gain additional insights into the dynamics and yields of *Eucalyptus hybrid* plantations. The investments in data already collected may offset the reductions in revenue due to reduced harvest levels relative to the costs of establishing and maintaining new trials.

The Weibull distribution is widely used because of its flexibility and capacity for fitting a variety of diameter distribution shapes (Poudel and Cao 2013), parameter estimation is straightforward and the parameters relate to commonly estimated stand-level attributes, and, because of the closed-form solution to the cumulative distribution function, the calculation of proportions of trees in diameter classes is straightforward (Cao 2012). As a result, the Weibull distribution is the most widely used distribution for generating diameter distributions (Burkhart & Tomé 2012) and one of the best-performing among many other distributions (Eisfeld et al. 2005). However, 32% of the estimated Weibull parameters differed significantly from the sample estimates based on plot data and maximum likelihood estimation (Table 3.8). Other probability density functions (e.g., beta, Johnson's SB, gamma or lognormal) are potentially worth examining or other forms of the Weibull distribution (left-truncated 2-parameter, for

example). Several variants of the Weibull distribution, as suggested by Goodwin (2020), also are worth future evaluation.

The increasing availability of airborne and ground-based LiDAR and high spatial resolution optical imagery from airborne and spaceborne programs has rapidly increased the availability of relevant remotely sensed data for forest inventories. The feasibility of modeling forest yield variables, such as basal area, volume, biomass and other stand attributes with LiDAR-derived variables (or LiDAR metrics) has been demonstrated in a variety of studies (Naesset 1997; Means et al. 2000; Andersen et al. 2005; Yang et al. 2020). Currently, APRIL is still in its early stages of integration of airborne LiDAR and other remote sensing technology into forest inventory. Developing predictive forest growth models that incorporate the stand dynamics model in this study, LiDAR, optical imagery, and other geospatial data have the potential to provide significant advances in APRIL capacity to estimate stand structure, wood attributes as well as other stand characteristics. The systems approach developed by Yang et al. (2021) is particularly relevant to APRILs inventory and growth and yield programs because it can leverage the vast array of historical data collected and provides estimates of the required inputs into the growth models developed here, thus providing the potential for wall-to-wall predictions of plantations yields at relatively high spatial resolutions.

Forest management regimes are constantly evolving as product demands shift and public perception demands more transparency and accountability. Sustainable management is more than maintaining volume flows. An integrated growth and yield program is one way forest industries, such as the APRIL group, can be responsive to these constant shifts in demands.

4.4 References

- Andersen, H.E., Clarkin, T., Winterberger, K., Strunk, J. 2009. An accuracy assessment of positions obtained using survey and recreational-Grade Global Positioning System Receivers across a range of forest conditions within the Tanana Valley of Interior Alaska. *Western Journal of Applied Forestry*. 24. 128-136.
10.1093/wjaf/24.3.128.
- Bailey, R.L., Burgan, T.M., Jokela, E.J. 1989. Fertilized mid-rotation-aged slash pine plantations-stand structure and yield prediction models. *South J Appl For*. 13:76-80
- Brooks, J.R, Borders, B.E, Bailey, R.L. 1992. Predicting diameter distributions for site-prepared loblolly and slash pine plantations. *South. J. Appl. For*. 16 130–133
- Bullock, B.P., Burkhart, H.E. 2005. Juvenile diameter distributions of loblolly pine characterized by the two-parameter Weibull function. *New Forest* 29, 233–244.
<https://doi.org/10.1007/s11056-005-5651-5>
- Burkhart, H.E., and Tomé, M. 2012. *Modeling forest trees and stands*. Dordrecht; New York: Springer.
- Cao, Q.V. 2004. Predicting parameters of a Weibull function for modelling diameter distribution. *Forest Sci*. 50, 682–685.
- Cao, Q.V. 2012. Use of the Weibull function to predict future diameter distributions from current plot data. In: Butnor, John R., ed. 2012. *Proceedings of the 16th biennial southern silvicultural research conference*. e-Gen. Tech. Rep. SRS-156. Asheville, NC: U.S. Department of Agriculture Forest Service, Southern Research Station. 53-58.

- Clutter, J. L. 1983. Timber management: a quantitative approach. New York: Wiley
- Coble, D.W., and Y.J. Lee. 2008. A new diameter distribution model for unmanaged slash pine plantations in east Texas. *South. J. Appl. For.* 32(2):89-94.
- Eisfeld, R.L., Sanquetta, C.R., Arce, J.E., Maestri, R., and Weber, K.S. 2005. Growth and yield modelling of *Pinus taeda* L. using probability function. *Floresta* 35(2): 317-328. doi:10.5380/rf.v35i2.4619
- Garcia, O. 1988. Experience with an advanced growth modelling methodology. In: A.R. Ek, S.R. Shifley and T.E. Burk (eds) *Forest Growth Modelling and Prediction. Proceedings of IUFRO Conference, August 23-27, 1987, Minneapolis, Minnesota. USDA For. Serv., Gen. Tech. Rep. NC-120. P. 668-675.*
- Hyink, D.M. and Moser, J.W. 1983. A generalized framework for projecting forest yield and stand structure using diameter distributions. *For. Sci.* 29: 85-95
- Inail, M., Hardiyanto, E. and Mendham, D.S. 2019. Growth responses of *Eucalyptus pellita* F. Muell plantations in South Sumatra to macronutrient fertilizers following several rotations of *Acacia mangium* Wild. *Forests*. 10. 1054. 10.3390/f10121054.
- Jiang, L., and Brooks, J.R. 2009. Predicting diameter distributions for young longleaf pine plantations in Southwest Georgia, *Southern Journal of Applied Forestry*, Volume 33, Issue 1, February 2009, Pages 25–28, <https://doi.org/10.1093/sjaf/33.1.25>
- Knoebel, B.R., Burkhart, H.E., Beck, D.E. 1986. A growth and yield model for thinned stands of yellow-poplar, *Forest Science*, Volume 32, Issue suppl_2, June 1986, <https://doi.org/10.1093/forestscience/32.s2.a0001>

- Knowe, S.A. 1992. Basal area and diameter distribution models for loblolly pine plantations with hardwood competition in the piedmont and upper coastal plain. *South. J. Appl. For.* 16: 93–98.
- Knowe, S.A., Radosevich, S.R., and Shula, R.G. 2005. Basal area and diameter distribution prediction equations for young Douglas-Fir plantations with hardwood competition: coast ranges. *West. J. Appl. For.* 20 (2), 73–93.
- Lee, Y.J., and Coble, D.W. 2006. A new diameter distribution model for unmanaged loblolly pine plantations in east Texas. *South. J. Appl. For.* 30(1):13–20.
- Lindsay, S. R., Wood, G.R and Wollons, R.C. 1996. Stand table modelling through the Weibull distribution and usage of skewness information. *For Ecology and Management* 81(1–3):19–23.
- Lohrey, R.E., and Bailey, R.L. 1976. Yield tables and stand structure for un-thinned longleaf pine plantations in Louisiana and Texas. Res. Pap. SO-133. New Orleans, LA: U.S. Department of Agriculture, Forest Service, Southern Forest Experiment Station. 53 p
- Matney, T.G., and Sullivan, A.D. 1982. Compatible stand and stock tables for thinned and unthinned loblolly pine stands. *Forest Sci.* 28, 161–171.
- McTague, J.P., and Bailey, R.L. 1987. Compatible basal area and diameter distribution models for thinned loblolly pine plantations in Santa Catarina, Brazil. *Forest Science* 33, 43–51.
- Means, J., Acker, S., Fitt, B., Renslow, M., Emerson, L., Hendrix, C. 2000. Predicting forest stand characteristics with airborne scanning LiDAR. *Photogrammetric Engineering and Remote Sensing.* 66. 1367-1371.

- Naesset, E. 1997. Estimating timber volume of forest stands using airborne laser scanner data. *Remote Sen. Environ.* 61 (2):246-253.
- Newton, P.F., Lei, Y., Zhang, S.Y. 2004. A parameter recovery model for estimating black spruce diameter distribution within the context of a stand density management diagram. *The Forestry Chronicle*, 3: 349–358
- Poudel, K. P., and Cao, Q.V. 2013. Evaluation of methods to predict Weibull parameters for characterizing diameter distributions. *For. Sci.* 59(2): 243-252.
doi:10.5849/forsci.12-001
- Temesgen, H., Monleon, V.J., and Hann, D. 2008. Analysis and comparison of nonlinear tree height prediction strategies for Douglas-fir forests. *Canadian Journal of Forest Research*. 38(3): 553-565. <https://doi.org/10.1139/X07-104>
- Weiskittel, A.R., Hann, D.W., Kershaw, J.A., and Vanclay, J.K. 2011. *Forest growth and yield modeling*. Hoboken, NJ: Wiley.
- Yang, T.-R., Kershaw, J.A., Ducey, M.J., 2021. The development of allometric systems of equations for compatible area-based LiDAR-assisted estimation. *Forestry: An International Journal of Forest Research*. 94(1): 36-53
- Vanclay, J. K. 1994. *Modelling forest growth and yield: applications to mixed tropical forests*.

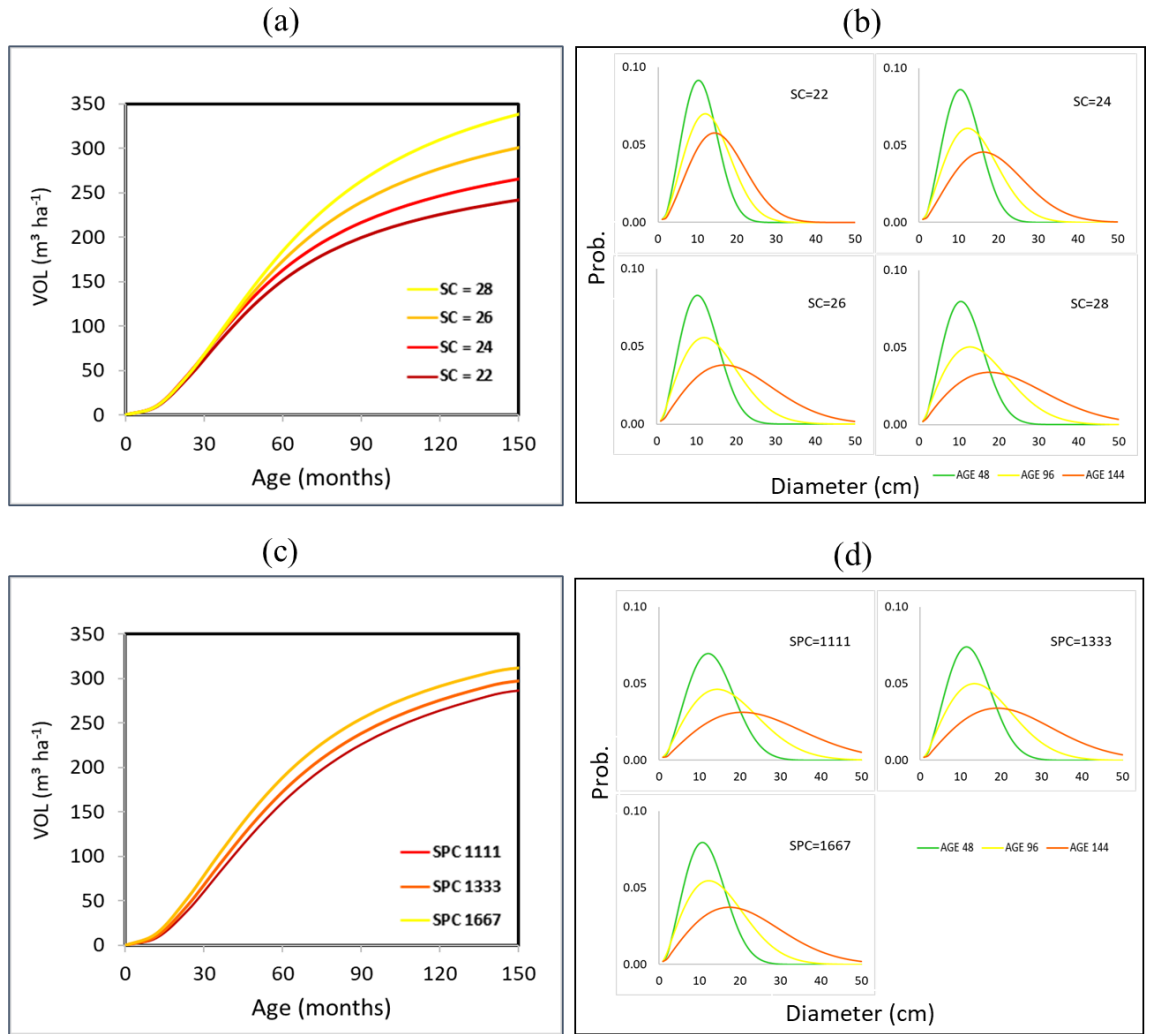


Figure 4.1 Stand dynamic model simulations of *Eucalyptus hybrid* for clone A. (a) Stand volume over time by site class (initial density 1667 trees·ha⁻¹); (b) Diameter distribution by site class for stand age 48, 96 and 144 months (initial density 1667 trees·ha⁻¹); (c) Stand volume over time by initial density (site class 26); (d) Diameter distribution by initial density for stand age 48, 96 and 144 months (site class 26).

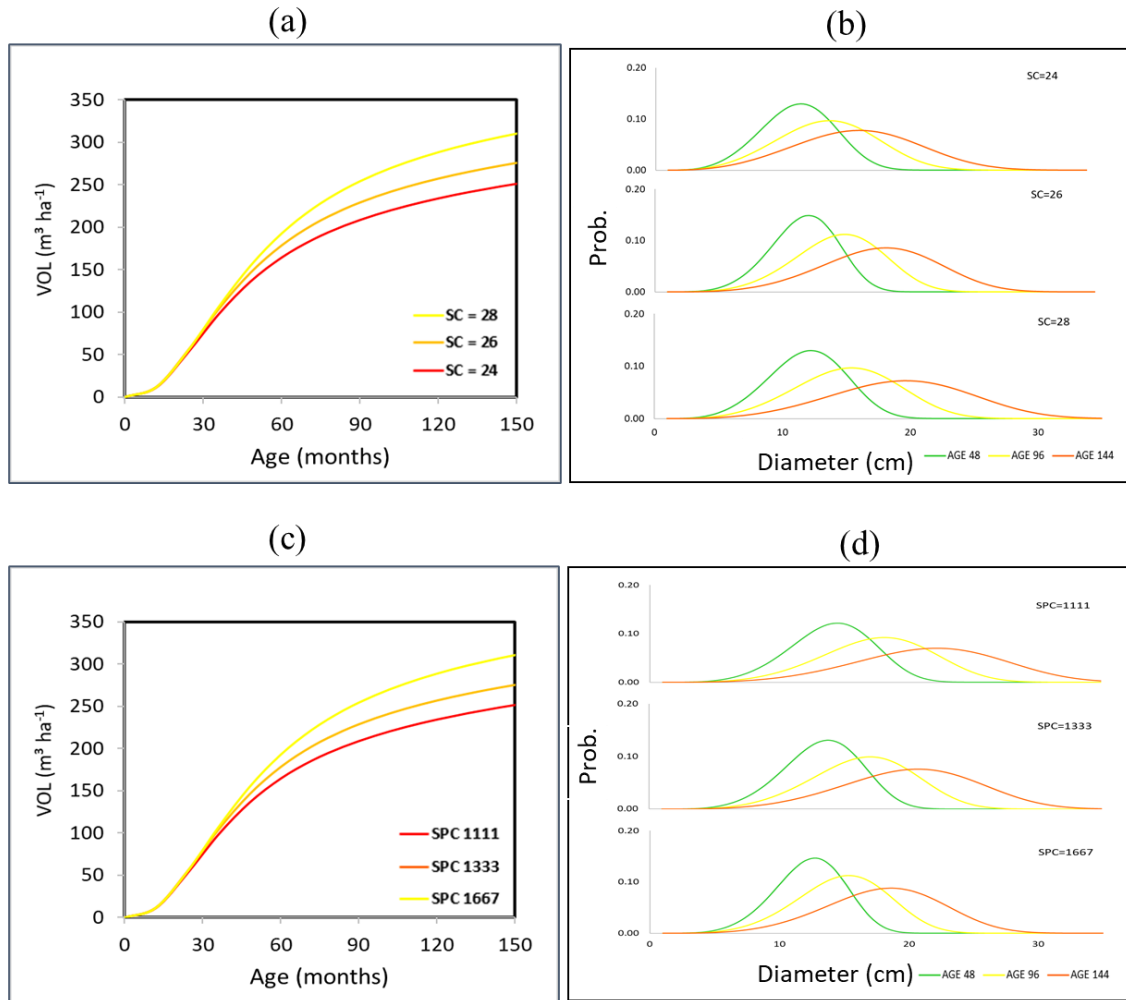


Figure 4.2 Stand dynamic model simulations of *Eucalyptus hybrid* for clone B. (a) Stand volume over time by site class (initial density 1667 trees·ha⁻¹); (b) Diameter distribution by site class for stand age 48, 96 and 144 months (initial density 1667 trees·ha⁻¹); (c) Stand volume over time by initial density (site class 26); (d) Diameter distribution by initial density for stand age 48, 96 and 144 months (site class 26).

Curriculum Vitae

Candidate's full name: Joni Waldy

Universities attended:

University of New Brunswick (2019 - 2021), Master of Science in Forestry

IPB University, Indonesia (2006 - 2010), Bachelor of Science in Statistics

Publications:

Walady, J., Kershaw, J.A., Weiskittel, A., Ducey, M.J. In Review. Diameter distribution model development of tropical hybrid Eucalyptus clonal plantations in Sumatera, Indonesia: A comparison of estimation methods. *New Zealand Journal of Forestry Science*.

Walady, J., Kershaw, J.A., Weiskittel, A., Ducey, M.J. In Revision. Comparison of time-based versus state-space stand growth models for tropical hybrid Eucalyptus clonal plantations in Sumatera, Indonesia. *Canadian Journal of Forestry Research*.

Wang, H., Yang, T.R., Walady, J., Kershaw, J.A. 2021. Estimating individual tree heights and DBHs from vertically displaced spherical image pairs. *Mathematical and Computational Forestry & Natural Resource Sciences*.

Conference Presentations:

Walady, J. 2021. Diameter distribution model development of tropical hybrid Eucalyptus clonal plantations in Sumatera, Indonesia: A comparison of estimation methods. Poster presentation, Winter 2021 Graduate Seminar, Faculty of Forestry and Environmental Management, University of New Brunswick (March 24th, 2021)

- Waldy, J. 2020. Comparison of time and state-space-based stand growth models for tropical hybrid *Eucalyptus* clonal plantations in Sumatera, Indonesia. Poster presentation, Fall 2020 Graduate Seminar, Faculty of Forestry and Environmental Management, University of New Brunswick (December 8th, 2020)
- Waldy, J. 2020. Time-based versus state-space stand growth models of tropical *Eucalyptus hybrid* plantations in Sumatera, Indonesia. Oral presentation, Western Mensurationists Conference, University of Idaho, Moscow, ID, U.S.A (June 14-16th, 2020; Virtual)
- Waldy, J. 2019. APRIL's overview and its challenges for forest growth and inventory. Oral presentation, Fall 2019 Graduate Seminar, Faculty of Forestry and Environmental Management, University of New Brunswick (December 9th, 2019)